The characterization of immune cells in Asm-overexpressed mice

Inaugural-Dissertation

zur

Erlangung des Doktorgrades

Dr. rer. nat.

der Fakultät für Biologie

an der

Universität Duisburg-Essen

vorgelegt von

Wing Yee Hung

aus

Hong Kong

Im August 2018

Die der vorliegenden Arbeit zugrunde liegenden Experimente wurden am Institut für Molekularbiologie, Universität Duisburg-Essen durchgeführt.

1. Gutachter: Prof. Dr. Erich Gulbins
2. Gutachter: Prof. Dr. Matthias Gunzer
3. Gutachter: Prof. Dr. Astrid Westendorf

Vorsitzender des Prüfungsausschusses: Prof. Dr. Astrid Westendorf

Tag der mundlichen Prüfung: 17th December, 2018

To my grandmother

Although you can't be here with us, we're truly not apart until the final breath we take. You will be living in our hearts.

Abbreviations

Ac	acid ceramidase
APRIL	proliferation-inducing ligand
Asm	acid sphingomyelinase
BAFF	B-cell-activating factor of the TNF family
BCR	B cell receptor
C1P	ceramide-1-phosphate
CD40L	CD40 ligand
cer	Ceramide
CerS	dihydroceramide synthases
CERT	ceramide transfer protein
CFTR	cystic fibrosis transmembrane conductance regulator
DCs	dendritic cells
DC-SIGN	DC specific intercellular adhesion molecule-grabbing non-integrin
DN	double negative
DP	double positive
ER	endoplasmic reticulum
FD	Farber disease
FIASMA	functional inhibitors of acid sphingomyelinase
fMLP	N-formylmethionylleucyl phenylalanine
FOXP3	foxhead box P3
fWT	female wildtype
HEV	high endothelial venules
ICAM-1	Intercellular Adhesion Molecule 1
IF	Immunofluorescence
IFN-γ	interferon gamma
Ig	immunoglobulin
IL	interleukin
IP-10	interferon gamma-induced protein-10
KC	keratinocyte chemoattractant
L-Asm	lysosomal Asm
LN	lymph node

MCP-1	monocyte chemoattractant protein
MFI	Median fluorescence index
MHC	major histocompatibility complex
MIP-1α	macrophage inflammatory protein-1α
mWT	male wildtype
MZB	Marginal B cells
NADPH	Nicotinamide adenine dinucleotide phosphate
NK	Natural killer
NSM	neutral sphingomyelinase
PALS	periarterial lymphatic sheaths
PAMPs	pathogen-associated molecular pattern
PKCδ	protein kinase C delta
ROR-γt	RAR-related orphan receptor gamma t
ROS	reactive oxygen species
S1P	sphingosine-1-phosphate
SphK	Sphingosine kinase
SM	sphingomyeline
SMase	sphingomyelinases
Sph	sphingosine
T-bet	T-box expressed in T cells
TCRβ	T cell receptor β
TD	T cell-dependent activation
Tg	transgenic
TGF-β	transforming growth factor
Th1	Th type 1
Th17	Th type 17
Th2	Th type 2
TI	T cell-independent activation
TLR	Toll-like receptor
TNF-α/β	tumor necrosis factors alpha/beta
Tregs	regulatory T cells
TSLP	thymic stromal lymphopoietin
WT	wildtype

List of figures

List of Tables

Abstract

Lysosomal enzyme acid sphingomyelinase (ASM) is known for regulating cellular ceramide, by converting sphingomyelin (SM) into ceramide. Mutations in *SMPD1*, the ASM encoding gene, cause Niemann-Pick disease with the symptoms of progressive hepatosplenomegaly, pulmonary defects, heart and brain disease. The alternation of Asm activity results in abnormal level of ceramide, and is involved in cancer, neurodegeneration, cardiovascular diseases, apoptosis, and cystic fibrosis. There are a few studies demonstrating the relation of Asm with immune cells, however, its role is yet to be confirmed.

The tAsm mouse model is a *Smpd1* (sphingomyelin phosphodiesterase 1) transgenic mouse line, in which Asm is overexpressed. Using this mouse model the direct relation in between Asm and immune system could be studied. Leucocytes are the major cell type in the immune system. These cells include lymphocytes, monocytes and neutrophils. They develop in the bone marrow and thymus and migrate to different lymphoid organs for their functions once mature. The present study focuses on the characterization of tAsm mice on T lymphocytes, B lymphocytes, and macrophages in the lymphoid organs spleen, lymph node and thymus.

The migration, innate and adaptive response were examined. Asm overexpression did not seem to have effect on T lymphocytes, B lymphocytes, and macrophages without immunization, because there was no obvious change in populations and localization. Interestingly, B cells and dendritic cells were seen closely related to ceramide-expressing cells. The current study confirmed that the tAsm mouse model provide a useful platform for immunological researches, since it showed baseline close to the wildtype (WT) healthy mice. Our findings also revealed the potential roles of B cells and dendritic cells in Asm overexpression.

Zusammenfassung

Das lysosomale Enzym saure Sphingomyelinase (Asm) reguliert zelluläre Ceramidspiegel, in dem es Sphingomyelin zu Ceramid hydrolysiert. Mutationen im *Smpd1*-Gen, welches die Asm kodiert, führen zur Niemann-Pick-Typ A bzw. B Erkrankung, deren Symptome neben einer progressiven Hepatosplenomegalie Beeinträchtigungen von Lungen-, Herz- und Hirnfunktionen umfassen. Änderungen der Asm-Aktivität und damit einhergehende veränderte Ceramidlevel, spielen bei diversen Krankheitsbildern eine Rolle. Diese umfassen unter anderem die Mukoviszidose, neurodegenerative Syndrome sowie Tumor- und Herz-Kreislauf-Erkrankungen. Es gibt Studien, die darauf hinweisen, dass die Asm auch in Immunzellen von Bedeutung ist, die konkreten Implikationen müssen jedoch noch aufgezeigt werden.

Als Mausmodell für die Asm-Überexpression dient ein für *Smpd1* transgener Mausstamm (tAsm). Anhand dieses Modells wurde die Bedeutung der Asm für das Immunsystem untersucht. Die zellulären Bestandteile des Immunsystems werden als Leukozyten, weiße Blutzellen, bezeichnet. Zu diesen zählen unter anderem Lymphozyten, Monozyten und Neutrophile. Ihre Entwicklung findet im Knochenmark und dem Thymus statt. Nach ihrer Reifung wandern sie in die verschiedenen lymphatischen Organe aus, um ihre jeweiligen Funktionen zu erfüllen. Die vorliegende Arbeit beschäftigt sich mit der Charakterisierung der lymphatischen Organe des tAsm Mausmodells, mit Fokus auf Makrophagen, T- und B-Zellen in der Milz, den Lymphknoten und dem Thymus. Hierfür wurden die Migration, sowie angeborene wie adaptive Immunantworten untersucht. Allein die Überexpression der Asm hat keinen Effekt auf die untersuchten Zelltypen, wenn man Änderungen der Populationsgröße oder die Lokalisierung der Immunzellen betrachtet. Interessanterweise wurden B-Zellen und dendritische Zellen in räumlicher Nähe zu ceramidreichen Zellen beobachtet.

Mit dieser Arbeit konnte bestätigt werden, dass das tAsm Mausmodell ein geeignetes Mittel zur Untersuchung des Immunsystems ist. Die transgenen Mäuse sind im Grundzustand gesunden Wildtyp-Mäusen sehr ähnlich und zeigen keine inhärenten Aberrationen von Immunzellen. Außerdem konnte gezeigt werden, dass B-Zellen und dendritische Zellen interessante Ziele für weiterführenden Studien sein können.

Table of Contents

Chapter 1 Introduction

Chapter 1.1 Sphingolipids

Sphingolipids are the second largest class of membrane lipids (Hawthorne, 1975), which are now also recognized as important bioactive lipids. They are composed of one polar head and two non polar tails (Coant, 2017). The backbone of sphingolipid is a sphingoid long chain base, with a fatty acid attached by an amide bond. The polar head ranges from a simple hydrogen (for example ceramide) to a number of complex species (phosphocholine for sphingomyelin and sugar residues for glycosphingolipid), and is attached at the primary hydroxyl (Merrill, 2008) (Fig. 1).

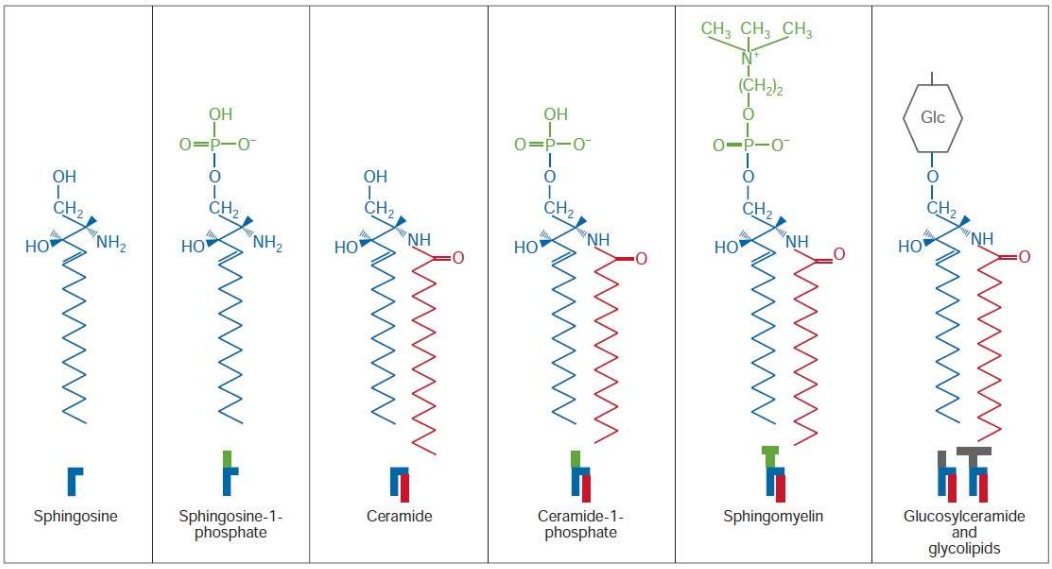

Figure 1. Chemical structure of sphingolipid. Adapted from Futerman, 2004

They are amphipathic molecules that have both hydrophobic and hydrophilic properties.

Sphingolipids metabolism is a complex system, with more than 40 enzymes involved. It stands to reason that they are named after the Greek mythical creature, the Sphinx, for being enigmatic in nature. They are primarily located in the plasma membrane, but are also found in intracellular membranes (van Meer, 2010). Their roles in the plasma membrane as the modulators of cell-cell interaction and also cell recognition have long been studied (Hannun, 2018). By regulating sphingolipid metabolism, cellular events including proliferation, differentiation, cell death, migration,

cell cycle arrest, senescence, cell adhesion, angiogenesis and inflammation are controlled. Ceramide, sphingosine (Sph) and sphingosine-1-phosphate (S1P) are popular amongst sphingolipid researchers (Hannun, 2018).

Chapter 1.1.1 sphingolipidoses

Sphingolipidoses are genetic disorders in genes encoding for enzymes metabolizing sphingolipids, result in the accumulation of substrate and ultimately the imbalance of substrates and products (Raas-Rothschild, 2004). They are also known as lysosomal storage disorders, since many of the enzymes in the sphingosine metabolism are stored in lysosomal (Hannun, 2018).

The majority of sphingolipidoses are autosomal recessive, apart from Fabry disease which is X-linked inherited (Desnick, 2001). The common sphingolipidoses are listed in Table 1.1.

Table 1.1. Sphingolipidoses. Adapted from Eckhardt, 2001.

Sphingolipidoses		
Disease	Deficient protein	Accumulating sphingolipids
Fabry	α-Galactosidase A	Digalactosylceramide, globotriaosylceramide (Gb3), Lyso-Gb3
Farber (lipogranulomatosis)	Ceramidase	Ceramide
Gaucher	β-Glucosidase	Glucosylceramide, glucosylsphingosine, GM1, GM2, GM3, GD3
Krabbe (globoid cell leukodystrophy)	Galactocerebrosidase	Galactosylceramide, psychosine
Metachromatic leukodystrophy (MLD)	Arylsulfatase A	Sulfatide, lysosulfatide, sulfolactosylceramide, GM2, GD3
Niemann–Pick Type A, B	Sphingomyelinase	Sphingomyelin, glucosylceramide, lactosylceramide, GM2, GM3
GM1-gangliosidosis	β-Galactosidase	GM1, lyso-GM1, GA1, GM2, GM3, GD1a, glucosylceramide, lactosylceramide
Tay–Sachs (GM2-gangliosidosis)	β-Hexosaminidase A	GM2, lyso-GM2
Sandhoff (GM2-gangliosidosis)	β-Hexosaminidase A and B	GM2, lyso-GM2, GA2, globoside
SapA deficiency	Saposin A	Galactosylceramide, psychosine
SapB deficiency (MLD variant)	Saposin B	Sulfatide, lactosylceramide, globotriaosylceramide
SapC deficiency (Gaucher like)	Saposin C	Glucosylceramide, glucosylsphingosine, lactosylceramide, lactosylsphingosine
GM2-gangliosidosis, AB variant	GM2 activator protein	GM2, GA2
Prosaposin deficiency	Saposin A, B, C, D	Glucosylceramide, lactosylceramide, galactosylceramide, sulfatide, globotriaosylceramide, GM1, GM2, GM3

The ASM related sphingolipidosis is known as Niemann-Pick disease. The deficiency of ASM is caused by mutation in *SMPD1* gene, which encodes for ASM (Brady, 1966).

Type A is characterized by neurodegeneration, early lethality, hepatosplenomegaly and psychomotor deterioration. Type B does not have early onset and do not affect

the neurological system as much. The symptoms include hepatosplenomegaly and pulmonary defects and cardiovascular diseases (Schuchman 2010).

Chapter 1.1.2 biosynthesis pathway

All key enzymes in the metabolism have been recognized. However, the metabolic pathways and subcellular compartmentalization have not been fully understood. Nonetheless, most of the scientists have agreed on three principle pathways, namely the de novo pathway, the salvage pathway and a direct hydrolytic pathway.

De novo pathway starts in cytosolic leaflet of smooth endoplasmic reticulum (ER). Palmitoyl-CoA together with serine are condensed to 3-ketodihydrosphingosine by palmitoyltransferase. 3-ketoreductase then converts the 3-ketodihydrosphingosine to dihydrosphingosine in a NADPH dependent manner. The product is N-acylated by dihydroceramide synthases (CerS) to produce dihydroceramide, and to ceramide by insertion of a double bond into the sphingoid base backbone with dihydroceramide desaturases (Coant 2017, Hannun, 2018, Michell, 1997). There are six identified CerS up to date and each has a preference of acyl Co-A to generate different species of ceramide (Merrill, 2008). Ceramide generated is trafficked to Golgi body, through ceramide transfer protein (CERT) or vesicles (Hanada, 2003).

Ceramide in the Golgi body is the centre of sphingolipid synthesis. Ceramide is then incorporated into various complex sphingolipids through modifications at the 1-hydroxyl position to generate ceramide-1-phosphate (C1P), sphingomyelin or glycoceramide, which in turn serves as the precursors for the various glycosphingolipids (Hannun, 2018).

The salvage pathway uses complex sphingolipids for example, SM and glycosphingolipids as substrates. Their sugar residues are degraded in lysosomes by lysosomal hydrolases, including sphingomyelinases (SMases), possibly glucocerebrosidase (acid-β-glucosidase), ceramidases, and (dihydro)ceramide synthases. Salvage pathway is therefore known as lysosomal degradation. In the degradation, glycosphingolipids are degraded into glucosylceramide and galactosylceramide and ultimately into ceramide and sphingosine (Sph). The sphingosine generated can move freely across lysosomal membrane to be reused, by ceramide synthase to ceramide (Kitatani, 2008).

The sphingomyelin hydrolysis is facilitated by sphingomyelinase, to generate ceramide and phosphocholine. Ceramide is converted by ceramidases to sphingo-

sine, which is further converted to sphingosine-1-phosphate (S1P) by sphingosine kinase. Ceramide generated in this process could be hydrolyzed either to sphingosine (Sph) and fatty acid by ceramidase, or phosphorylated to ceramide-1-phosphate through ceramide kinase. These reactions are reversible. Sphingolipids leave the metabolism by the action of S1P lyase. This action cleaves S1P to fatty aldehyde and ethanolamine phosphate. The fatty aldehyde then forms palmitoyl-CoA and exits the metabolism (Hannun, 2018)

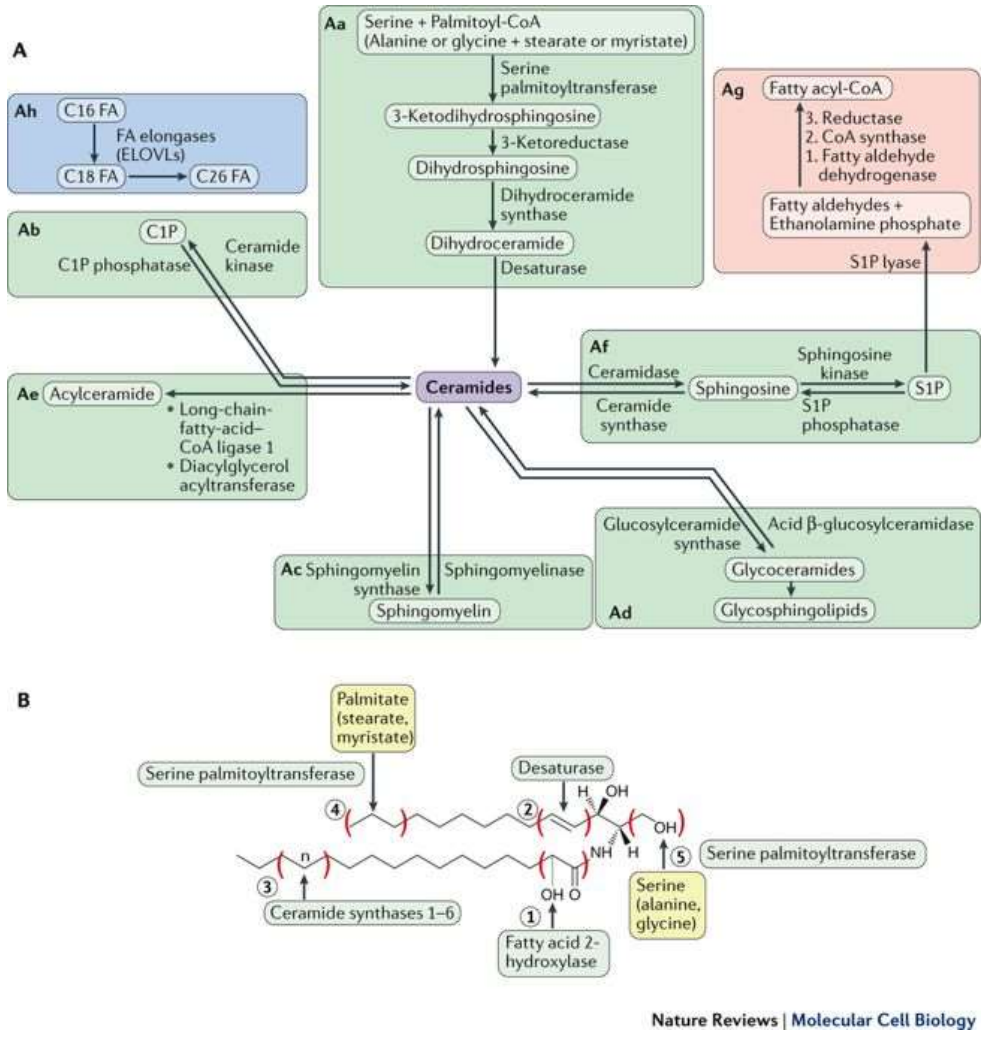

Figure 2. Sphingolipid biosynthesis. Adapted from Hannun, 2018.

Chapter 1.2 Acid sphingomyelinase

Sphingomyelinases are classified by the optimal pH they work in. As described by their name, neutral sphingomyelinase and alkaline sphingomyelinase work in neutral and basic pH respectively (Marchesini, 2004). Acid sphingomyelinase consists of lysosomal Asm (L-Asm) and secretory Asm, both work best at acidic pH. All of them function to hydrolyze sphingomyelin into ceramide and phosphocholine (Schuchman 2010).

Asm responds to cellular stress by generating ceramide and changing the plasma membrane dynamics. The alternation of Asm activities, through increasing or decreasing, causes pathological consequences.

SMPD1 is found on chromosome 11. It encodes for a polypeptide of 629 amino acids (Schuchman, 1992). After translation the precursor protein in the Golgi body undergoes glycosylation and forms two types of ASM, the lysosomal form with a molecular weight of 75 kDa and the secretory form with 57 kDa (Ferlinz, 1994). Asm is a zinc metalloprotein. While the zinc molecule is already bound with lysosomal Asm, the secretory form requires exogenous zinc for its full activity (Beckmann, 2014).

Upon activation by various stimuli, the Asm translocates to the extracellular leaflet of the plasma membrane by fusion of lysosomes with the plasma membrane. Ceramide released by the Asm forms ceramide-enriched membrane platforms subsequently: The enzyme is in close proximity to the sphingomyelin on the plasma membrane and therefore converts the sphingomyelins to ceramides. These ceramides start associating with each other to form microdomains and eventually fuse to form a ceramide-enriched platform (Beckmann 2014).

Chapter 1.2.1 Increased activity of Acid Sphingomyelinase

The stimuli for Asm activations are summarized in Table 1.2 (Beckmann, 2014). Asm can be activated by various mechanisms, for example phosphorylation, or with modification of C-terminal cysteine. With the phosphorylation, protein kinase C delta (PKCδ) phosphorylates the Asm at Ser508, causing translocation of Asm to the plasma membrane (Zeidan and Hannun, 2007) and cleavage by caspase-7 (Edelmann, 2011). After the modification of cysteine 629, the enzyme activity is increased by higher coordination with active site of zinc (Qiu, 2003).

Deficiency of ASM has been shown to be involved in many neurological diseases. It is no surprise that the activation of ASM is found to affect the neurological dynamic and is associated with neuropsychiatric disorders, such as Alzheimer's dementia (He, 2008) or status epilepticus (Mikati, 2008). An example of lung defect with elevated Asm level is lung edema occurring during acute lung injuries (Goggel, 2004).

Apart from disease, higher levels of Asm activity are found in many dysfunctions of cellular events. An increase in Asm activity leads to the increase in ceramide levels. It has been found that ceramide is the cause of apoptosis (Lang, 2007).

Table 1.2. List of stimulus inducing Asm activation and/or ceramide-enriched membrane platforms formation (Adapted from Beckmann, 2014).

Stimulus	References
PATHOGENS	
Listeria monocytogenes	Utermöhlen et al., 2003
Measles virus	Gassert et al., 2009; Avota et al., 2011
Mycobacterium avium	Utermöhlen et al., 2008
Neisseria gonorrhoeae	Grassmé et al., 1997; Hauck et al., 2000
Pseudomonas aeruginosa	Grassmé et al., 2003a; Zhang et al., 2008
Rhinoviruses	Grassmé et al., 2005; Dreschers et al., 2007; Miller et al., 2012
Salmonella typhimurium	McCollister et al., 2007
Sindbis virus	Jan et al., 2000
Staphylococcus aureus	Esen et al., 2001
CLUSTER OF DIFFERENTIATION MOLECULES	
CD5	Simarro et al., 1999
CD14	Pfeiffer et al., 2001
CD20	Bezombes et al., 2004
CD28	Boucher et al., 1995
CD32 (FCγRII)	Abdel Shakor et al., 2004; Korzeniowski et al., 2007
CD38	Jia et al., 2008
CD40	Grassmé et al., 2002
CD95	Cifone et al., 1994; Gulbins et al., 1995; Cremesti et al., 2001; Perrotta et al., 2010
CD95-DISC	Kirschnek et al., 2000; Grassmé et al., 2001a,b, 2003b
CD253 (TRAIL)	Dumitru and Gulbins, 2006; Dumitru et al., 2007; Li et al., 2013
IL-1 receptor	Mathias et al., 1993

Stimulus	References
SOLUBLE MOLECULES	
Platelet activating factor	Samapati et al., 2012; Predescu et al., 2013
Tumor necrosis factor	Schütze et al., 1992, 1994; Garcia-Ruiz et al., 2003; Edelmann et al., 2011; Ardestani et al., 2013
Visfatin	Boini et al., 2010a
DRUGS AND OTHER STRESSES	
Cisplatin	Lacour et al., 2004; Zeidan et al., 2008
Cu^{2+}-treatment	Lang et al., 2007
Doxorubicin	Dumitru et al., 2007
Heat damage	Chung et al., 2003
Ischemia-reperfusion injury	Yu et al., 2000
Oxidative stress	Zhang et al., 2007; Li et al., 2012
Oxygen radicals	Scheel-Toellner et al., 2004
UV-light	Zhang et al., 2001; Charruyer et al., 2005; Kashkar et al., 2005; Rotolo et al., 2005
γ-irradiation	Santana et al., 1996; Paris et al., 2001; Lee et al., 2011

Chapter 1.2.2 Decreased activity of Acid Sphingomyelinase

Researchers used Asm deficient mice or functional inhibitors of acid sphingomyelinase (FIASMA) to mimic the effects of decreased Asm activity. FIASMA do not inhibit Asm directly, but rather, change the attachment to the lysosomal membrane to cause the degradation of the detached ASM (Beckmann, 2014). The deficiency or functional inhibition of Asm neutralizes the ceramide and eases the ceramide-mediated apoptosis (Gulbins, 2006). It has been found in some studies, that the decrease in Asm activity provides protections for example, autoimmune hepatitis (Kirschnek, 2000), ischemia (Yu,2000), radiation (Paris, 2001) and chemotherapy (Dimanche-Boitrel, 2005).

Chapter 1.3 Sphingomyelin

Sphingomyelin (SM) is the substrate for generating ceramide through Asm. As a component of cell membrane, it has a hydrophobic ceramide tail, and a phosphoryl-

choline headgroup. The fatty acid chain of SM ranges from 16 to 26 carbons (Gulbins, 2006). Nieman-Pick disease is a result of the accumulation of sphingomyelin (Eckhardt, 2010).

Chapter 1.4 Ceramide

Ceramide is an amphipathic sphingolipid which has a sphingoid base linked to a fatty acid with amide bond, and a hydrogen head. This structure is essential for a membranes lipid. Ceramide has restricted intrabilayer movement (Bai and Pagano 1997). It is not defined as a particular molecule but by family of more than 200 ceramide species, with various lengths, saturation, hydroxylation of fatty acid and sphingoid base (Hannun, 2011).

The fatty acid chain length of ceramide can vary from 2 to 28 carbons, but C16 to C24 ceramide is the most abundant in mammalian cells (in Merrill, 2007). The nomenclature of ceramide indicates the length of the sphingoid base and the fatty acid saturation (Hannun, 2017).

Asm upon stimulation translocates to the outer leaflet of the plasma membrane from the lysosome. It converts the SMs on the plasma membrane to ceramides by hydrolysis. These ceramides associate with each other to form lipid rafts and eventually a membrane platform (Beckmann 2014) (Fig. 3). The lipid platform is held by hydrophobic van der Waals forces in between saturated acyl chains (Artetxe, 2013). This has been observed under the microscope in both *in vivo* (Grassmé, 2001) and *in vitro* studies (Holopainen, 1998).

The platform interacts with various molecules such as receptors and proteins, for example CD95 (Grassmé, 2001) and CD40 (Grassmé, 2002), on the plasma membrane selectively. And by this mean, they amplify the signaling transduction. This is how ceramide can control cellular events, such as apoptosis, autophagy, inflammation and senescence (Beckmann, 2014).

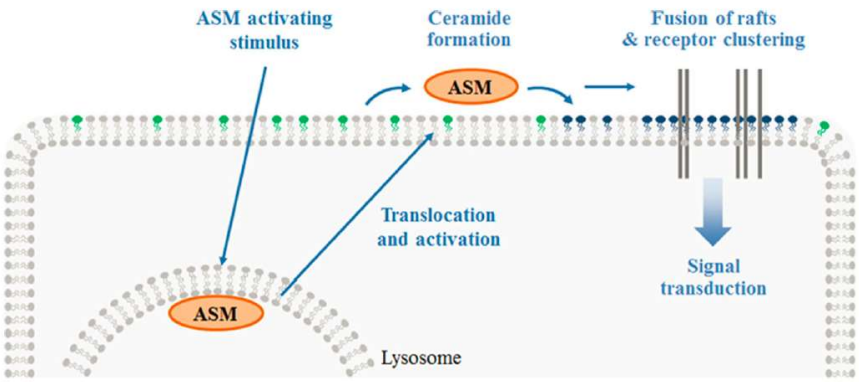

Figure 3. Asm translocation to the plasma membrane. Adapted from Beckmann, 2014.

Ceramide has been shown to inhibit proliferation and promote apoptosis (Marchesini and Hannun 2004). It has also been shown to be involved in lung edema in response to platelet activating factor, LPS or acid instillation (Goggel, 2004). In the immune system, ceramide was reported to activate PI3K and Akt phosphorylation (Monick, 2001), and take part in the formation of TLR4 raft complex in macrophages in response to LPS (Cuschieri, 2007). C2-ceramide has been reported to increase superoxide production in N-formylmethionylleucyl phenylalanine (fMLP)-primed neutrophils (Richard, 1996). Ceramide has been reported to be related to cystic fibrosis. It has been shown that the ceramide levels were increased in cystic fibrosis CFTR deficient mice (Teichgräber, 2008).

Chapter 1.5 acid ceramidase

Acid ceramidase (Ac) is the enzyme for the conversion of ceramide to sphingosine and free fatty acid. It is the downstream component of the sphingomyelinase reaction and is critical for maintaining the sphingolipid rheostat between ceramide and S1P. The hydrolysis reactions occur at pH 4.5, as suggested by the enzyme's name. One distinctive feature of Ac is that the catalytic reaction is reversed when the enzyme is at pH 6.0 (Okino, 2003). The enzyme is crucial because apart from the conversions to Sph, it regulates the downstream level of S1P and upstream level of SM (in Mao and Obeid, 2008).

Farber disease (FD) is the genetic disorder from the mutation of the ASAH1 gene, which encodes for AC. The resulting deficiency in AC causes accumulations of ceramide in the lysosome. The typical symptoms include deformation of joint,

hoarseness, subcutaneous nodules and childhood lethality

There are also problems in the immune system. Dysfunction of leukocyte leads to inflammation in airways and joints in patients, as well as granuloma formation (Ehlert, 2007). Macrophages infiltrate into joints, skin, lung, spleen, lymph node, thymus and liver (Antonarakis, 1984). It was proposed that the infiltration was caused by high level of cytokines, monocyte chemoattractant protein (MCP-1), keratinocyte chemoattractant (KC), macrophage inflammatory protein-1α (MIP-1α), and the inflammatory cytokine interferon gamma-induced protein-10 (IP-10) in plasma (Dworski, 2017).

Chapter 1.6 Immune cells

Chapter 1.6.1 T cell development in the thymus

Thymus is the site for T cell development. It consists of the subcapsular region, the cortex, the corticomedullary junction and the medulla. The lymphoid progenitors that originated from bone marrow travel through blood and enter thymus for maturation processes. They first enter the corticomedullary junction, then accumulate in the cortex, move to the medulla and exit as naïve T cells. In the cortex, they first undergo 4 double negative ($CD4^-CD8^-$) stages, which are marked by, $CD44^+CD25^-$ (DN1), $CD44^+CD25^+$ (DN2), $CD44^{-/lo}CD25^+$ (DN3), and $CD44^{-/lo}CD25^-$ (DN4). At DN3 and DN4, the β, γ and δ loci are rearranged, which leads to T cell receptor β (TCRβ) rearrangement and pre-TCRα chains expression. The thymocytes now express a random and antigen-specific TCRαβ receptor from the rearrangement and become double positive cells (DP, $CD4^+CD8^+$). The TCRs on these cells are tested for their ability to recognize MHC-peptide complex. The DP thymocytes, which have a high affinity for MHC-peptide complex pass through positive selection and proliferate, whereas the auto-reactive thymocytes are eliminated. The proliferating cells eventually would become either $CD4^+$ or $CD8^+$ single positive cells in the medulla.

T cells in spleen or lymph node (LN) are mostly single positive cells. The $CD4^+$ cells are called helper T cells and the $CD8^+$ cells are known as the cytotoxic T cells. The helper T cells produce cytokines, and are divided into subsets including Th1, Th2, Th17 and regulatory T cells (Tregs) (Shah, Zúñiga-Pflücker, 2014; Murphy, 2011).

Chapter 1.6.2 T cell activation

These cells entering secondary lymphoid organs such as spleen and LN are known

as naïve T cells. They encounter foreign antigen there and differentiate into effector T cells. Once they have carried out their functions, they would undergo apoptosis to maintain the immune homeostasis. Unlike effector T cells, memory T cells are long-lasting (Shah, Zúñiga-Pflücker, 2014; Murphy, 2011).

The classification of T cells agreed by most of the research is into two subtypes, helper T cells ($CD4^+$) and cytotoxic T cell ($CD8^+$). Cytotoxic T cells recognize MHC I – antigen complex, then lyse the infected cell or induce apoptosis (Soloski, 2000). Helper T cells recognize MHC II-antigen complex (Plate, 1988), and function according to their own subtypes.

Helper T cells are made up of several lineages, Th type 1 (Th1), Th type 2 (Th2), Th type 17 (Th17) and regulatory T cells (Tregs). Th1 cells work against intracellular pathogens in response to IL-12 and interferon gamma (IFN-γ). Th1 cells secrete pro-inflammatory cytokines, such as IFN-γ, interleukin (IL) -2, IL-10 and tumor necrosis factors alpha/beta (TNF-α/β), which mediate activation and phagocytosis of macrophages (Mukhopadhyay, 2006). This function is helped by transcription factors T-box expressed in T cells (T-bet), which suppressed differentiation of other lineages, and control the cytokine (Albert, 2002; Murphy, 2011).

Th2 cells function in response to IL-4, as well as TSLP and secrete IL-4, IL-5, IL-9, and IL-13. These cytokines mediate the activations of eosinophils and basophils. They also activate B cell by CD40:CD40 ligands and induce class switching (Jakobi and Petry, 2008). Their target is extracellular pathogens. Their transcription factor GATA-3 has similar functions like T-bet.

Th17 cells regulate chronic inflammation against specific fungi and extracellular bacteria, as well as autoimmune diseases. Their transcription factor RAR-related orphan receptor gamma t (ROR-γt) promotes Th17 differentiation and mediates the production of pro-inflammatory cytokines IL-17 and IL-22. These cytokines help the recruitment and activation of neutrophils (Albert, 2002; Murphy, 2011).

The last one is the Treg cells. Their functions are to maintain the balance between other T cells, and keep the self-tolerance by suppressing the functions of other T cells. Their transcription factor is foxhead box P3 (FOXP3), which promotes the secretion of immunosuppressive cytokines, IL-10 and transforming growth factor (TGF-β). These cytokines inhibit the pro-inflammatory effects by other cytokines, such as recruitment, proliferation, differentiation and activation of immune cells (Albert, 2002; Murphy, 2011).

Chapter 1.6.3 B cells development

B cells are responsible for humoral immune response because they produce antibodies against antigens.

B cells are originated in bone marrow from where they develop into immature B cells. The early development is antigen-independent and pre-pro-B cells, pro-B cells, and pre-B cells arise from the B cell progenitors. During the process of development, early pro-B cells undergo V(D)J recombination to assemble B cell receptor. The B cells then undergo a series of selections, including B cell receptor (BCR) editing and clonal deletion, which remove self-reactive B cells. Through this process the BCR on each B cell is highly specific and diversity of B cell repertoire is obtained. Transitional B cells leave bone marrow and home to spleen to develop into naïve mature B cells. Most of these cells develop into follicular B cells, while the rest develop into marginal zone B cells. Upon antigen-dependent activation, follicular B cells differentiate into memory B cells or plasma cells in germinal centre (Wardemann, 2003; Murphy, 2011).

Chapter 1.6.4 B cell activation

The first signal of B cell activation is the binding of antigen to BCR. There are two ways of B cell activations, T cell-dependent or T cell-independent.

In a T cell-dependent (TD) activation, an antigen binds to BCR and being internalized. The B cell then presents it on a MHC-II molecule, which attracts helper T cell. The helper T cell gives second signals and activates the B cell in return via CD40 ligand (CD40L) and cytokines such as IL-21, IL-4, and IL-10 (Cerutti, 2012). Follicular B cells are usually involved in TD activation. When activated, they either differentiate into plasma cells, or move into germinal centre (Cyster, 2000) (Fig.4).

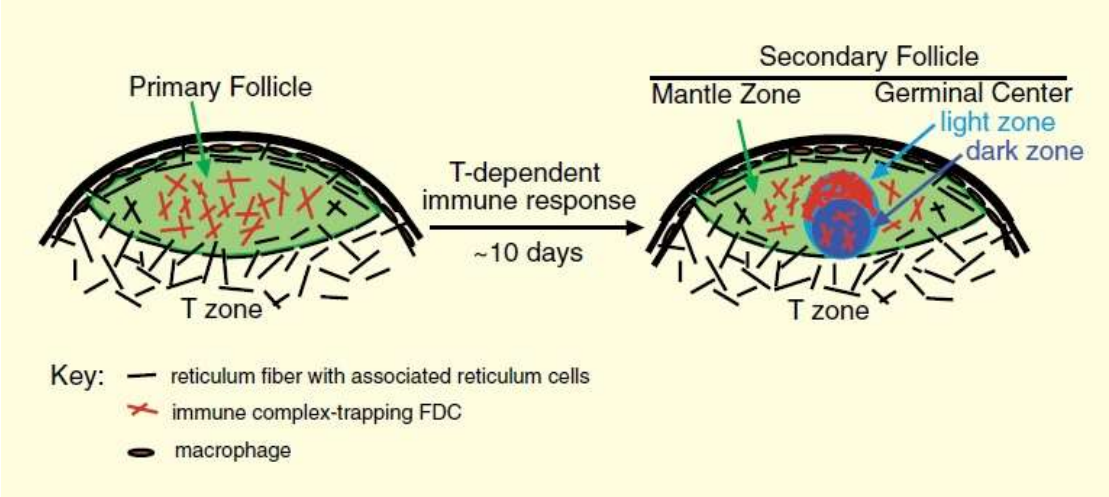

Figure. 4. Germinal centre formation in spleen. Adapted from Cyster, 2000.

As described by its name, T cell-independent activation (TI) does not depend on T cells.

The TI antigens include foreign polysaccharides, unmethylated CpG DNA and bacterial epitopes. They function with the help of a CD40L-like cytokines, B-cell-activating factor of the TNF family (BAFF) and a proliferation-inducing ligand (APRIL) (Cerutti, 2012). The second signal is Toll-like receptor (TLR) stimulation or BCR engagement of antigen or microbial particles for TI-I or TI-II accordingly. The marginal zone B cells and B1 cells differentiate into plasma cells and produce vast percentage of IgM and lower percentage of other isotypes (Cerutti, 2012).

Even undergoing TI activation, innate-like B cells, which are marginal zone B cells and B1 cells, were found to respond to TI antigens TI-1. B cells encounter TI antigen, such as microbial polysaccharides, glycolipids as well as self-antigens and differentiate into short-lived plasma cells (Cerutti, 2012).

Chapter 1.6.5 Macrophages

Innate immune cells, such as macrophages, dendritic cells (DCs) and NK cells work with pattern-recognition receptors, for example, toll-like receptors, when they detect pathogen-associated molecular pattern (PAMPs). These cells can eliminate the pathogens directly, or communicate with lymphocytes, for the cytokines signaling or other adaptive immune responses. Therefore, these cells are also known as antigen presenting cells. Macrophages are derived from circulating monocytes, but are mature when they are at the site for their functions (Murphy, 2011).

In LN and thymus, macrophages function to present antigen to lymphocytes. However, they have a variety of population in spleen to carry out different functions. Phagocytic macrophages in the marginal zone clear blood borne pathogens, while metallophilic macrophages play a role in viral infections (O'Riordain, 1999; Takahashi., 1994).

There are two ways of activating macrophages, classical for M1 macrophages and alternative activation for M2 macrophages.

M1 happens when the resting macrophages are primed cytokines. First, they are primed by IFN-γ produced by helper T cells, cytotoxic T cells and natural killer cells (Dalton, 1993). They then have to encounter the second signal, for example the cytokine TNF-α, or microbial products (Gordon 2003). Once activated, they secrete pro-inflammatory cytokines such as IL-1β, TNF, and IL-23. They also perform antimicrobial activities by phagocytosis of either foreign particles or apoptotic polymorphonuclear cells and by releasing reactive oxygen species (ROS). They also work as antigen presenting cells to helper T cells. They differentiate under IFN-γ, TNF, and microbial stimuli. The markers of classical activation are nitric oxide production for pathogen killing and release of cytokine TNF-α and IL-12 to increase Th1 differentiation and IFN-γ production (Murphy, 2011).

Alternative activation (M2) happens when macrophages are exposed to IL-4, IL-10 or IL-13 from Th2cells and Th1 cells. M2 functions to inhibit inflammation, and promote immune cell growth, angiogenesis and tissue repair when activated. It is also involved in reverse cholesterol transport, B cells class switching and antibody production. Macrophages can be found in both lymphoid organs and non-lymphoid organs, such as Kupffer cells in livers, alveolar macrophages in lung and microglia in nervous system (Gordon, 2003).

Asm has been found to be correlated to macrophages on apoptosis, survival, differentiation, cytokine secretion, phagocytosis, infection and inflammation.

A study by Wang and team (2007) has shown that the stimulation of TLR4 on macrophages inhibits the Asm activity and promotes the survival of macrophages. Another team (2004) has shown that by stimulating TLR4, the sphingosine kinase (SphK) is activated, and generates S1P, which is pro-inflammatory and pro-survival.

Our group has reported that with *Staphylococcus aureus* infection, CD44 was activated and produced ROS, which led to translocation of Asm and generation of ceramide. The CD44 then clustered in ceramide-enriched membrane platforms on plasma membrane and activated Rho-family GTPases. These macrophages showed

cytoskeleton rearrangement and phagosome-lysosome fusions (Li, 2017).
Another study from our group demonstrated the cytokines releases and inflammation in macrophages in response to Asm activation. *Ex vivo* macrophages were infected with *S. aureus*, and Asm was activated. The ceramide generated localized to the lysosome, and cathepsins were released into the cytosol. Inflammasomes were activated, resulting in IL-1β and TNF-α formation (Ma, 2017).
Macrophages are known to be involved in inflammation in cystic fibrosis. It has been demonstrated that in cystic fibrosis mice, CF mice have found to have ceramide accumulation, which triggers inflammatory responses including recruitment of neutrophils and macrophages (Döring, 2009).

Chapter 1.6.6 Dendritic cells

Dendritic cells are mononuclear phagocytes, which are responsible for phagocytosis and antigen presentation to naïve T cells. To perform antigen presentation, DCs take up antigen from an infected site and migrate to lymphoid organs spleen and LN. They travel through either high endothelial venules (HEV) or afferent lymphatic vessels. By presenting antigen, they activate naïve and memory $CD4^+$ cells, as well as stimulate cytotoxic T cells by MHC I. They also play a role in T cells in tolerance in self antigen (Cools, 2007). Apart from phagocytosis and antigen presentation, they also secrete cytokines to mediate immune responses (Reis e Sousa, 2006).
Dendritic cells are classified as conventional and non-conventional DCs. Conventional DCs are derived from dendritic cell precursor. They migrate from bone marrow to tissue and lymphoid organs as the immature form. Upon exposure to incoming antigen, they become mature, differentiate and up-regulate co-stimulatory molecules such as CD40, CD80 and CD86. They are characterized by their expression of CD11c (Liu, 2009). Non-conventional DCs can be monocyte-derived or plasmacytoid-derived. They circulate in blood and can be found in the bone marrow, spleen, thymus, lymph nodes, and the liver. They are CD11c negative but CD103 positive. They arise in response to inflammation.
Asm is involved in DC survival and apoptosis. It has been shown that bacteria *Escherichia. coli* can induce Asm-dependent apoptosis in immature DCs. Asm level in mature DC was found to be lower than those in immature DC, which suggests that the mature DCs are protected from Asm-induced apoptosis, and have the immune response prolonged (Falcone, 2004).

Asm is also found to regulate the ability of DCs in pathogen uptake. DC specific intercellular adhesion molecule-grabbing non-integrin (DC-SIGN) has been reported to activate Asm and neutral sphingomyelinase (nSM) when ligated. The subsequent formation of ceramide-enriched platform then promoted the transient recruitment of CD150 to the plasma membrane. CD150 then co-clustered with DC-SIGN in ceramide enriched-platform, where it functioned as measle virus uptake receptor and microbial sensor (Avota, 2011).

Exogenous molecules such as zinc or thymol, alter the Asm level. Thymol was found to activate and translocate Asm to the cell surface, leading to ceramide formation. Ceramide then downregulates Bcl-2 and Bcl-xL to trigger apoptosis (Xuan, 2010).

Chapter 1.6.7 Neutrophils

Neutrophils are derived from bone marrow and function as phagocytes during inflammation. Migration and activation are crucial for neutrophil to carry out its functions (Bunting, 2002; Cheretakis, 2006). A mature neutrophil forms its characteristic multi-lobed nucleus and is released into the bloodstream from bone marrow. When an infection occurs, activated neutrophils undergo cytoskeleton rearrangement and are drawn by chemoattractants to the injury sites (Chemotaxis), for phagocytosis and bacterial killing (Cicchetti, 2002; Fenteany and Glogauer, 2004;). Neutrophils recognize opsonins or sometimes non-opsonized ligands, for example lipopolysaccharides. The binding of ligands to the surface receptors of neutrophils initiates the phagocytosis. The neutrophils then undergo a series of events, including cytoskeleton remodeling, lipid metabolism, and engulfment of the pathogens (Niedergang, 2004). Phagosomes then mature to phagolysosome for bacterial killing, by producing degradative enzyme, bactericidal peptides and superoxides (Vieira, 2002). Neutrophils were shown to detect PAMPs by TLR2, TLR7 and TLR8 (Wang, 2008). They were found to perform microbicidal effects and prolong survival via NF-kB nuclear factor (Kobayashi, 2005).

It has been shown that ROS is produced and released upon pyocyanin stimulation in neutrophils (Managò, 2015). This results in Asm activation and ceramide is generated. The cytochrome C is released from mitochondria and causes cell death (Managò, 2015). This finding is similar to the research from Scheel-Toellner and colleagues (2004). They reported apoptosis in neutrophils, as a result of ROS activation of Asm, followed by ceramide platform formation and clustering of CD95.

One of the symptoms of cystic fibrosis is the inflammation in lung. Neutrophil accumulation was found in lung of CF mice, but Asm inhibition and heterozygosity of Asm mice normalized the situation (Teichgräber, 2008).

Chapter 1.7 Histology of lymphoid organs

Thymus is divided into many lobules, connected with connective tissue septae. Within each lobule there are subcapsular, cortical, corticomedullary and medullary regions. Epithelial reticular cells are the majority cell type in the subcapsular area, and they support the infrastructure of the whole thymus (Pearse 2006).

The main population found in cortex is the immature lymphocytes, with small population of epithelial cells, and transient bone-marrow derived macrophages. The lymphocytes are shorted-lived and phagocytosed by the macrophages after apoptosis. Corticomedullary junction is the transition from cortex to medulla and therefore having both immature and mature lymphocytes. There are plenty of blood vessels, and also some B cells, plasma cells and dendritic cells. Medulla is not as congested as cortex, with densely distributed mature T cells, epithelial cells, admixed macrophages, dendritic cells, B cells and Hassall's corpuscles. Hassall's corpuscles are a particular type of epithelial cells in medulla. Usually it is hard to visualize in rodent compare to human (Pearse 2006).

Spleen consists of white pulp and red pulp areas. Within the white pulp, there are B cell follicles surrounding the T cells zone in the centre. The outer layer of the B cell follicles is the marginal zone. It is the transition area where the cells from blood enter white pulp via red pulp (Steiniger, 2015). B cell follicles are the site where T cell-dependent immune responses occur. Marginal B cells (MZB) however, are involved in T cell-independent immune response. MZB are closer to marginal sinus to pick up antigens and present them to the follicular cells. Within the T cells zone there are central arteries and periarterial lymphatic sheaths (PALS). Extending from T cell zone directly into the red pulp is the bridging zone (Steiniger, 2015).

LN is comprised of cortex and medulla. In the cortex, there are B cell follicles, with some follicular DCs and T cells zone. Within the B cell follicle there is a germinal centre. It is the site for class switching and B cells differentiation into plasma cells. Lymphocytes and macrophages are found in the medulla. The lymph brings in activated lymphocytes through medullary sinuses (Murphy, 2011).

Chapter 1.8 Aims

There are two primary aims in this project.

My first aim is to characterize the phenotype of the tAsm mouse model in terms of immune system. The mouse model was generated by introducing *Smpd1* gene into the mouse genome. After some carefully controlled breedings, a mouse line with Asm overexpression was established and maintained stably. The mouse model has been used in depression studies (Gulbins,2013), cystic fibrosis studies (Grassmé, 2017) and alcoholism studies (Müller, 2017), but has not been described in studies of immune system. In this project, the phenotype was characterized when there was no immunization, so as to provide a baseline for further study.

The second aim is to establish a correlation of Asm overexpression with immune system. There were studies showing Asm affects the immune system, either by its activation or deficiency. However, there have only been few studies with Asm overexpression. Using this mouse model, the immune system *in vivo* with respect to Asm overexpression was studied. It provides information of immune cells as a whole, so that in the future particular cells could be work on in detail.

In the study, a validation on the increased Asm activity and the effects on the subsequent sphingolipid level were provided. The populations and the localization of T cells, B cells, macrophages, and dendritic cells, and neutrophils in lymphoid organs, thymus, lymph node and spleen were then examined. The activation of T cells by T cell activation markers was also assessed.

Chapter 2 Materials and Methods

Chapter 2.1 Materials

Chapter 2.1.1 Chemicals

Acetic acid (100 %)	Merck KGaA, Darmstadt, Germany
BODIPY-sphingomyelin	Thermo Fisher Scientific, Waltham, MA, USA
Bovine serum albumin (BSA), fatty acid free	Sigma-Aldrich Chemie GmbH, Steinheim, Germany
Bradford Protein assay	Biorad Laboratories GmbH, München, Germany
Chloroform	AppliChem GmbH, Darmstadt, Germany
Eosin	Carl-Roth GmbH & Co, Karlsruhe, Germany
Ethanol (absolute, anhydrous)	Diagonal GmbH & Co. KG, Münster, Germany
Ethyl acetate	Diagonal GmbH & Co. KG, Münster, Germany
FBS	GE Healthcare Europe GmbH, Freiburg, Germany
Hematoxylin	Carl-Roth GmbH & Co, Karlsruhe, Germany
Hydrochloric acid (fuming, 37 %)	Sigma-Aldrich Chemie GmbH, Steinheim, Germany
Methanol (≥ 99.8 %)	Diagonal GmbH & Co. KG, Münster, Germany
Mowiol-488	Hoechst GmbH, Frankfurt, Germany
NBD-ceramide	Thermo Fisher Scientific, Waltham, MA, USA
NP-40 (Igepal)	Sigma-Aldrich Chemie GmbH, Steinheim, Germany
Paraformaldehyde (powder, 95 %)	Sigma-Aldrich Chemie GmbH, Steinheim, Germany
Polyoxyethyle glycol sorbitan monolaurate (Tween20)	Sigma-Aldrich Chemie GmbH, Steinheim, Germany
Potassium chloride (≥ 99 %)	Carl-Roth GmbH & Co KG, Karlsruhe, Germany
Sodium chloride (≥ 99,5 %)	Carl-Roth GmbH & Co KG, Karlsruhe, Germany
Sodium citrate (tribasic, dehydrate)	Sigma-Aldrich Chemie GmbH, Steinheim, Germany
Tissue-Tek O.C.T Compound	Sakura Finetek Germany GmbH, Staufen, Germany
Trypan Blue solution	Sigma-Aldrich Chemie GmbH, Steinheim, Germany

Chapter 2.1.2 Buffers

Ac/Asm assay buffer	250 mM sodium acetate 0.1 % NP-40 pH 4.5 (Ac) or pH 5.0 (Asm)
Ac/Asm lysis buffer	250 mM sodium acetate 1 % NP-40 pH 4.5 (Ac) or pH 5.0 (Asm)
Ac substrate solution	1 µl NBD-Cer 27.2 mL Ac assay buffer
Asm substrate solution	0.5 µl BODIPY-Sphingomyelin 1 mL Asm assay buffer
Mowiol	20-25 % Mowiol-488 2.5 % Dabco
Paraformaldehyde (PFA), 4 %	4 % PFA 1 x PBS pH 7.2 – 7.4 adjusted with HCl and NaOH
Phosphate buffered saline (PBS)	137 mM NaCl 2.7 mM KCl 10 mM Na2HPO4 • 2 H20 2.0 mM KH2PO4 pH adjusted with HCl and NaOH
Phosphate buffered saline Tween (PBST)	1 x PBS 0.1% Tween 20

Chapter 2.1.3 Consumables

Cuvettes	Corning Inc., New York, NY, USA
Embedding cassettes	Greiner Bio-One GmbH, Frickenhausen, Germany
Microscopic slides	Carl-Roth GmbH & Co, Karlsruhe, Germany
Microtiter plates	Sarstedt AG & Co, Nümbrecht, Germany
Reaction tubes, 1.5 mL	Carl-Roth GmbH & Co, Karlsruhe, Germany
Reaction tubes, 2 mL	Langenbringen Labor- und Medizintechnik, Emmendingen, Germany
Stainless steel beads, 5 mm	Sarstedt AG & Co, Nümbrecht, Germany
Thin layer chromatography (TLC) Silica G60 plates	Sarstedt AG & Co, Nümbrecht, Germany

Chapter 2.1.4 Equipment

Attune NxT Flow Cytometer	Thermo Fisher Scientific, Waltham, MA, USA
Confocal fluorescence (TCS-SP5)	Leica Mikrosysteme Vertrieb GmbH, Wetzlar, Germany
Mass spectrometer (Q-TOF 6530)	Merck KGaA, Darmstadt, Germany
pH Meter (HI9025)	Binder GmbH, Tuttlingen, Germany
Rotary microtome (Microm HM 3555)	Intern. Laborat. App GmbH, Dottingen, Germany
Spectrophotometer	Agilent Technologies, Waldbronn, Germany
SpeedVac	Hanna instruments, Woonsocket, RI, USA
TissueLyser	Thermo Scientific, Waltham, MA, USA
Typhoon FLA 9500	Eppendorf AG, Hamburg, Germany
Ultrasonic bath (sonorex RK 102 H)	Thermo Fisher Scientific, Waltham, MA, USA
Vortexer (Reax 2000)	Qiagen GmbH, Hilden, Germany
Water bath (1o12)	GE Healthcare Europe GmbH, Freiburg, Germany

Chapter 2.1.5 Software

GraphPad Prism (5.01)	GraphPad Software, La Jolla, CA, USA
ImageQuant	GE Healthcare Europe GmbH, Freiburg, Germany
Leica advanced Fluorescence – Application Suite (2.61)	Leica Mikrosysteme Vertrieb GmbH, Wetzlar, Germany
MassHunter Software	Agilent Technologies, Waldbronn, Germany
Microsoft Office (2016)	Microsoft Corporation, Redmond, WA, USA

Chapter 2.1.6 Antibodies for flow cytometry

	Surface marker	Fluorophore	cat #	Supplier	Dilution
Immune cells	CD45	Brilliant violet 605	103155	Biolegend	1:40
Dead cell	Zombi Aqua	Violet 405nm	423101	Biolegend	1:200
T cell	CD3	Percp/5.5	100218	Biolegend	1:20
T helper	CD4	PE/Cy7	100422	Biolegend	1:80
T cytotoxic	CD8	PE	100708	Biolegend	1:80
Act. Marker	CD69	FITC	104516	Biolegend	1:200
Act. Marker	CD25	APC	17025181	Invitrogen	1:160
B cell	CD19	PE	12019381	Invitrogen	1:160
B cell	B220	Percp/5.5	103228	Biolegend	1:100
Neutrophil	Ly6G	AF647	127610	Biolegend	1:200
DC	CD11c	FITC	117306	Biolegend	1:200
Macrophage	F4/80	PE/Cy7	123114	Biolegend	1:80
monocyte	CD11b	PE	101208	Biolegend	1:80
Blocking	TruStain fcX	-	101319	Biolegend	1:100

Chapter 2.1.7 Antibodies for immunofluorescence (IF)

	Surface marker	Fluoro-phore	cat #	Supplier	Dilution
T cell	CD3	FITC	100306	Biolegend	1:100
T helper	CD4	FITC	11004182	Invitrogen	1:100
T cytotoxic	CD8	PE	100708	biolegend	1:100
T cytotoxic	CD8	APC	17008182	Invitrogen	1:100
Act. Marker	CD69	FITC	104516	Biolegend	1:100
Act. Marker	CD25	APC	17025181	Invitrogen	1:100
B cell	B220	eFluor 660	50045280	Invitrogen	1:100
Neutrophil	Ly6G	AF649	127610	Biolegend	1:200
DC	CD11c	FITC	117313	Biolegend	1:100
Macro-phage	F4/80	APC	123113	Biolegend	1:100
monocyte	CD11b	FITC	53011258	Invitrogen	1:100
Ceramide	ceramide	-	MAB-0011	Glycobi-otech	1:100
Cy3	Cy3	Cy3	715-166020	Jackson	1:200

Chapter 2.2 Methods

Chapter 2.2.1 Animal husbandry

All mice were bred and housed under pathogen-free conditions. They were kept on 12h/12h light dark cycle. The husbandry followed guidelines from the Federations of European Laboratory Animal Science Associations (FELASA). Genotyping were performed with PCR. The procedures in this study were approved by the State Agency for Nature, Environment and Consumer Protection (LANUV) NRW in Düsseldorf, Germany.

Chapter 2.2.2 Generation of the tAsm mouse model

The current mouse model was generated by GenOway (Lyon, France) by knocking in SMDP1 cDNA into the deleted HPRT locus on the x-chromosome. The vector was driven by ubiquitous CAG promoter (CMV immediate early enhancer / chicken ß-actin promoter fusion), with a *loxP* flanked stop cassette downstream, to ensure the expression is under the action of Cre-recombinase. It then was inserted into E14 ES cells by electroporation. After screening for the homologous recombination, the corresponding ES cell clones were injected into the blastocytes, which were then implanted into pregnant female mice. The male chimeras were bred with wildtype C57BL/6J female, and the breeding was continued for 10 generations. To express the transgene, the mice were crossed with E2a-Cre mice for the excision of the stop cassette. Genotyping was performed by PCR.

Chapter 2.2.3 Sphingolipids quantification

Sphingolipid levels were determined in University of Potsdam by rapid resolution liquid chromatography/mass spectrometry, with the help of Dr. Fabian Schumacher (University of Duisburg-Essen and University of Potsdam) (Huston, 2016). In brief, lipids extracted from tissues were analyzed by rapid-resolution liquid chromatography-MS/MS using a Q-TOF 6530 mass spectrometer operating in the positive ESI mode. C17-ceramide and C16-d31-sphingomyelin are used as internal standards. Ceramide precursor ions (C16-ceramide (*m/z* 520.508), C17-ceramide (*m/z* 534.524), C18-ceramide (*m/z* 548.540), C20-ceramide (*m/z* 576.571), C22-ceramide (*m/z* 604.602), C24-ceramide (*m/z* 632.634) and C24:1-ceramide (*m/z* 630.618)) were cleaved into the fragment ion m/z 264.270 while sphingomyelin precursor ions

(C16-sphingomyelin (*m/z* 703.575), C16-d31-sphingomyelin (*m/z* 734.762), C18-sphingomyelin (*m/z* 731.606), C20-sphingomyelin (*m/z* 759.638), C22-sphingomyelin (*m/z* 787.669), C24-sphingomyelin (*m/z* 815.700) and C24:1-sphingomyelin (*m/z* 813.684)) were cleaved into the fragment ion *m/z* 184.074. MassHunter Software was used for quantification and data analysis.

Chapter 2.2.4 Asm and Ac activity determination

The frozen tissues were incubated with NP40 lysis buffer (1% NP40, 250mM sodium acetate, pH 4.5) on ice for 2 minutes. The tissue was then homogenized by TissueLyser for 5 minutes at 50 Hz. Bradford assay was used to determine the protein concentration. Tissue corresponding to 0.5 µg (Asm) and 30 µg (Ac) of protein was used and the sample was made up to 20 µl. The NBD-ceramide or BODIPY-sphingomyelin substrate was added to substrate buffer (0.1% NP40, 25mM sodium acetate), and vortex for 30 seconds. Lysate and diluted substrate were sonicated for 10 minutes in separate tubes for the micelle formation. After sonication 100 pmol substrate was added to each substrate. The reaction mixture was incubated at 37°C for their corresponding time (Asm, 2 hours; Ac for spleen 4 hours, for LN and thymus, 5 hours). The reaction mixture 250 µl of chloroform/methanol (2:1) was added to reaction mixture, and vortexed for 20 seconds. It was then centrifuged at 14000 rpm for 5 minutes. 100 µl of the lower phase was transferred to new microcentrifuge tube. The solution was dried by speedvac for 40 minutes. The dried pellet was resuspended with 20 µl chloroform/methanol. 3 µl of the mixture was dipped onto thin layer chromatography (TLC) plate. The plate was inserted in the diffusion chamber with chloroform-methanol solvent (80:20) for diffusion. It is then scanned with Typhoon FLA 9500 fluorescent scanner.

Chapter 2.2.5 Flow cytometry

Thymus, spleen and lymph node were taken from the sacrificed mice. The tissues were slowly pressed through 70µM cell strainers to obtain single cell suspension in 5 ml of working buffer. The cell suspensions were washed by centrifuging at 400G for 5 minutes at 4°C. They were then counted under the microscope, with trypan blue staining the dead cell. 20 million cells were resuspended per 1 ml PBS and 1 million cells were added to each well in a round bottom 96 well-plate. Zombi Aqua (1:200) were added to each sample, for the detection of dead cell, for 20 minutes incubation

on ice. The samples were centrifuged, washed and resuspended in working buffer. FC block (1:100) was added to each sample for 5 minutes on ice. The cells were blocked by TruStain fcX anti-mouse CD16/32 (Biolegend, 1:100). The antibodies were added to the single stain control and the samples, and incubated for 30 minutes in dark (Table 2.16). 4% PFA were added to fix the cells in room temperature for 10 minutes. The cells suspensions were washed and resuspended for the analysis by Attune® NxT Acoustic Focusing Cytometer.

Chapter 2.2.6 Immunofluorescent imaging

Mice are sacrificed and thymus, spleen and LN were frozen in Tissue-Tek O.C.T Compound (Sakura). The frozen blocks were cut by cryotome to 6 μM sections. The sections were fixed by ice-cold acetone in fridge for 20 minutes, then washed with PBS. Blocking was done by 2% FBS for 20 minutes. Next, the sections were labeled with antibodies for 1 hour at room temperature. In case of anti-ceramide staining, the sections were incubated with secondary antibody for 30 minutes. They were mounted in DAPI mounting medium, and observed under Leica SP5 confocal microscope. Antibodies used are listed in Table 2.17.

Chapter 2.2.7 Statistics

Data is presented as arithmetic mean ± standard deviation. Analysis of variance (ANOVA) was then employed to assess significant differences between selected pairs.

Chapter 3 Results

3.1 Asm and Ac activity

Initially, the Asm activity of thymus, LN and spleen were analyzed. This is to confirm the overexpression in the mouse model, which is fundamental for this study (Fig. 5).

The analysis on thymus in this thesis is only on 4 months old mice, because of the thymic involution. Two ages, 4 and 6 months old mice were investigated. The tAsm mice were generated by knocking in the transgene to the *Hprt* locus in the x-chromosome. Therefore, male Tg (hemizygous) and female Tg (homozygous) mice were analyzed with their corresponding WT mice.

The specific activity in thymus of hemizygous male mice was on average 228 pmol/mg/min, which was more than 10 times than that of the male WT mice (19 pmol/mg/min). The difference in between female WT and Tg mice was not as great, which was around 2.6 folds (WT, 37 pmol/mg/min and Tg, 97 pmol/mg/min).

In LN, the specific Asm activity of 4 months old male WT mice was 21 pmol/mg/min, while that of the hemizygous mice was on average 241 pmol/mg/min. The rise was more than ten folds. The Asm activity of 4 month-old female WT mice was on average 14 pmol/mg/min, and that of the homozygous mice was 84 pmol/mg/min. The increase was around 6.5 fold. In the LN of 6 month-old mice, the Asm activities of Tg mice (male, 83 and female, 109 pmol/mg/min) were higher than those of WT mice (male, 38 and female, 19 pmol/mg/min), with 2.1 and 5 fold change respectively.

In the spleen of the 4 months old male WT mice Asm activity (19 pmol/mg/min) was shown to be similar with those in thymus and LN. The Asm activity in hemizygous mice was 208 pmol/mg/min. The fold change was more than ten times, and was consistent with that of thymus. In female, the fold change was around 6.5, with the mean 32 and 209 for WT and homozygous respectively. The Asm activities of male 6 months old WT and hemizygous were 46 and 124 pmol/mg/min respectively, having around a 3 fold rise. Female mice showed similar fold increase. The specific Asm activity was 19 pmol/mg/min in female WT mice, and 68 pmol/mg/min in homozygous mice

All of the mice demonstrated increases in Asm activity from WT to Tg, even though not all of them were statistically significant. Only three to five mice were used in the Asm activity quantification currently. Increasing n number might be able to improve the statistical verification of the Asm overexpression in the mouse model. Genotyping was performed to all the mice (data not shown) and the transgenic mice were proven to have the target gene expressed. With the consistent trend in all three organs, it is believed that the thymus, LN and spleen of all the Tg mice used in this study were overexpressing Asm and that they could be used for further investigations

4 months old hemizygous mice had the highest increase in Asm activity in all three organs, consistently over 10 folds from WT to Tg.

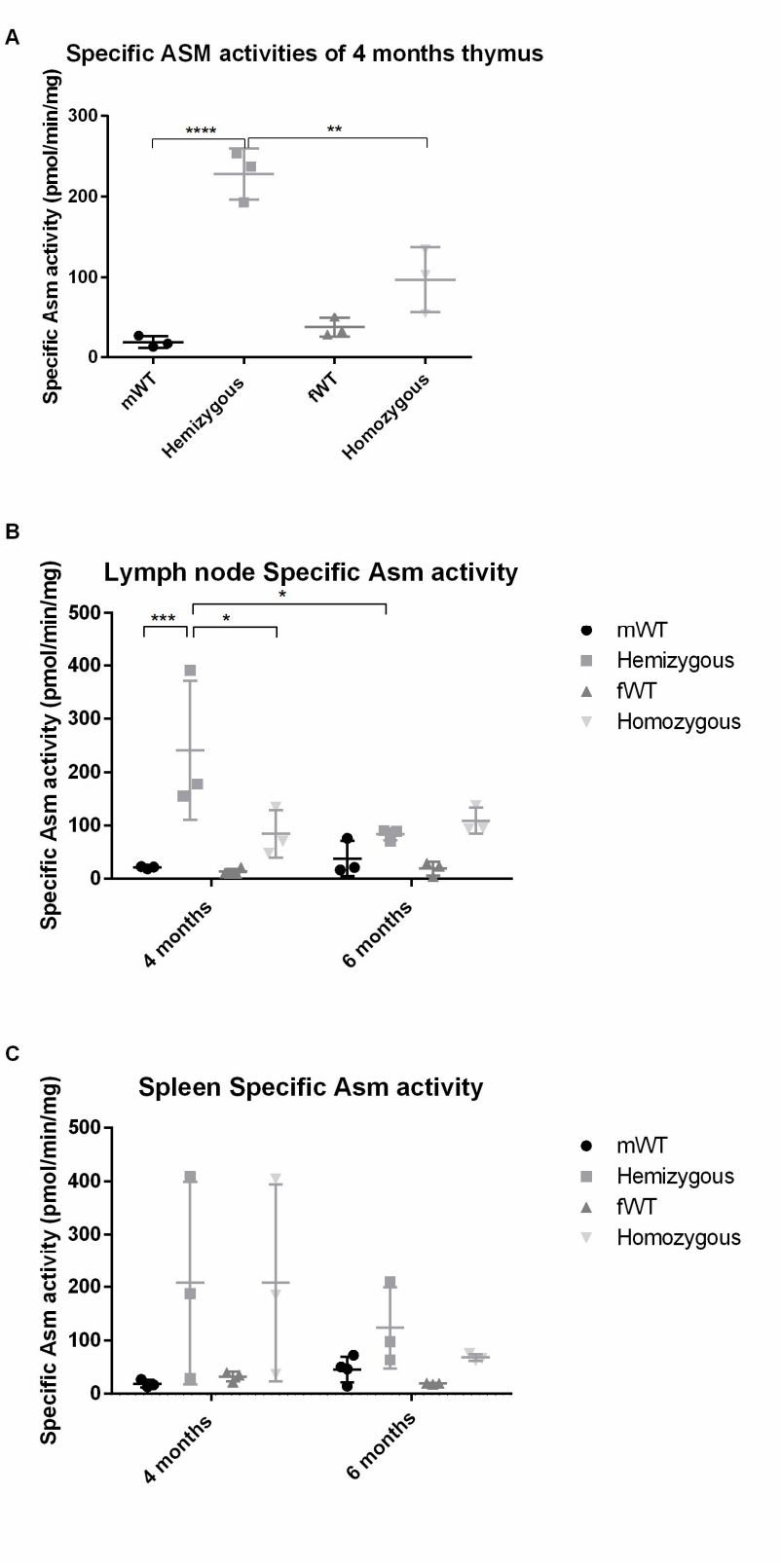

Figure 5. Acid sphingomyelinase activity of (A) Thymus (B) Lymph node (C) Spleen. Means ± SD from n = 3-5 mice are analysed. Asterisks indicate significant differences as assessed by two-way ANOVA (Spleen and lymph node) and one-way ANOVA (thymus): * $p < 0.05$, ** $p < 0.01$; *** $p < 0.001$, **** $p < 0.0001$. Abbreviation: mWT,male wildtype; fWT, female wild-type; Asm, acid sphingomyelinase.

Acid sphingomyelinase and acid ceramidase are the two key enzymes in maintaining the ceramide/S1P rheostat. Ac activities were examined to see if the rheostat has been altered by the Asm overexpression (Fig. 6)

In thymus, Ac activities from different genotypes ranged from 0.45 to 0.66 pmol/mg/min, whereas in LN, they ranged from 0.37 to 0.75 pmol/mg/min and in spleen, they ranged from 0.21 to 0.83 pmol/mg/min. The mean Ac activities amongst genotypes fluctuated, with no trend observed.

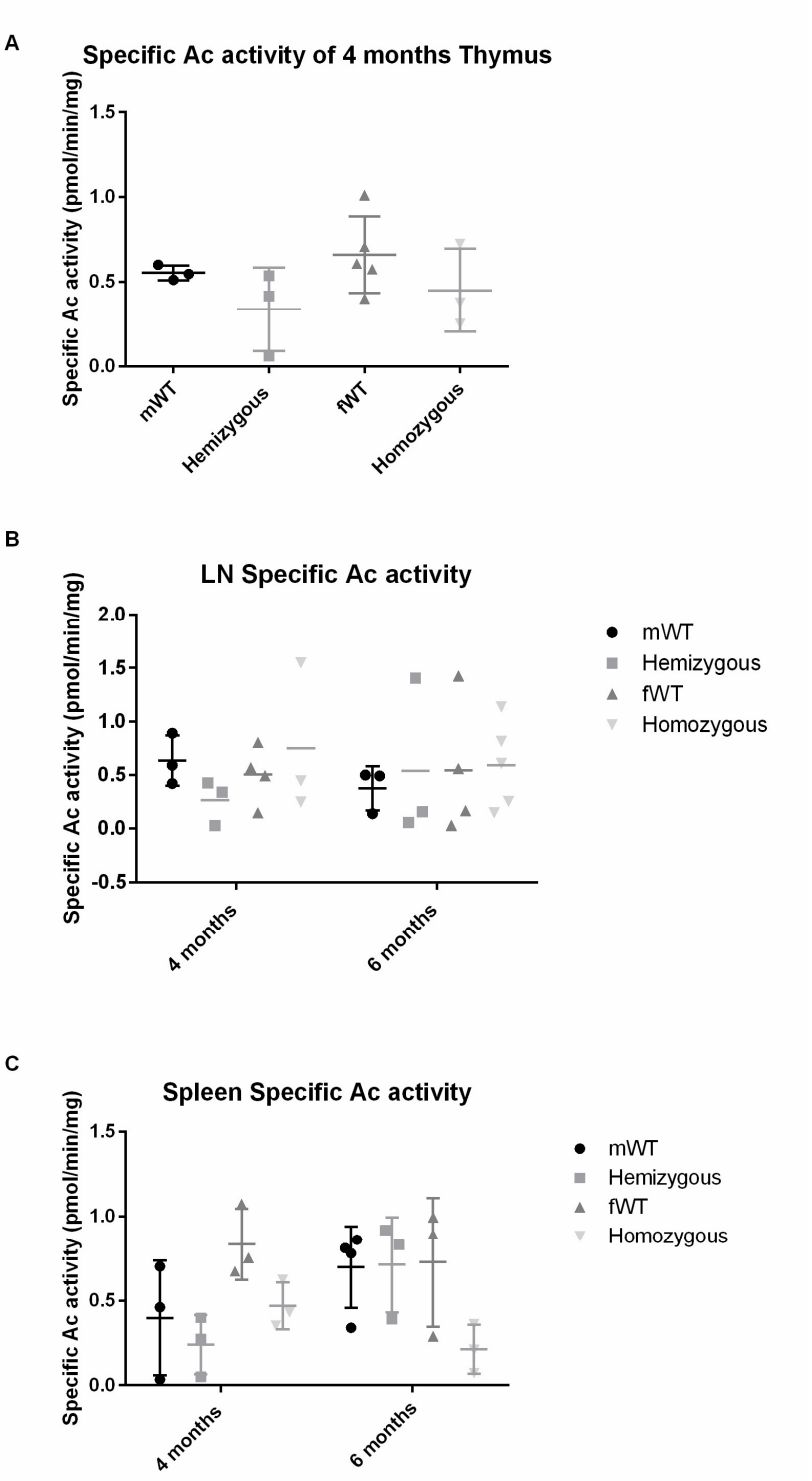

Figure 6. Acid ceramidase activity of (A) Thymus (B) Lymph node (C) Spleen. Means ± SD from n = 3-5 mice are analysed. Asterisks indicate significant differences as assessed by two-way ANOVA (spleen and lymph node), and one-way ANOVA (thymus). Abbreviation: mWT,male wildtype; fWT, female wildtype; Ac, acid ceramidase.

3.2 Sphingolipid level

SM, ceramide and Sph levels were checked to see whether the increase in Asm activities would affect the SM and the downstream sphingolipid level. For ceramide and SM, species ranged from C16-C24, C24:1 and total amount were examined (Fig. 7-11). Mass spectrometry was employed. The most abundant ceramide is C24:1 and that of SM is C16. In 6 months old mice, there was an increase of C24:1 from male WT to Tg in LN, whereas in spleen, the increase was in female mice. However, the C24:1 level was the other way round in thymus. A drop in 6 months old female from WT to Tg was observed.

Surprisingly, with a few exceptions, no significant changes of sphingomyelin and ceramide were detected.

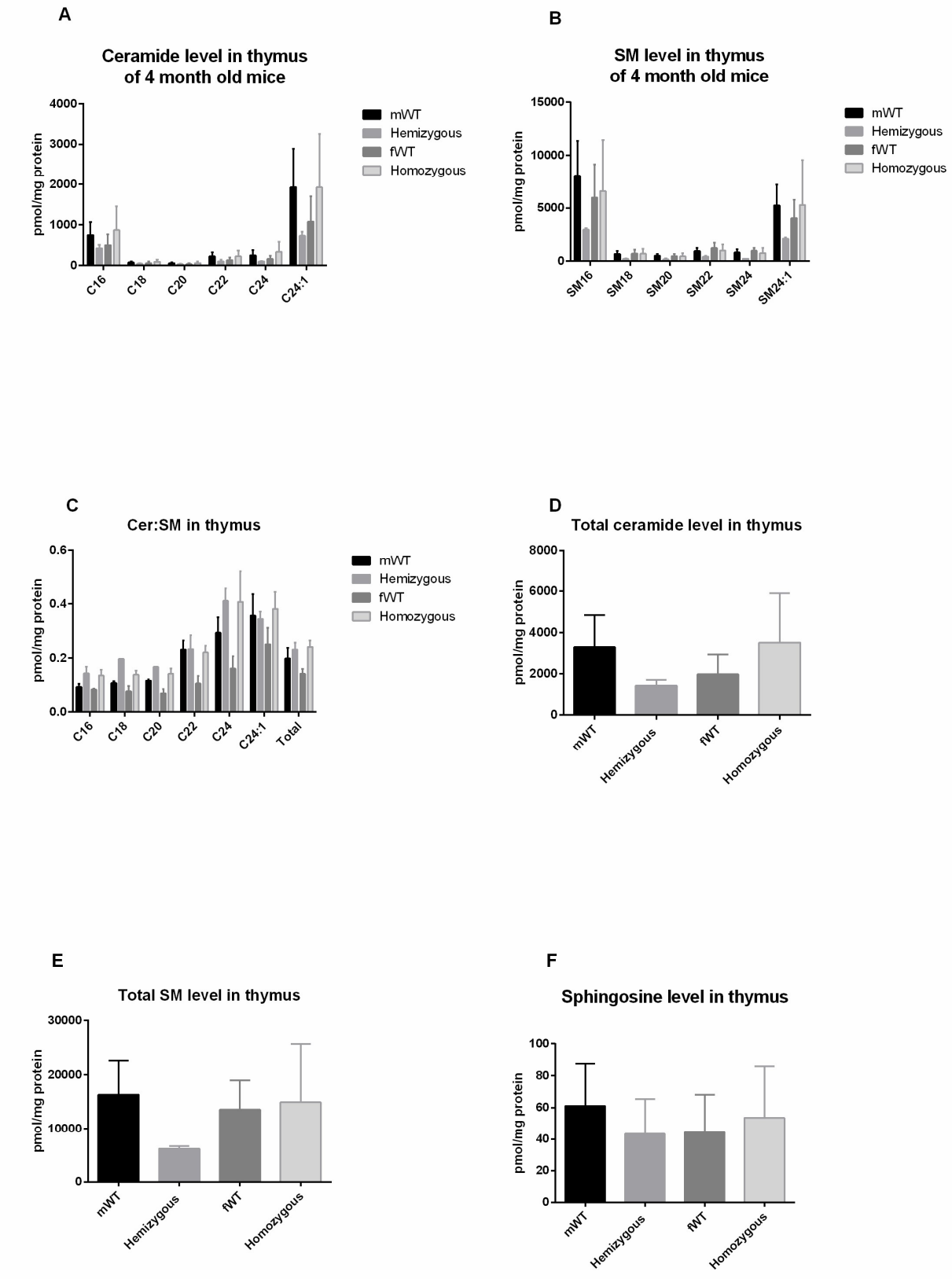

Figure 7. Ceramide, sphingomyelin and sphingosine quantification in thymus of (A) ceramide level, (B) SM level of, (C) Cer: SM level, (D) Total ceramide level, (E) Total SM level, (F)Sphingosine level. Means ± SD from n = 2- 5 mice are depicted. Asterisks indicate significant differences as assessed by one-way ANOVA. Abbreviation: mWT,male wildtype; fWT, female wildtype. SM, sphingomyelin; Cer, ceramide.

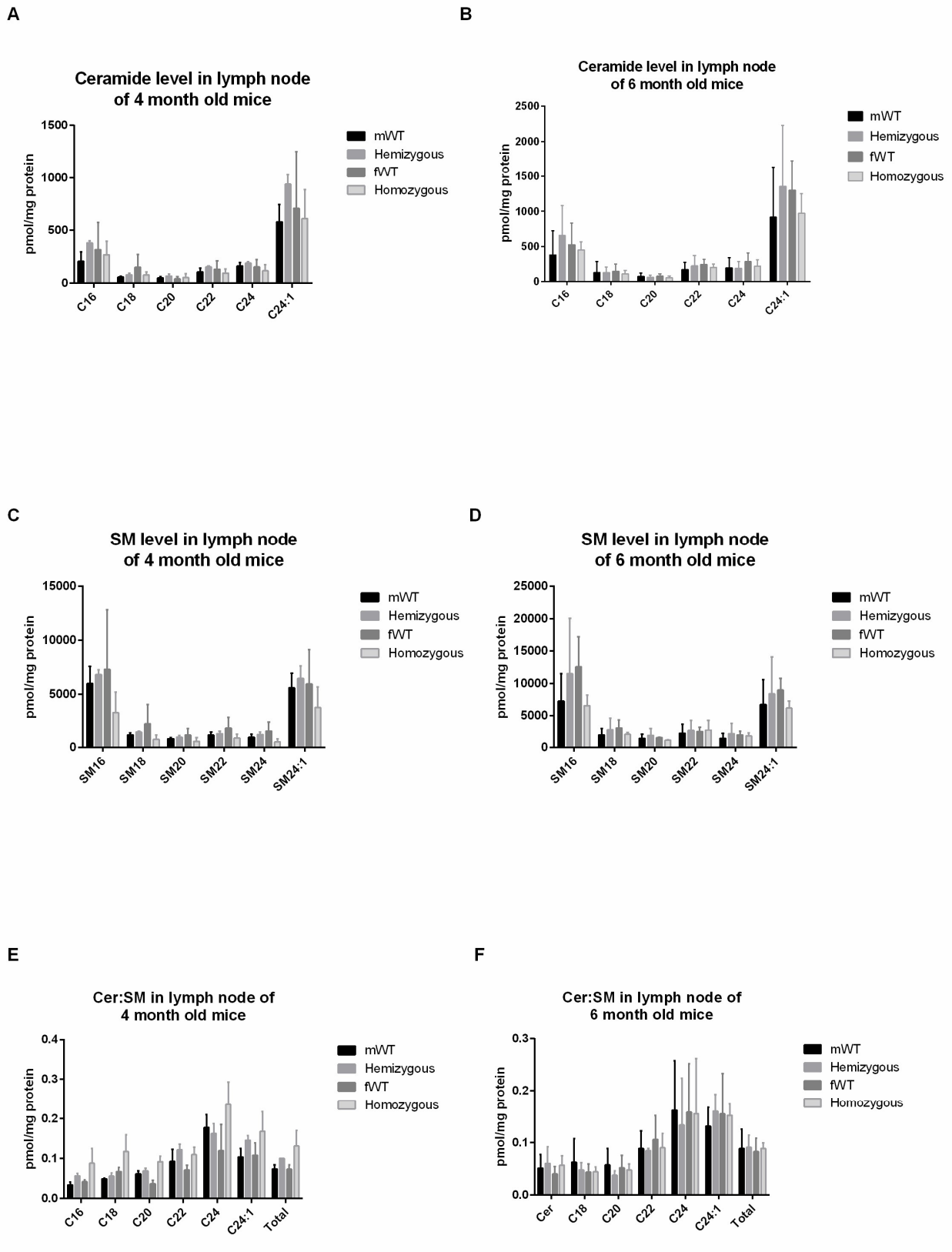

Figure 8. Ceramide and sphingomyelin quantification in lymph node of (A) ceramide level of 4 months old mice, (B) ceramide level of 6 months old mice, (C) SM level of 4 months old mice, (D) SM level of 6 months old mice, (E) Cer:SM level of 4 months old mice, (F)SM level of 4 months old mice. Means ± SD from n = 2- 5 mice are depicted. Asterisks indicate significant differences as assessed by two-way ANOVA:. Abbreviation: mWT,male wildtype; fWT, female wildtype. SM, sphingomyelin; Cer, ceramide.

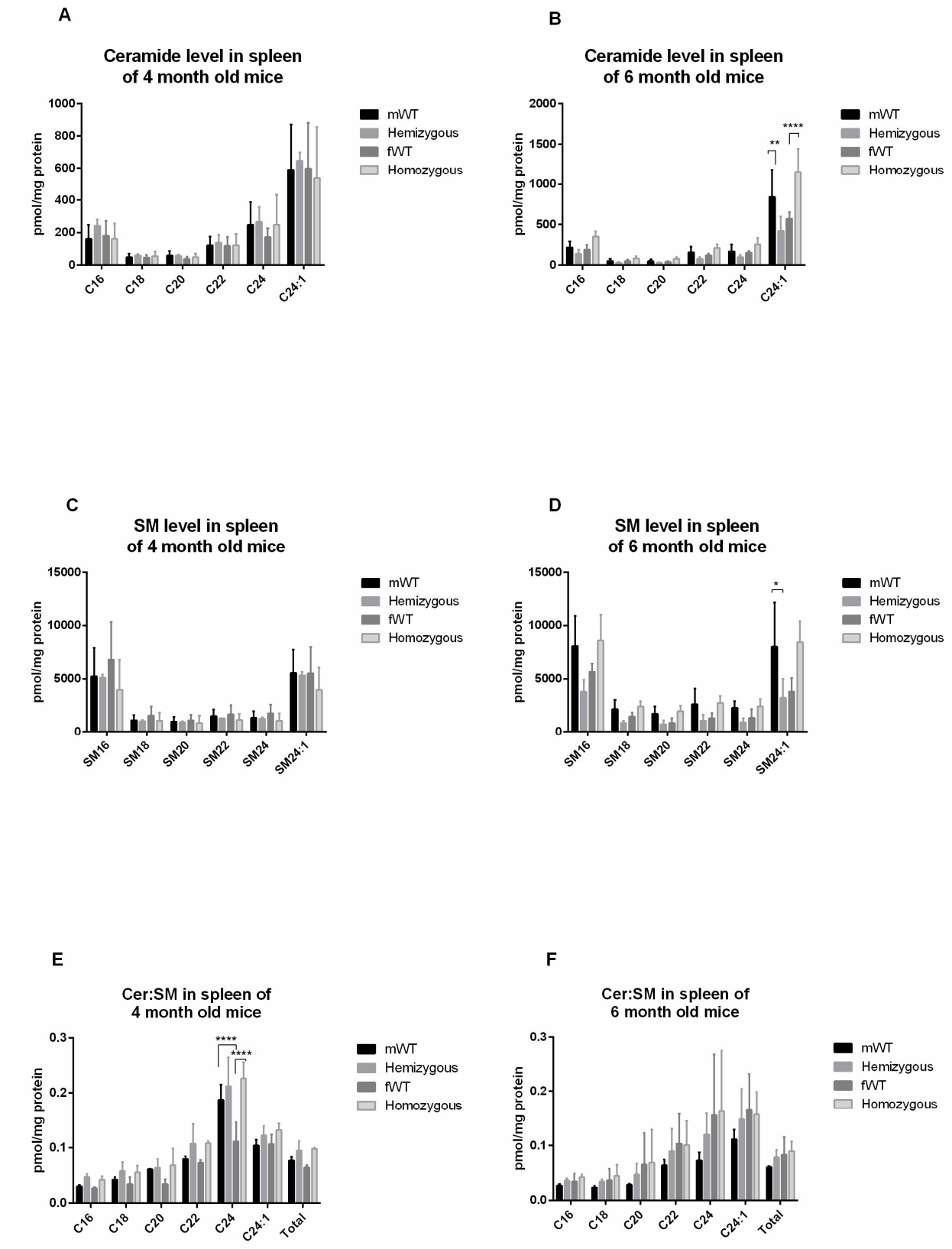

Figure 9. Ceramide and sphingomyelin quantification in spleen of (A) ceramide level of 4 months old mice, (B) ceramide level of 6 months old mice, (C) SM level of 4 months old mice, (D) SM level of 6 months old mice, (E) Cer:SM level of 4 months old mice, (F) SM level of 4 months old mice. Means ± SD from n = 2- 5 mice are depicted. Asterisks indicate significant differences as assessed by two-way ANOVA): * $p < 0.05$, ** $p < 0.01$, **** $p < 0.0001$. Abbreviation: mWT,male wildtype; fWT, female wildtype. SM, sphingomyelin; Cer, ceramide.

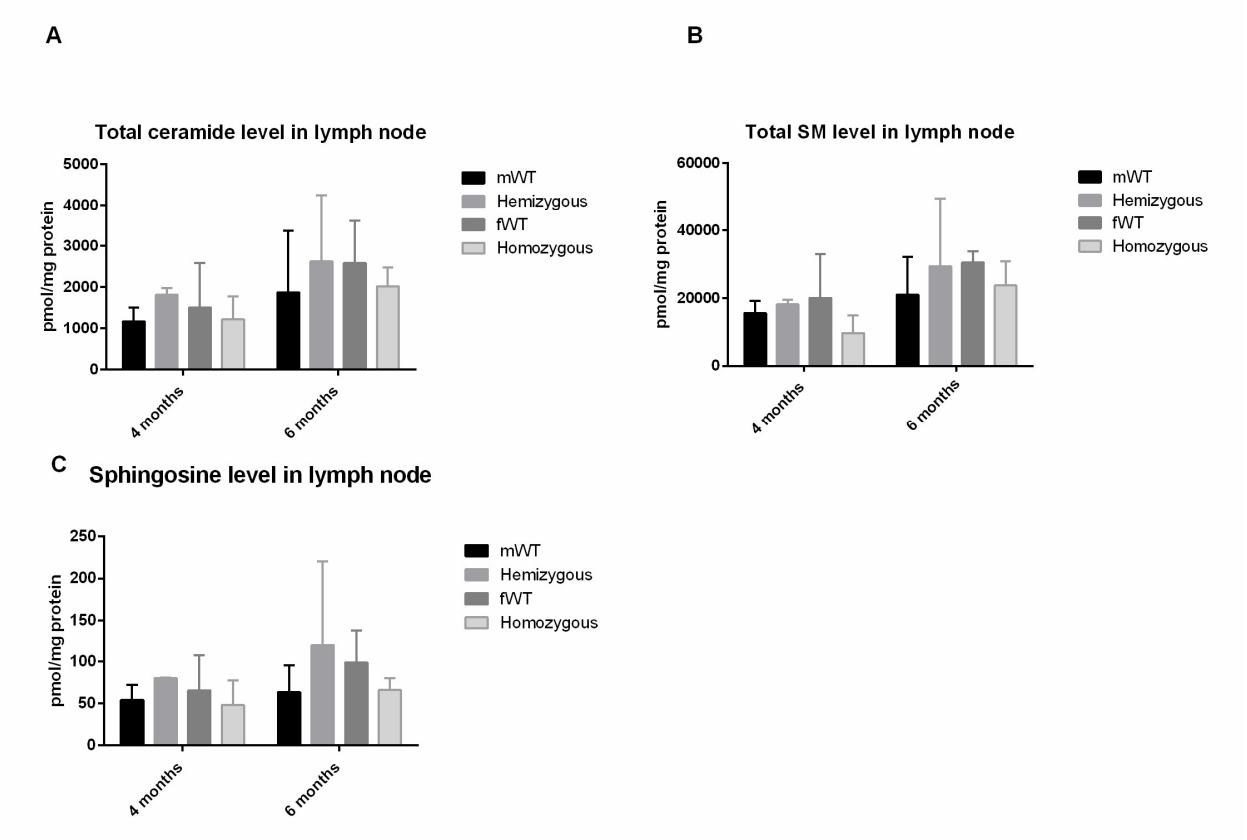

Figure 10. Ceramide and sphingomyelin quantification in lymph node of (A) Total ceramide level (B) Total SM level (C) sphingosine level. Means ± SD from n = 2- 5 mice are depicted. Asterisks indicate significant differences as assessed by two-way ANOVA. Abbreviation: mWT,male wildtype; fWT, female wildtype. SM, sphingomyelin.

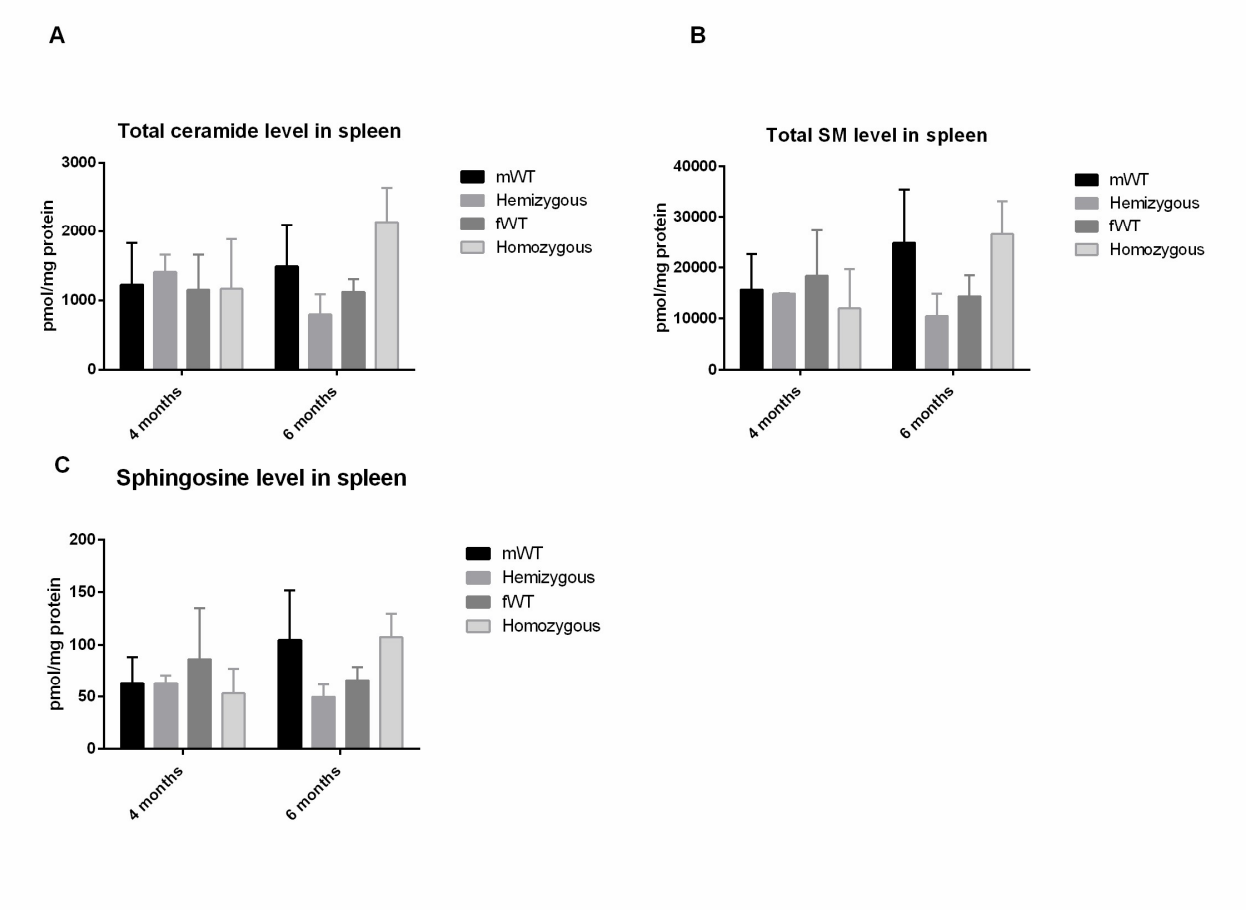

Figure 11. Ceramide and sphingomyelin quantification in spleen of (A) Total ceramide level (B) Total SM level (C)Sphingosine level. Means ± SD from n = 2- 5 mice are depicted. Asterisks indicate significant differences as assessed by two-way ANOVA. Abbreviation: mWT,male wildtype; fWT, female wildtype. SM, sphingomyelin.

3.3 Cell number

Thymus, LN and spleen were taken out from sacrificed mice. Cell numbers from each organ were counted under the light microscope (Fig. 12). Only viable cells without trypan blue dye were counted. Tg and WT showed similar cell counts regardless of the genders. The total splenocyte numbers of both ages were approximately the same. The slight drop in LN cell number with age was not statistically significant. There was a fluctuation in thymus cell number, and the difference is not statistically confirmed. Asm did not seem to have effects on the basal cell numbers in the organ as a whole. Cell number analysis is a preliminary indication of and the events such as proliferation, haematopoiesis, migration, egress and cell death. Further examination has to be carried out for populations of a particular cell type.

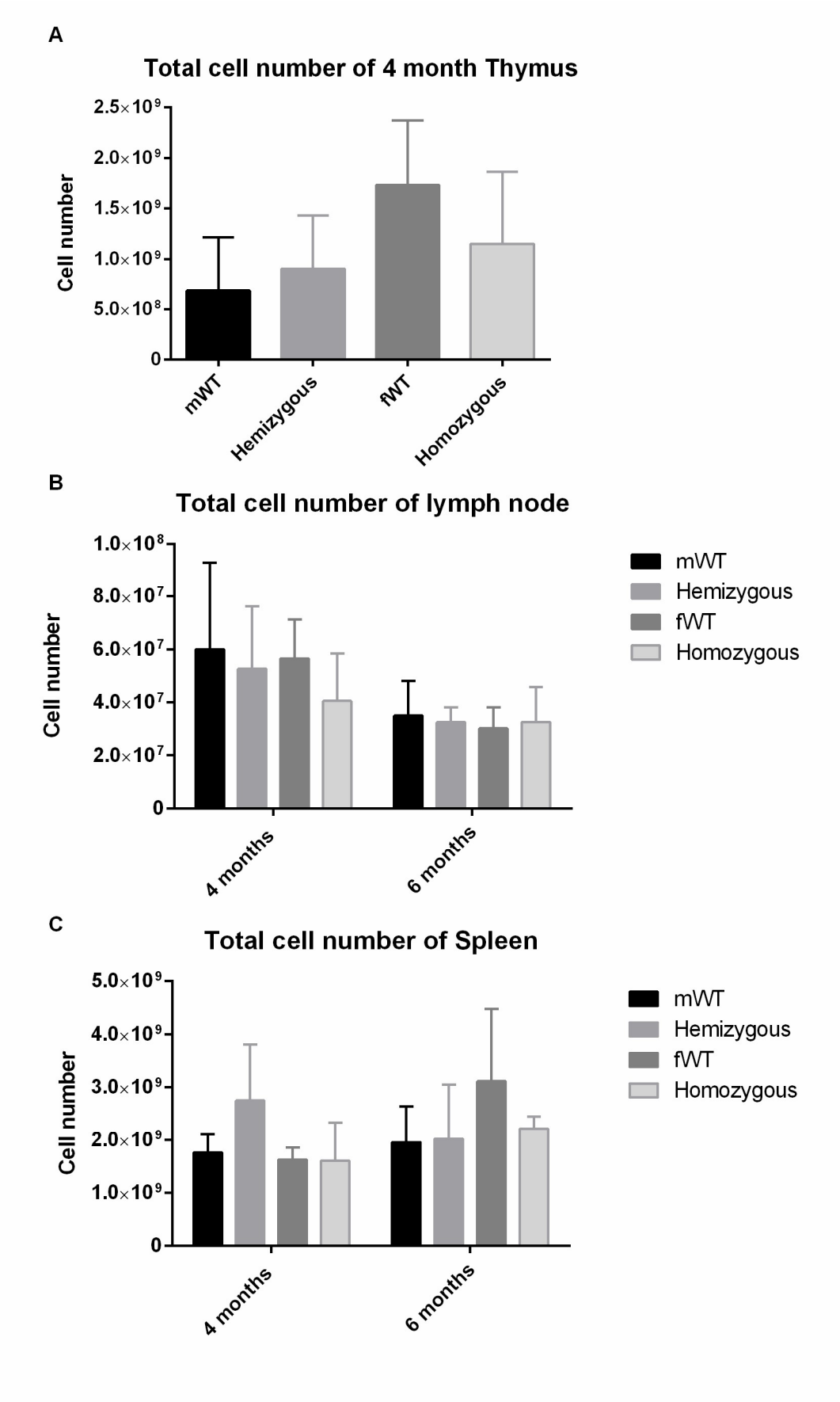

Figure 12. Total cell number of (A) thymus, (B) lymph node, (C) spleen. Mean ± SD. n = 3-5 mice. Significant differences were assessed by one-way ANOVA in thymus, and 2-way ANOVA in lymph node and spleen. Abbreviation: mWT,male wildtype; fWT, female wildtype.

3.4 T cell population

To quantify the T cell population, flow cytometry was performed (Fig. 13-15).

CD3 antigen appears on most of the T cells at all developmental stage, therefore known as a T cell marker. The percentage upon $CD45^+$ immune cells and the cell number were analyzed. The $CD3^+$ cells were not altered between the genotypes in the three organs.

The distributions of different T cell subtypes were then studied. There are many T cell subtypes, for example, cytotoxic T cells, helper T cells, memory T cells, natural killer T cells and regulatory T cells. In this project, $CD4^+$, $CD8^+$, double positive cells, double negative cells out of the $CD3^+$ cells were investigated. These cells represent helper T cells, cytotoxic T cells, T cells in developmental stage and T cells before selections, and they predominate the T cell population. Again, the percentage of $CD45^+$ immune cells and the cell number were analyzed. $CD4^+$, $CD8^+$ and double positive cells did not have their populations changed from WT to Tg in all three organs. All the populations remained similar, which suggested that Asm overexpression did not impose observable effects on T cell resting population.

The distributions of the T cell subtypes are shown in Figures 13-15. No differences were detected between WT and Tg, in all three organs. No abnormal distribution was observed in all three organs: in spleen and LN, double negative cells had the highest population, then $CD4^+$, $CD8^+$, and double positive cells followed; whereas in thymus, the highest population was double positive cells, then $CD4^+$ and $CD8^+$, and the least was double negative cells.

There were changes in double negative cells percentage with age and gender in LN (Fig. 10). Both 6 month-old female WT and homozygous mice showed their populations doubled of that of the other genotypes. It suggests that there are phenotypic differences in between age and gender, and should be considered when using this mouse model.

3.5 T cell subtypes distribution

In thymus, the immature (double negative) thymocytes are located at the outer cortex, when the mature cells (single and double positive) are located at the T cell zone and medulla.

Images of T cell zone in spleen and LN, medulla in thymus were captured. There was hardly any difference in between genotypes in terms of the CD4/CD8/double positive cells distribution. It was difficult to distinguish the cell types using IF (Fig.16-18).

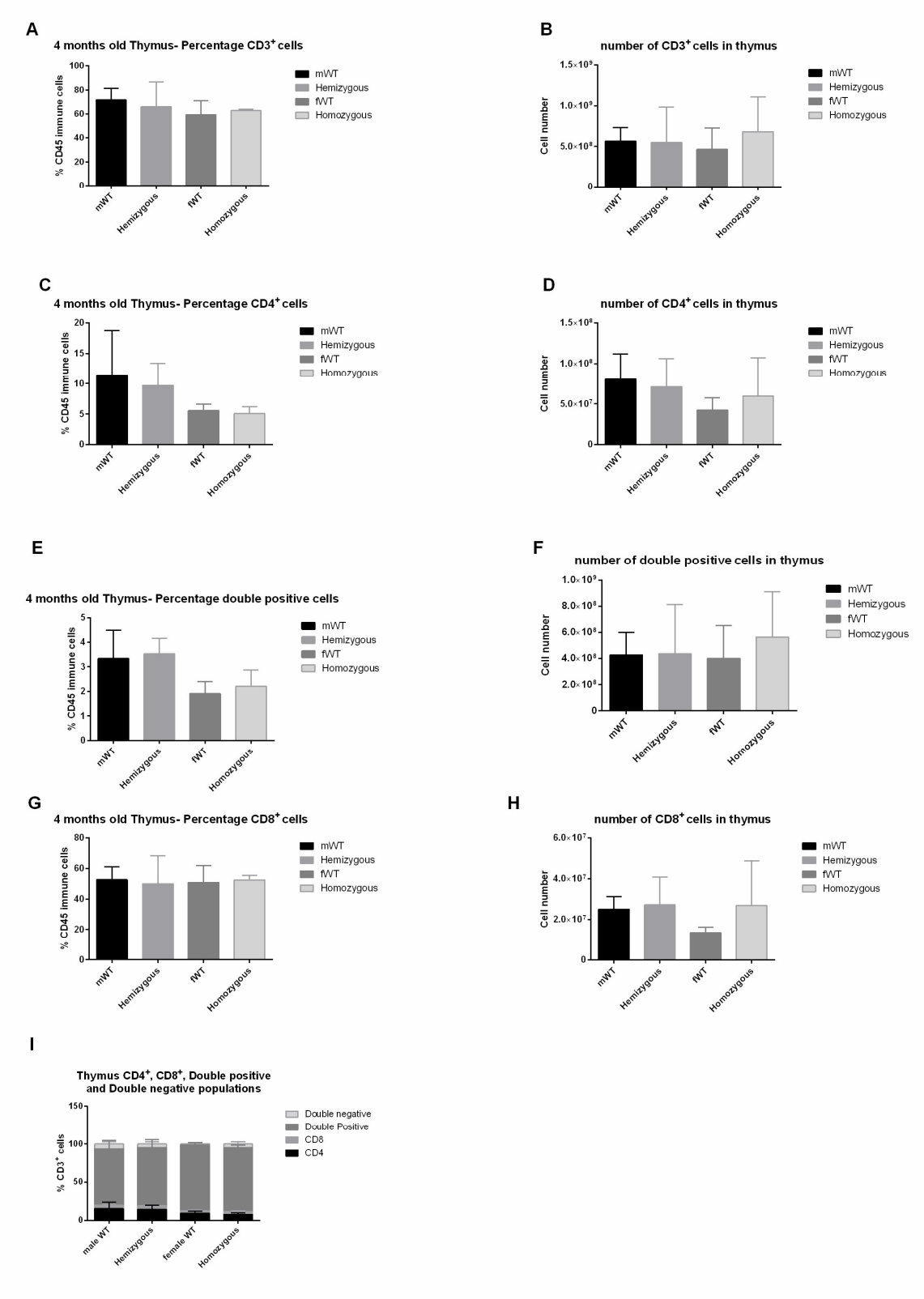

Figure 13. T cell population analysis of thymus on (A) CD3+ percentage of immune cells, (B) cell number, (C) CD4+ percentage of immune cells, (D) cell number, (E) CD8+percentage of immune cells, (F) cell number (G) double positive percentage of immune cells, (H) cell number (I) distribution of subtypes. Mean ± SD. n = 3-5 mice. Significant differences were assessed by one-way ANOVA. Abbreviation: mWT,male wildtype; fWT, female wildtype.

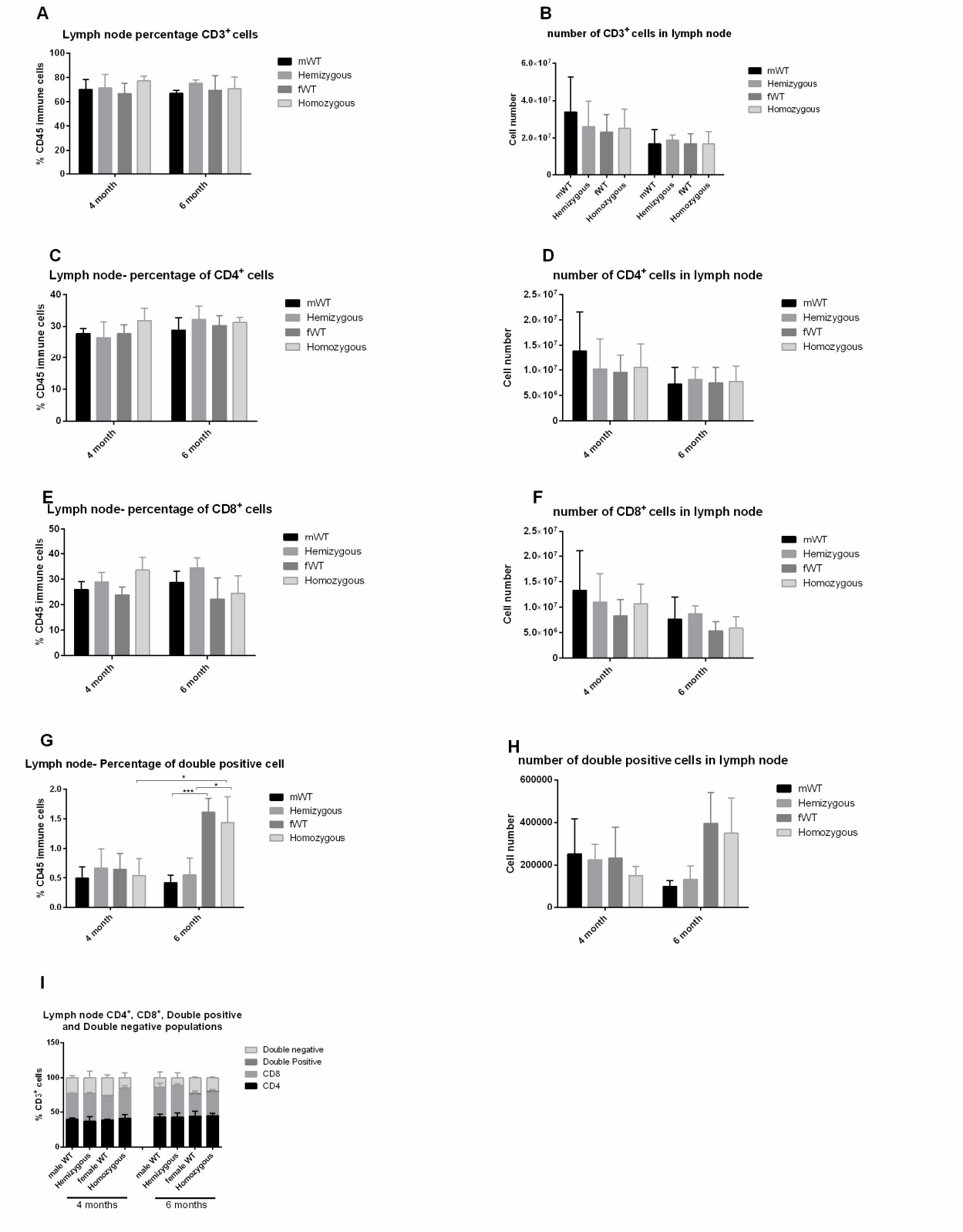

Figure 14. T cell population analysis of lymph node on (A) CD3+ percentage of immune cells, (B) cell number, (C) CD4+ percentage of immune cells, (D) cell number, (E) CD8+percentage of immune cells, (F) cell number (G) double positive percentage of immune cells, (H) cell number (I) distribution of subtypes. Mean ± SD. n = 3-5 mice. Significant differences were assessed by two-way ANOVA: * $p < 0.05$, *** $p < 0.001$. Abbreviation: mWT,male wildtype; fWT, female wildtype.

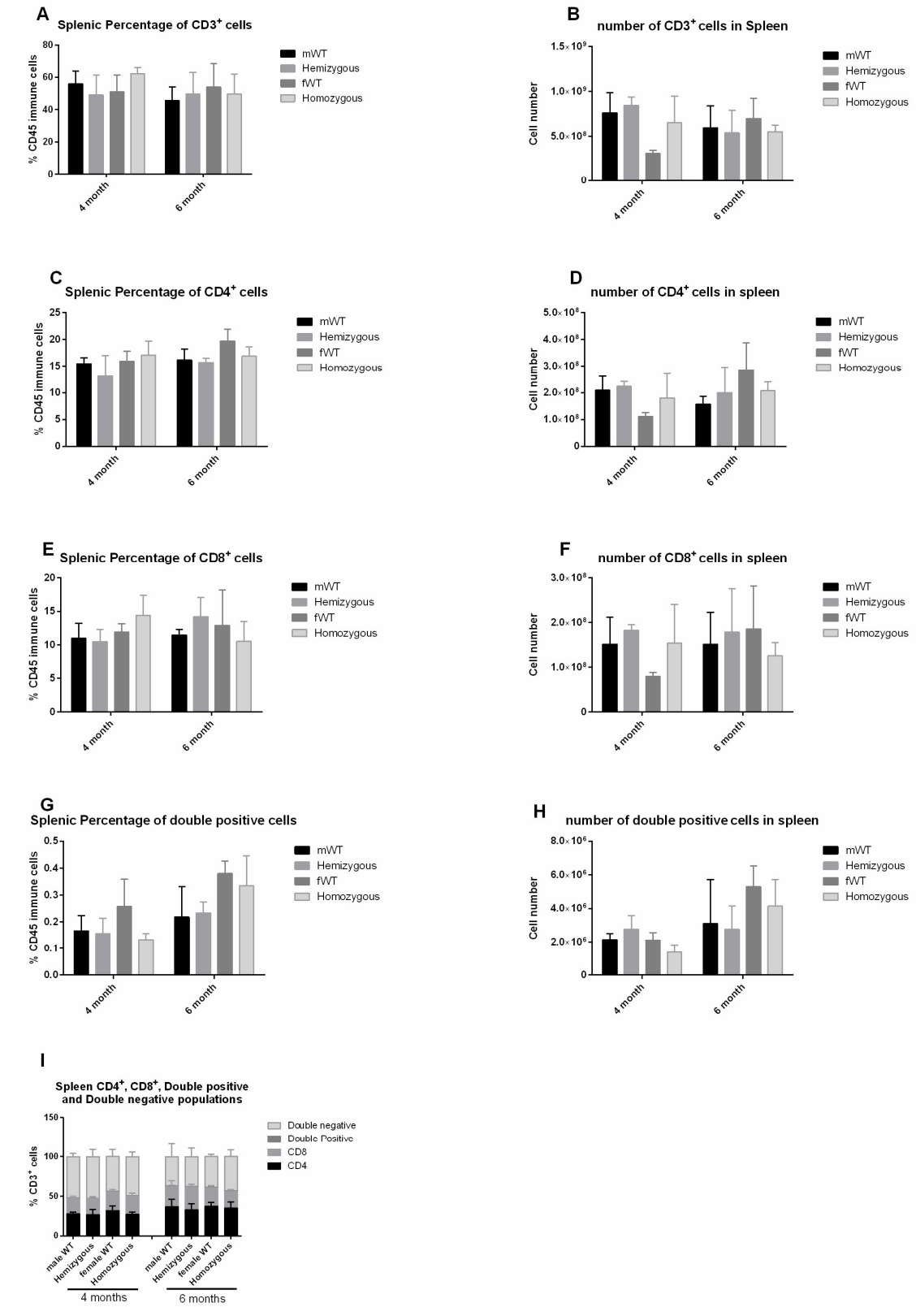

Figure 15. T cell population analysis of Spleen on (A) CD3+ percentage of immune cells, (B) cell number, (C) CD4+ percentage of immune cells, (D) cell number, (E) CD8+percentage of immune cells, (F) cell number (G) double positive percentage of immune cells, (H) cell number (I) distribution of subtypes. Mean ± SD. n = 3-5 mice. Significant differences were assessed by two-way ANOVA. Abbreviation: mWT,male wildtype; fWT, female wildtype.

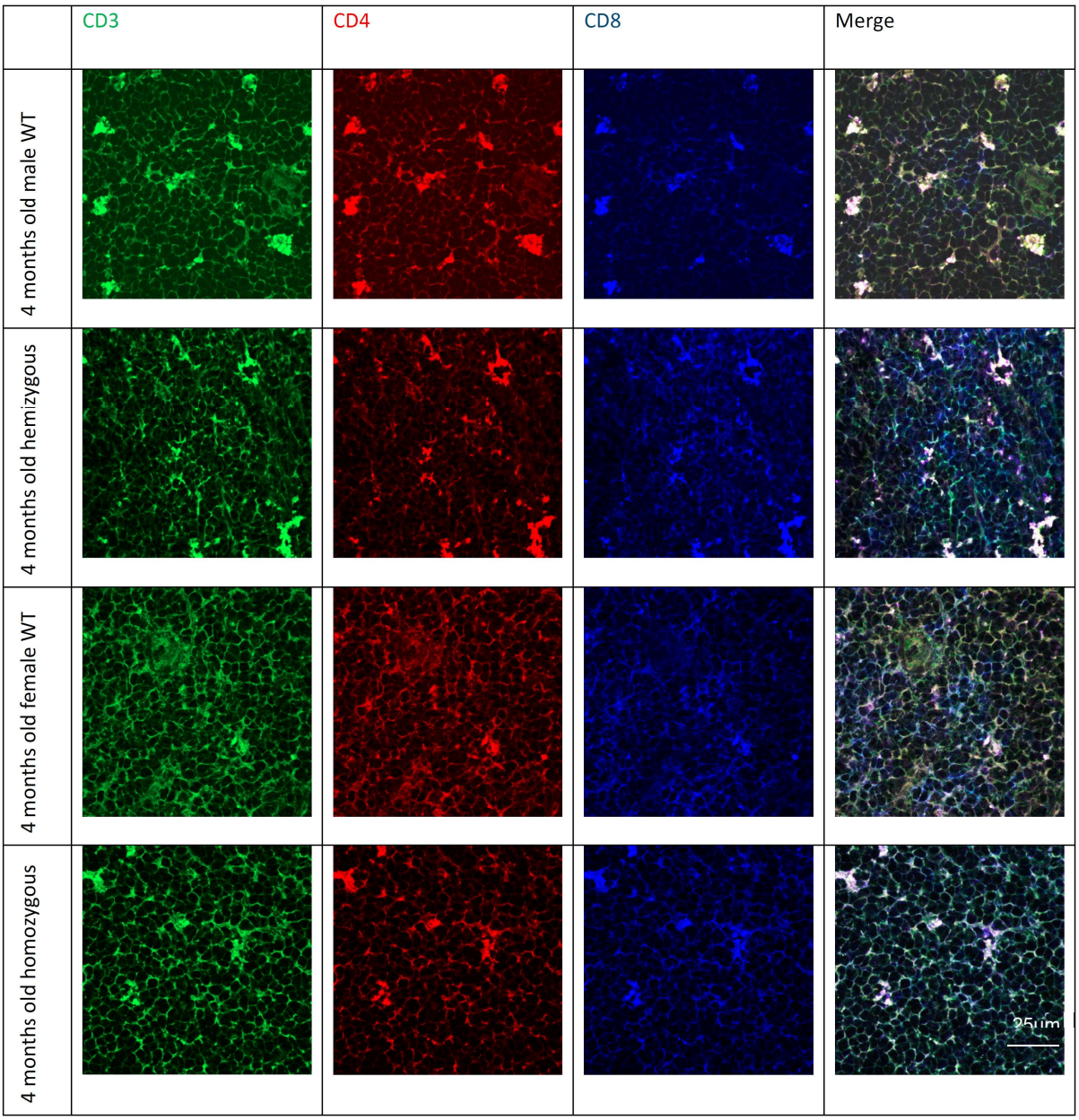

Figure16. Immunofluorescent staining of thymus with antibodies directed against T cell (CD3, green), CD4 (red) and CD8 (blue). n=2-3 mice. Representative images are shown. Abbreviation: WT, wildtype. Scale bar: 25 µm.

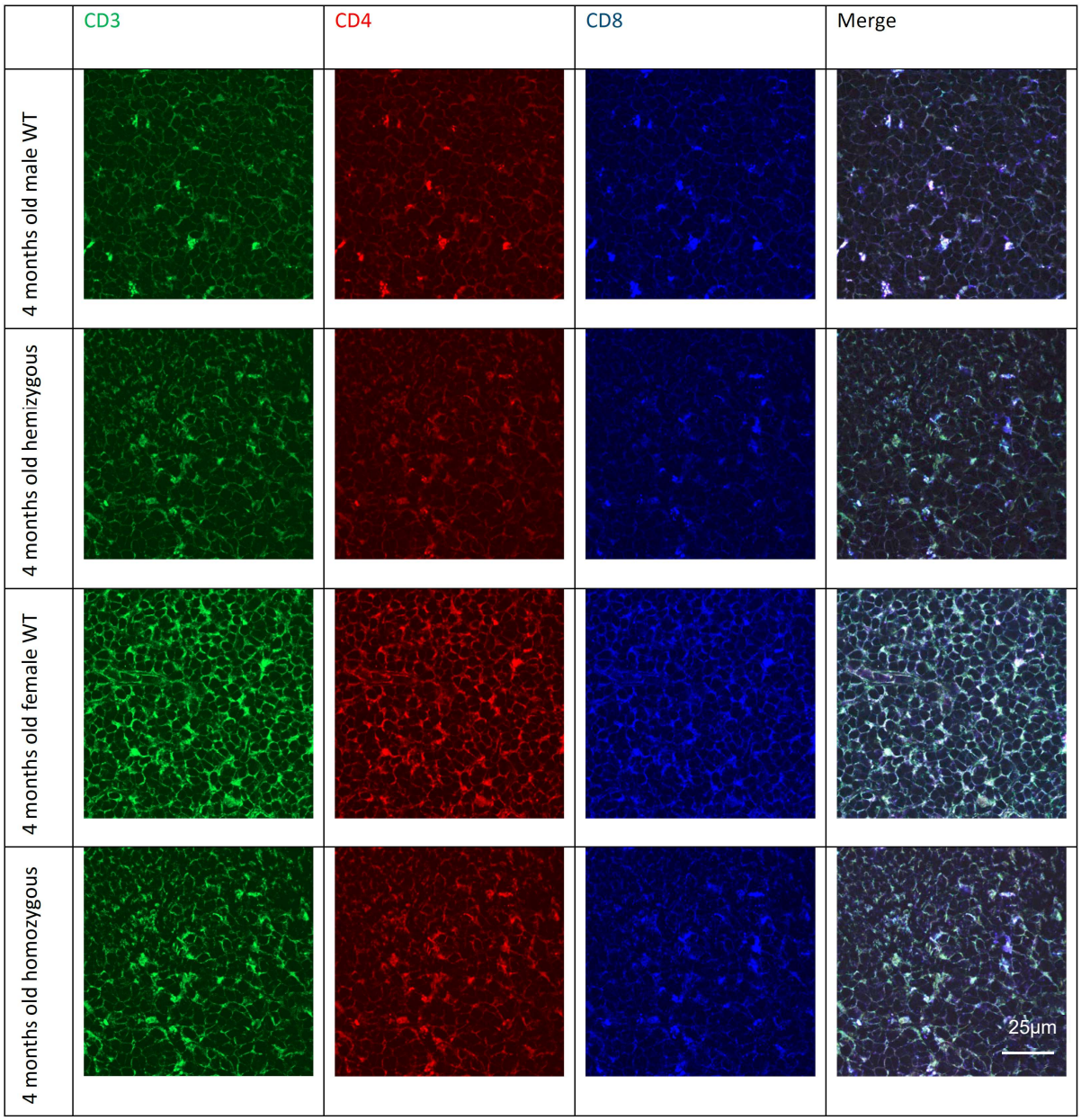

Figure17a. Immunofluorescent staining of lymph node with antibodies directed against T cell (CD3, green), CD4 (red) and CD8 (blue). n=1-3 mice. Representative images are shown. Abbreviation: WT, wildtype. Scale bar: 25 µm.

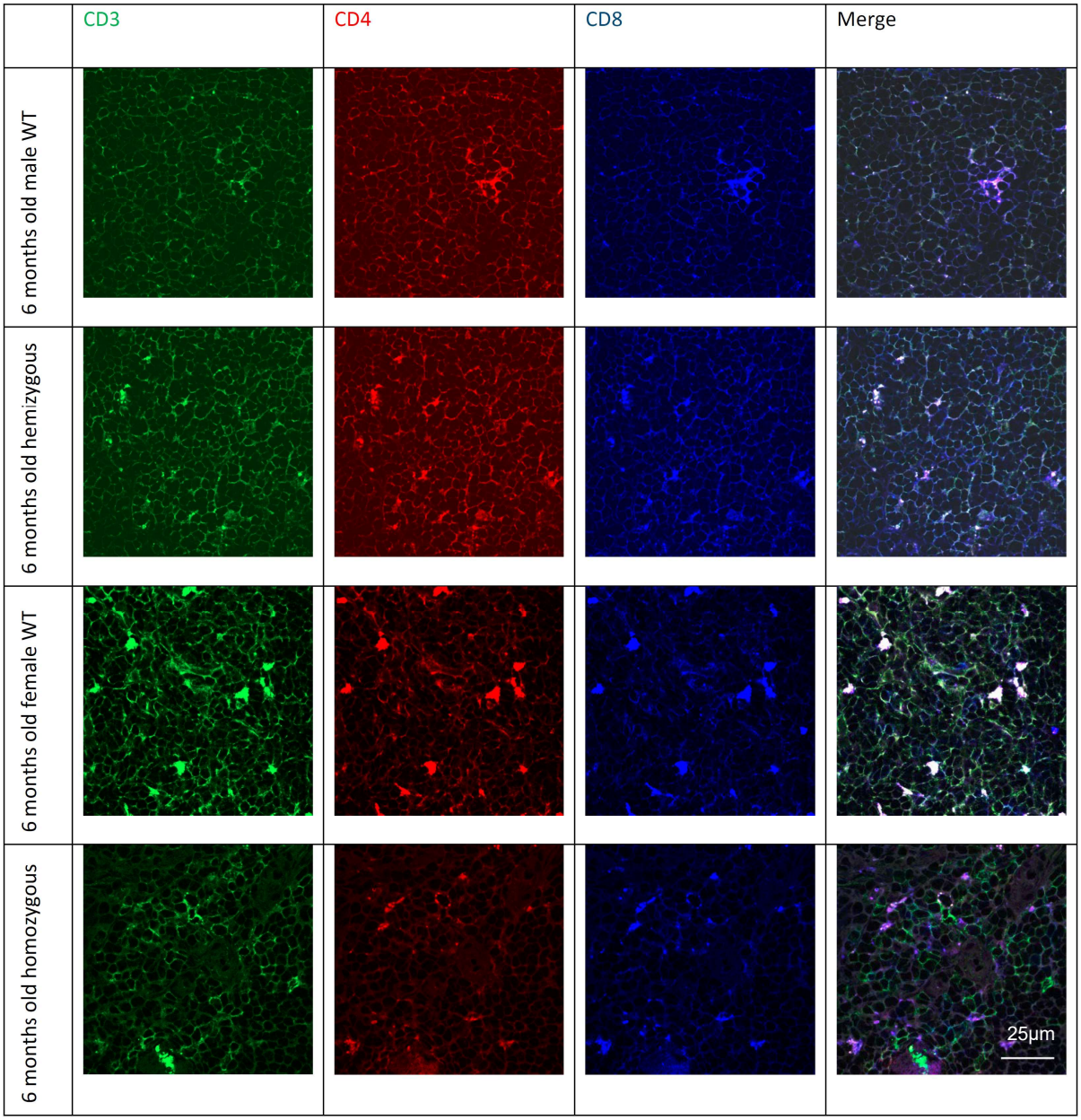

Figure17b. Immunofluorescent staining of lymph node with antibodies directed against T cell (CD3, green), CD4 (red) and CD8 (blue). n=1-3 mice. Representative images are shown. Abbreviation: WT, wildtype. Scale bar: 25 µm.

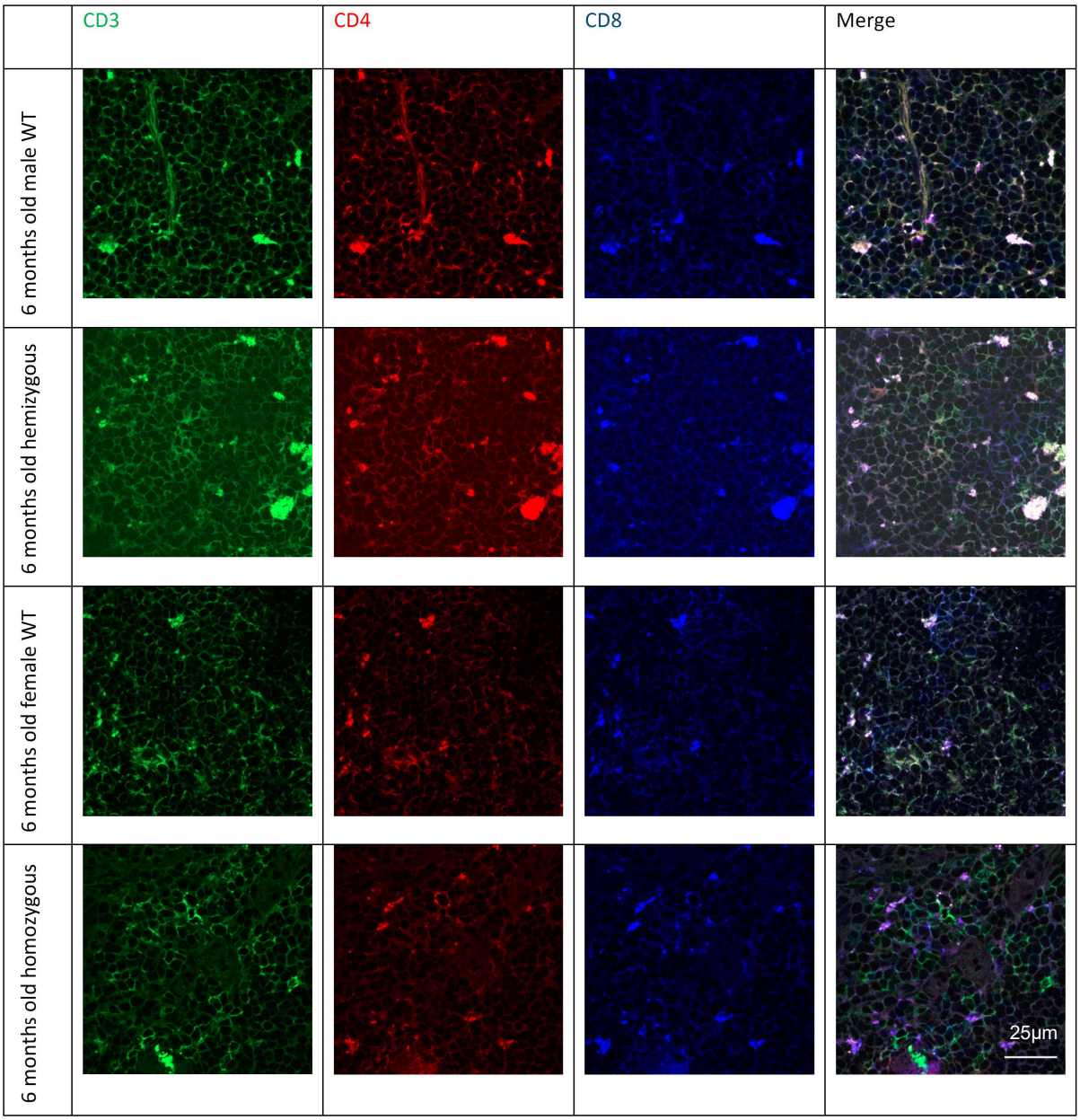

Figure18a. Immunofluorescent staining of spleen with antibodies directed against T cell (CD3, green), CD4 (red) and CD8 (blue). n=1-3 mice. Representative images are shown. Abbreviation: WT, wildtype. Scale bar: 25 µm.

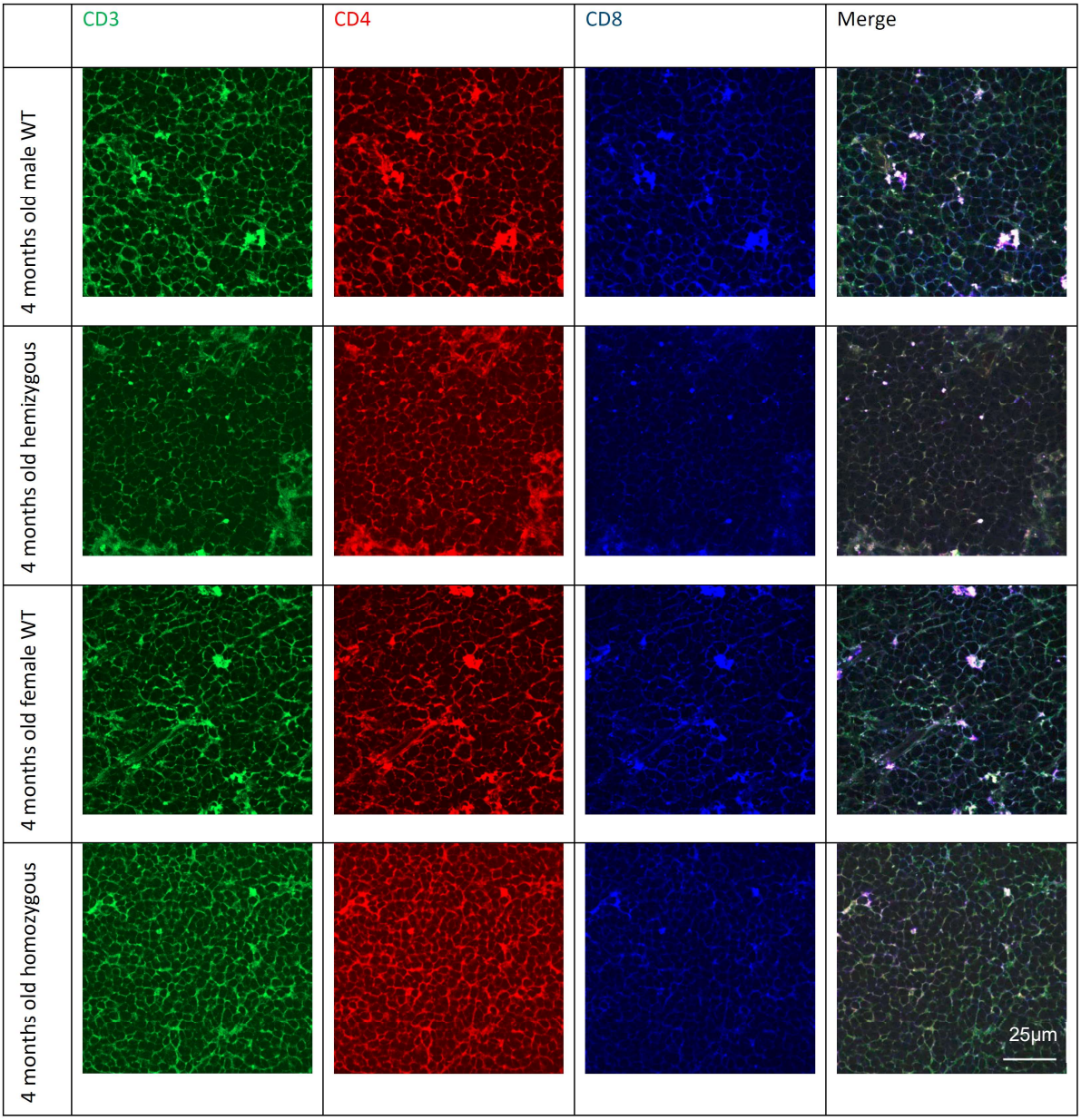

Figure18b. Immunofluorescent staining of spleen with antibodies directed against T cell (CD3, green), CD4 (red) and CD8 (blue). n=1-3 mice. Representative images are shown. Abbreviation: WT, wildtype. Scale bar: 25 µm.

3.6 T cell activation

CD69 is an early activation marker of many immune cells including T cells, B cells, neutrophils, macrophages, eosinophils and NK cells. It is also used to identify some residential thymocytes, monocytes and platelets. It was found (Reddy, 2004) to have induced expression as soon as two hours after T cell activation. Expressions of other activation markers, such as CD25, follow. CD25 is the α-chain of the interleukin 2 (IL-2) receptor. The role of CD25 is to respond to and produce IL-2 for its function such as proliferation, survival and expansion of T cells upon activation (Bajnok, 2017). To study the T cell activation in the transgenic mice, I evaluated the expressions of CD69 and CD25 by flow cytometry and IF.

To look at the population of activated T cells (Fig. 19-21), $CD69^+$ and $CD25^+$ according to their parent $CD4^+$, $CD8^+$ and double positive T cells were gated. In LN, both the percentage of CD69 and the number of $CD69^+$ fluctuated amongst all genotypes. No trend and no significant difference could be seen. In spleen and thymus, the percentage of all genotypes within their corresponding T cells subtypes were roughly the same, regardless of their gender and age. The splenic and thymic $CD69^+$ cell numbers fluctuated, but no significant difference was found in between genotypes. The same observation was found in $CD25^+$ population. There was no correlation of the CD69 and CD25 population with any species of ceramide, SM and Sph.

The median fluorescent intensity of CD69 and CD25 were also assessed. In the 6 months old mice, the expressions of CD69 were similar, with no significant difference among all genotype within all T cell subtypes. In 4 months old mice, the CD69 expression fluctuated within $CD4^+$, $CD8^+$ and double positive T cells, however, no significant differences between the genotypes were detected.

The CD25 expressions of all genotypes fluctuated in thymus and LN, while it was stable in spleen. Nonetheless, there was no trend or significant difference in CD25 expression between WT and Tg observed in all three organs. There was no correlation of the CD69 and CD25 expression with any species of ceramide, SM and Sph. Asm did not activate T cell without challenges in this study.

The CD69 and CD25 expressions by IF were also studied (Fig. 22-27). CD69 or CD25 were co-stained with CD4 and CD8. Images of T cell zones in LN and spleen, and medulla in thymus were taken. There was no outstanding fluorescence of CD69

and CD25 observed in all genotypes in all three organs. Asm did not seem have any effect on T cell activation without stimulation.

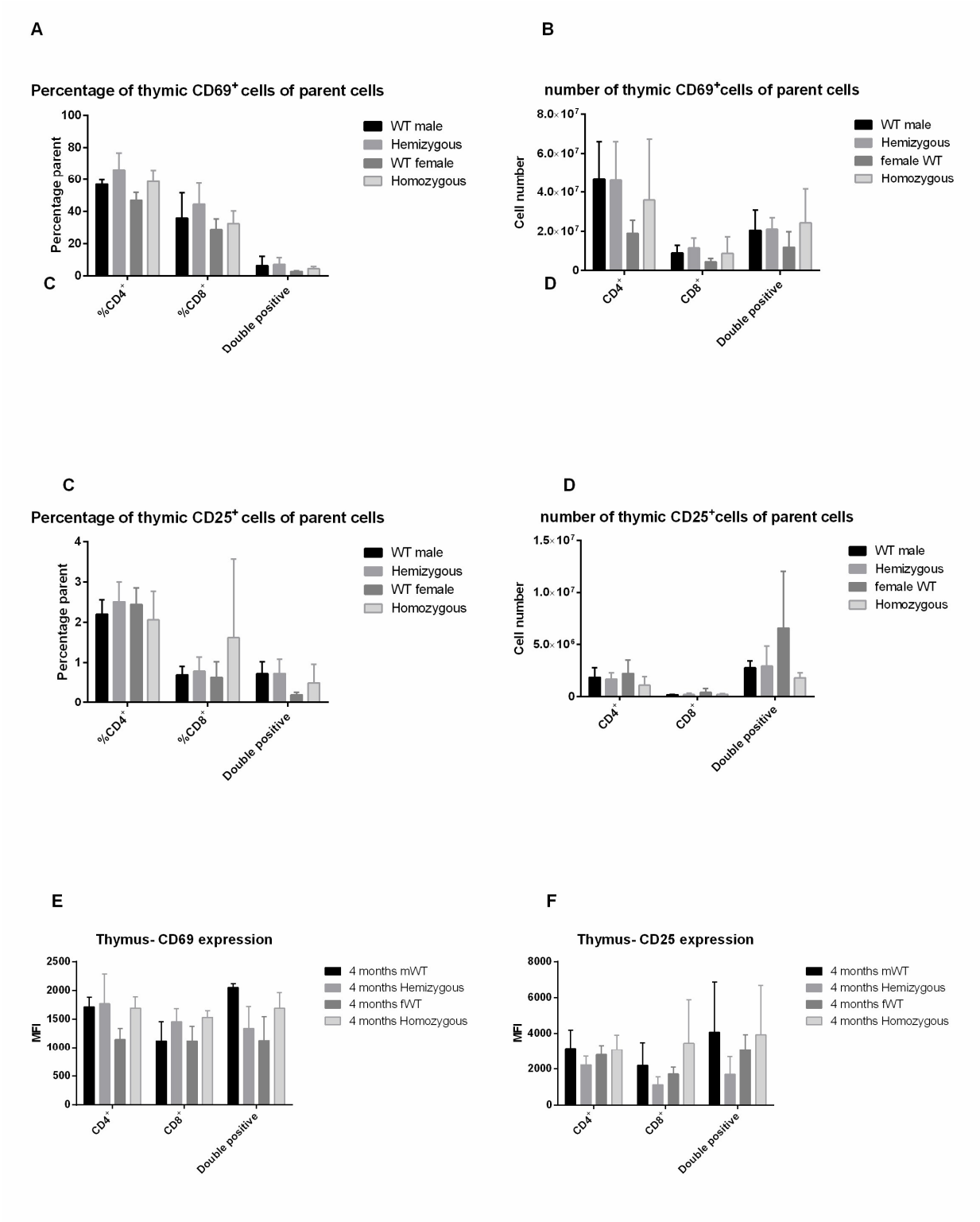

Figure 19. Analysis of thymic CD69 and CD25 expression and population on (A) CD69+ percentage, (B) cell number, (C) CD25+ percentage, (D) cell number, (E) CD69 expression, (F) CD25 expression Mean ± SD. n= 3-5 mice. Significant differences were assessed by one-way ANOVA. Abbreviation: mWT,male wildtype; fWT, female wildtype.

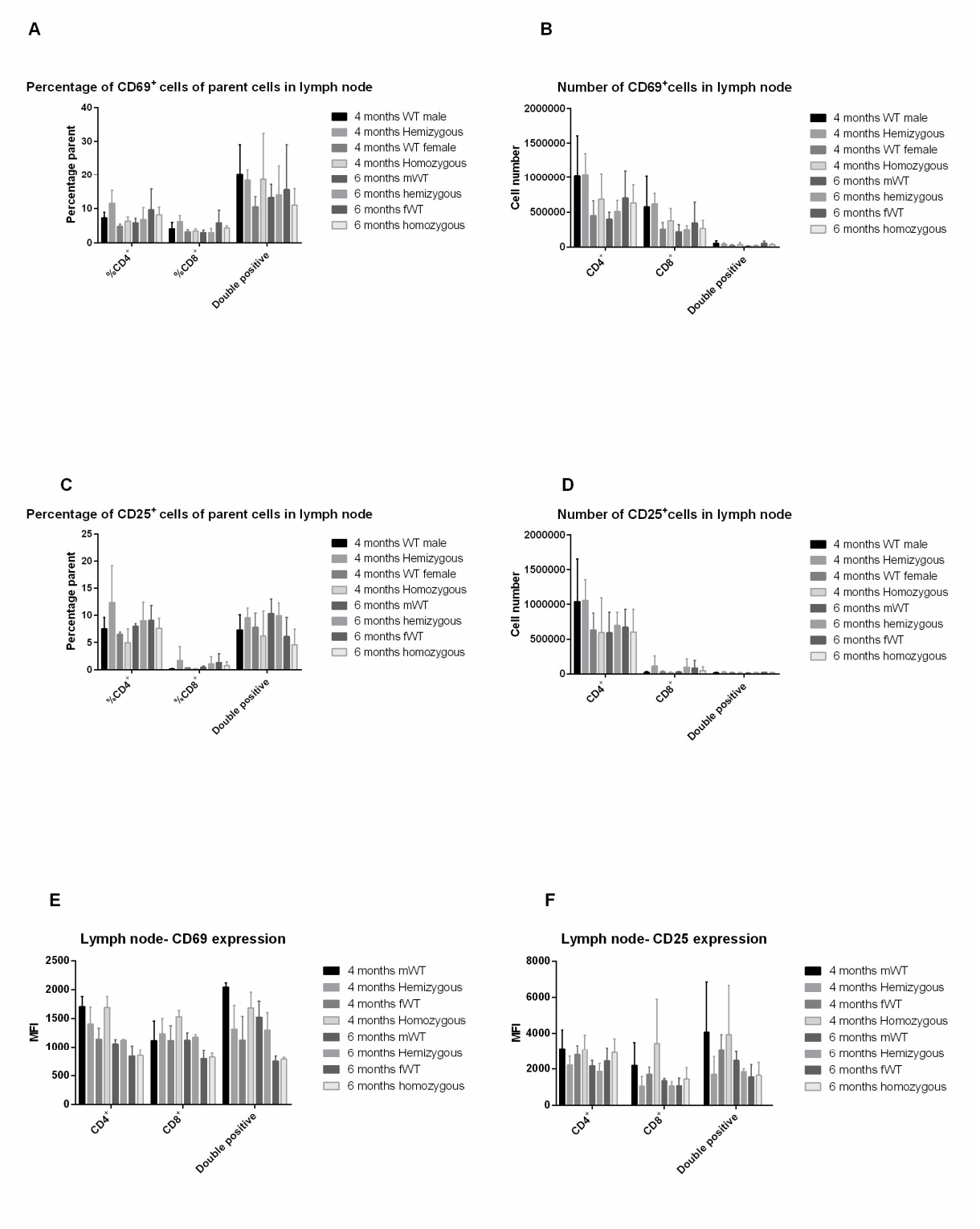

Figure 20. Analysis of lymph node CD69 and CD25 expression and population on (A) CD69+ percentage, (B) cell number, (C) CD25+ percentage, (D) cell number, (E) CD69 expression, (F) CD25 expression Mean ± SD. n= 3- 5 mice . Significant differences were assessed by two-way ANOVA. Abbreviation: mWT,male wildtype; fWT, female wildtype.

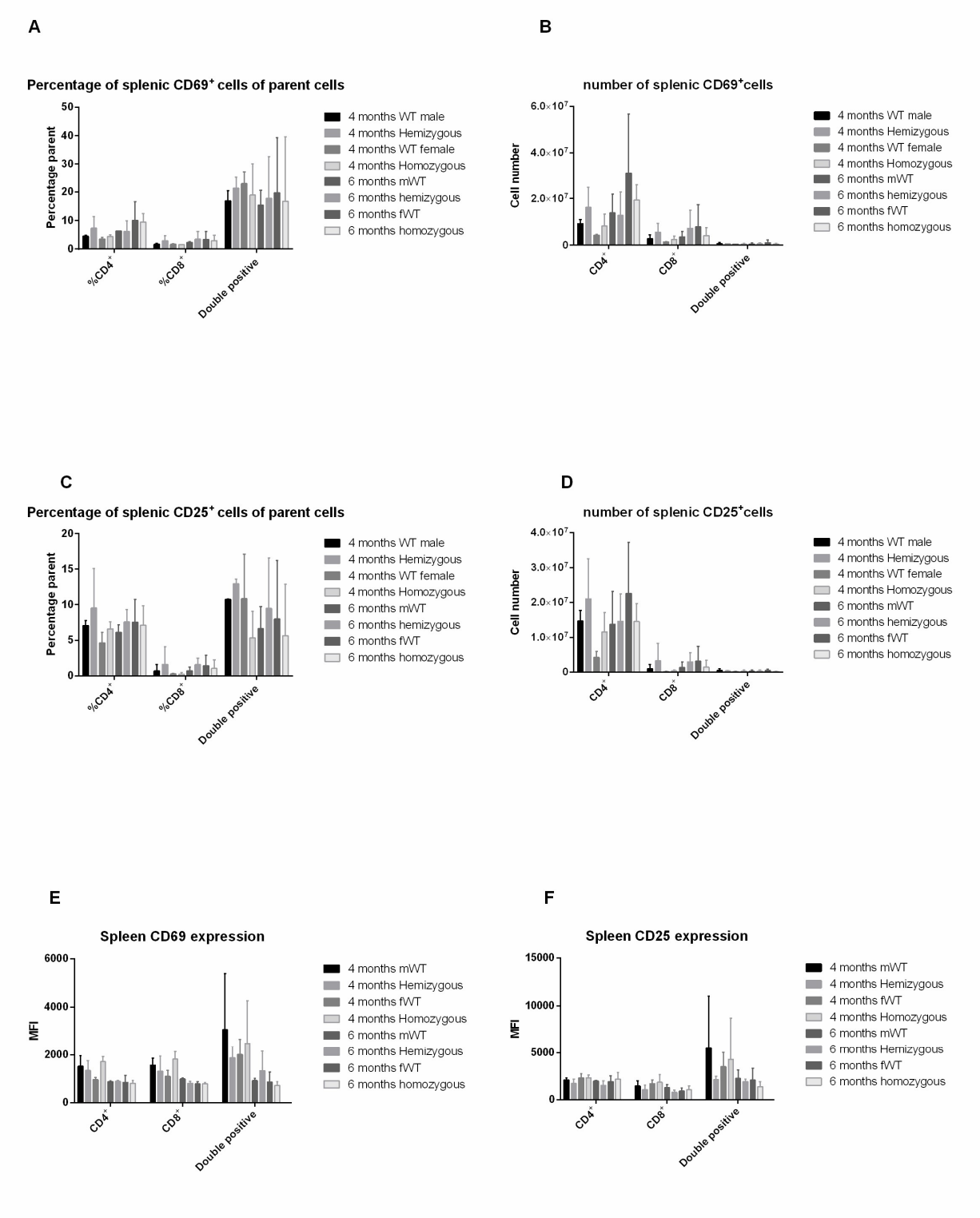

Figure 21. Analysis of splenic CD69 and CD25 expression and population on (A) CD69+ percentage, (B) cell number, (C) CD25+ percentage, (D) cell number, (E) CD69 expression, (F) CD25 expression Mean ± SD. n= 3- 5 mice . Significant differences were assessed by two-way ANOVA. Abbreviation: mWT,male wildtype; fWT, female wildtype.

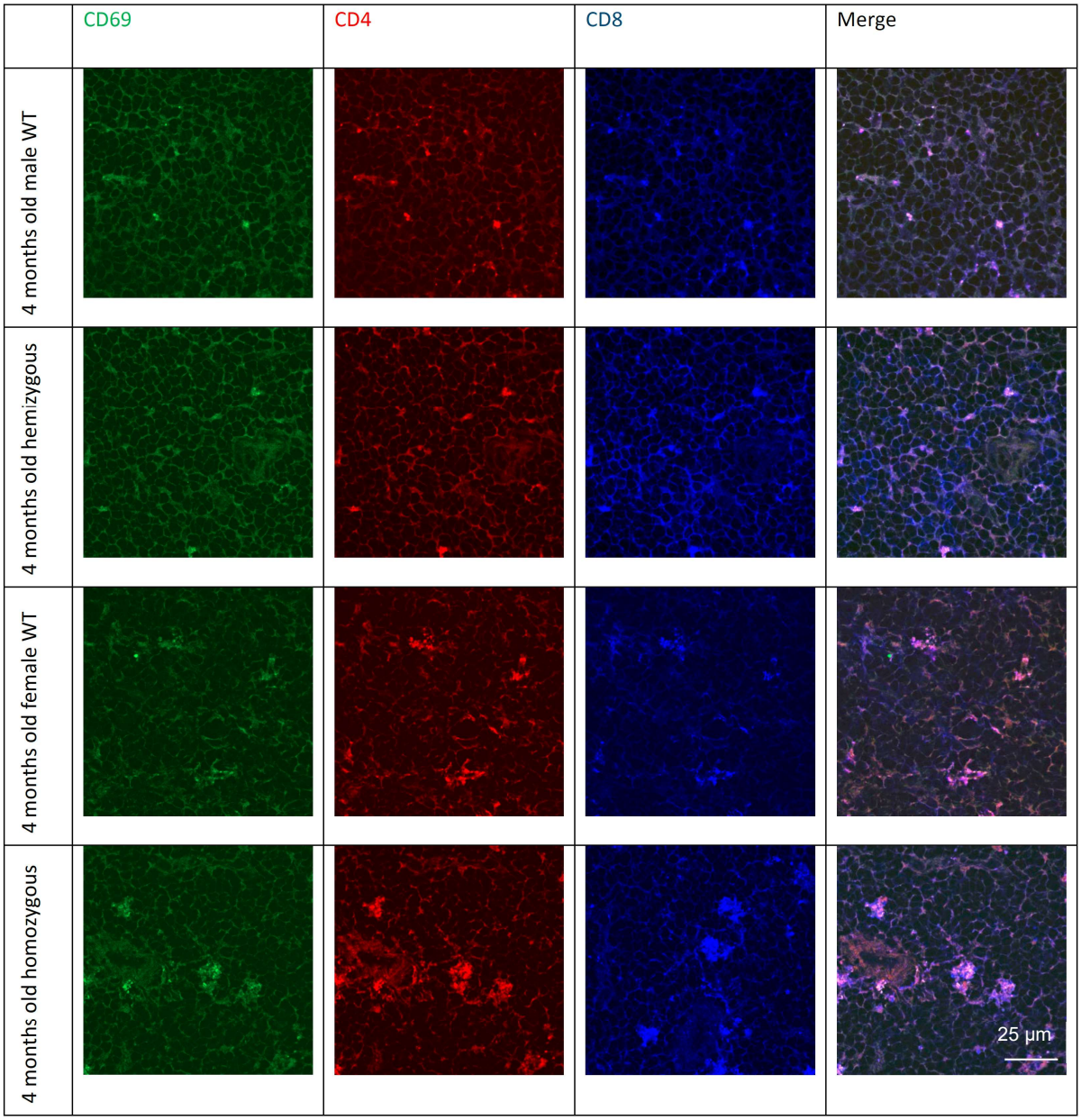

Figure 22. Immunofluorescent staining of thymus with antibodies directed against T cell activation marker (CD69, green), CD4 (red) and CD8 (blue). n=2-3 mice. Representative images are shown. Abbreviation: WT,wildtype. Scale bar: 25 µm.

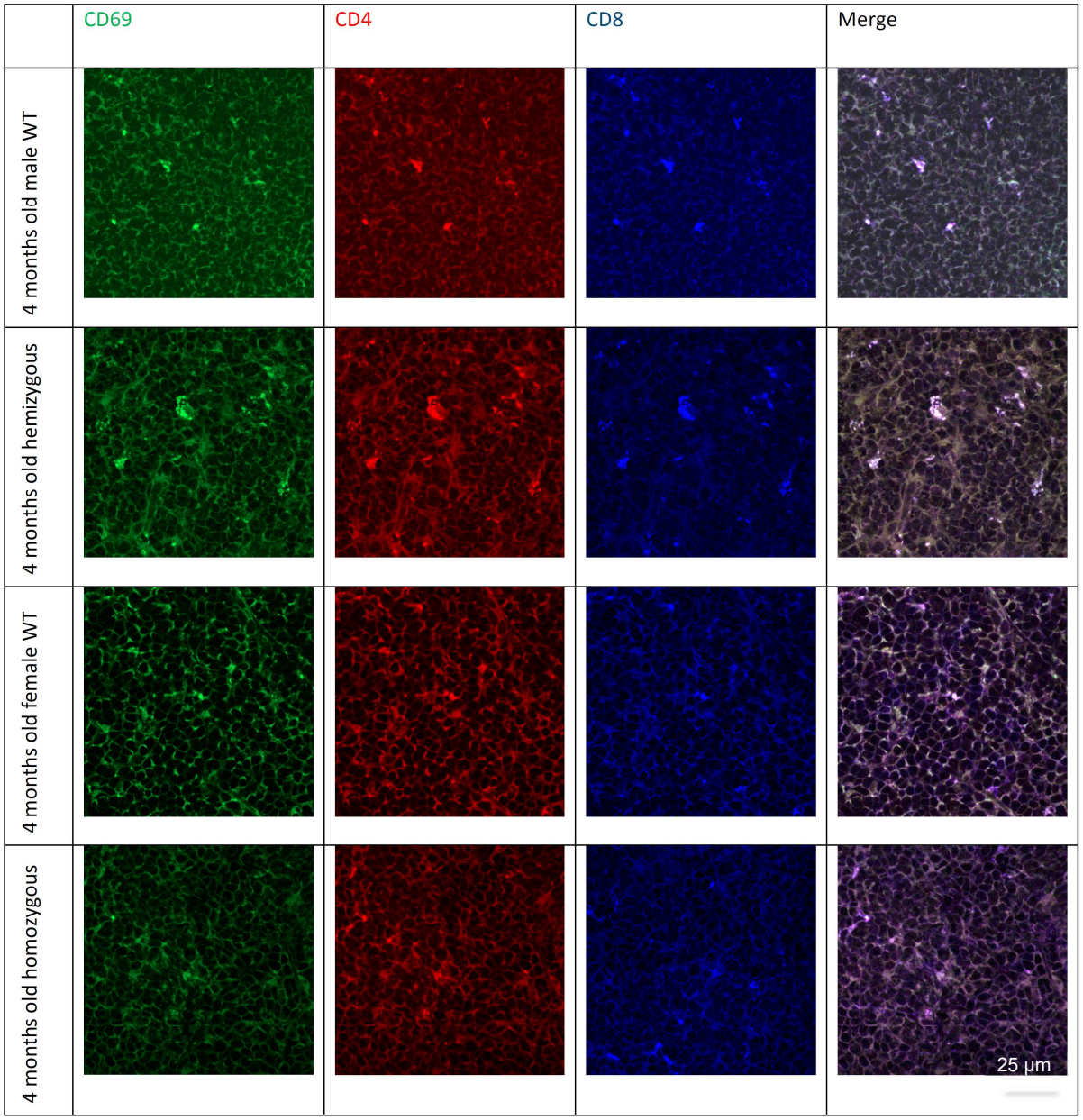

Figure 23a. Immunofluorescent staining of lymph node with antibodies directed against T cell activation marker (CD69, green), CD4 (red) and CD8 (blue). n=1-3 mice. Representative images are shown. Abbreviation: WT,wildtype. Scale bar: 25 µm.

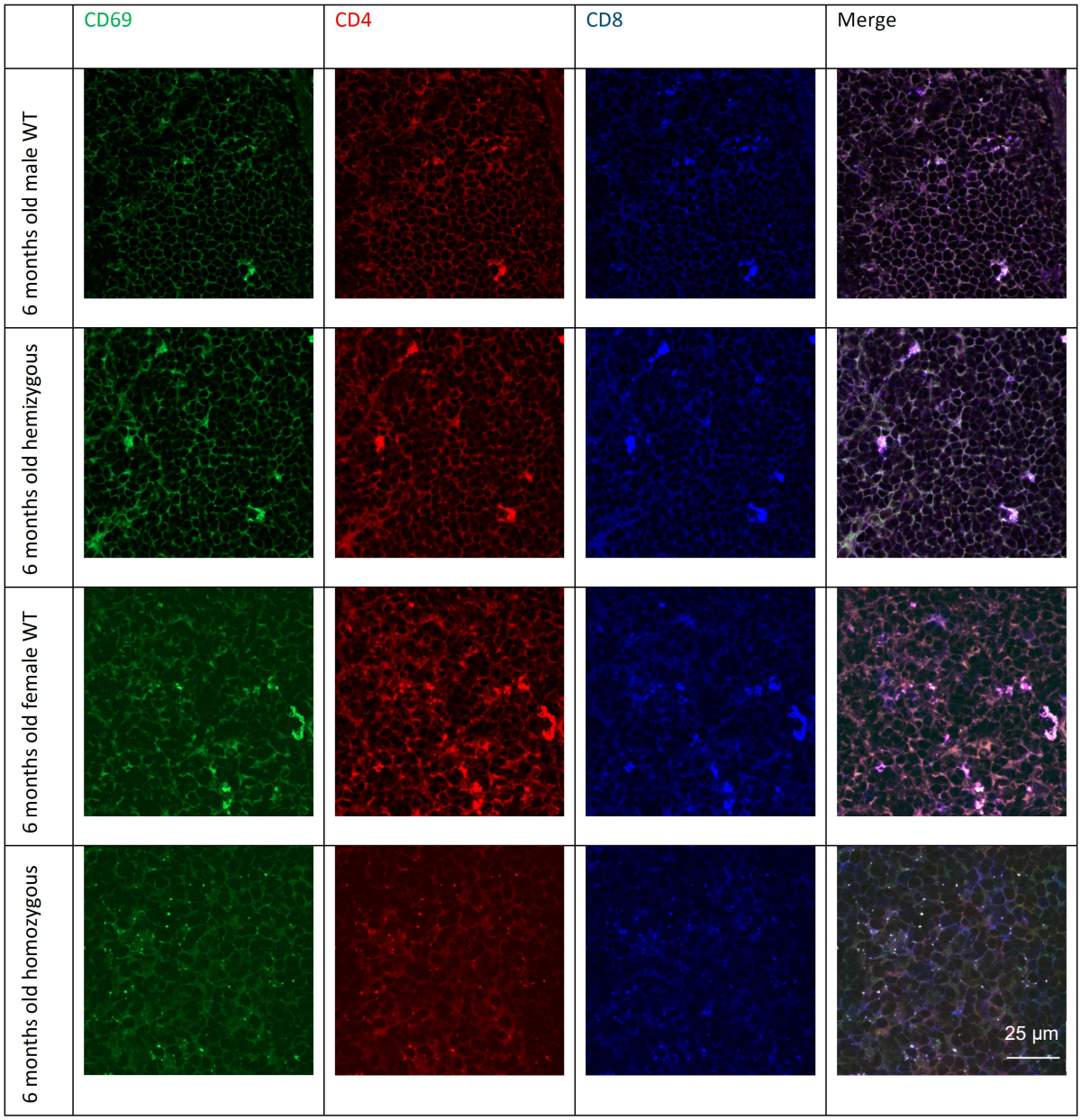

Figure 23b. Immunofluorescent staining of lymph node with antibodies directed against T cell activation marker (CD69, green), CD4 (red) and CD8 (blue). n=1-3 mice. Representative images are shown. Abbreviation: WT,wildtype. Scale bar: 25 µm.

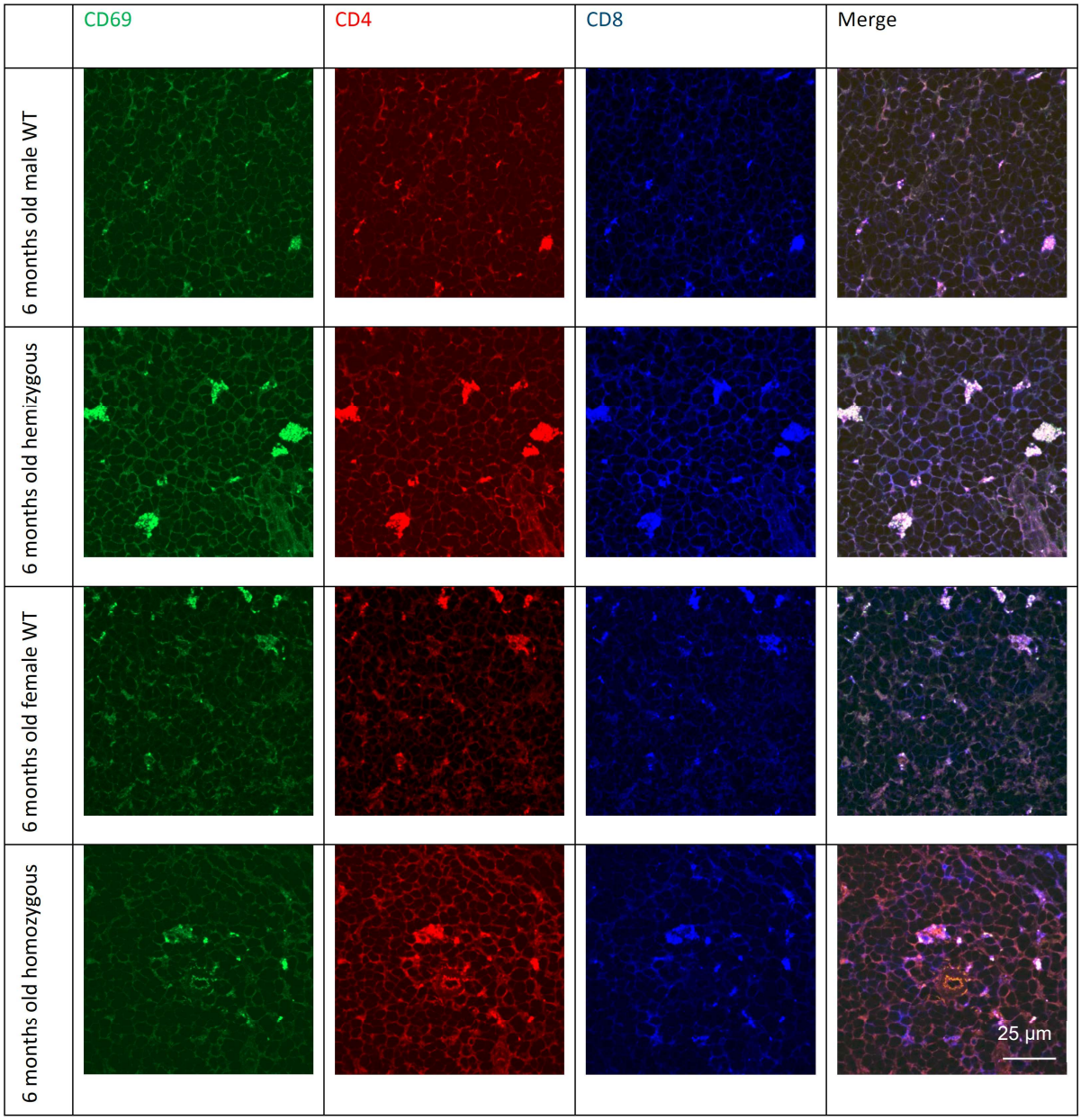

Figure 24a. Immunofluorescent staining of spleen with antibodies directed against T cell activation marker (CD69, green), CD4 (red) and CD8 (blue). n=1-3 mice. Representative images are shown. Abbreviation: WT,wildtype. Scale bar: 25 µm.

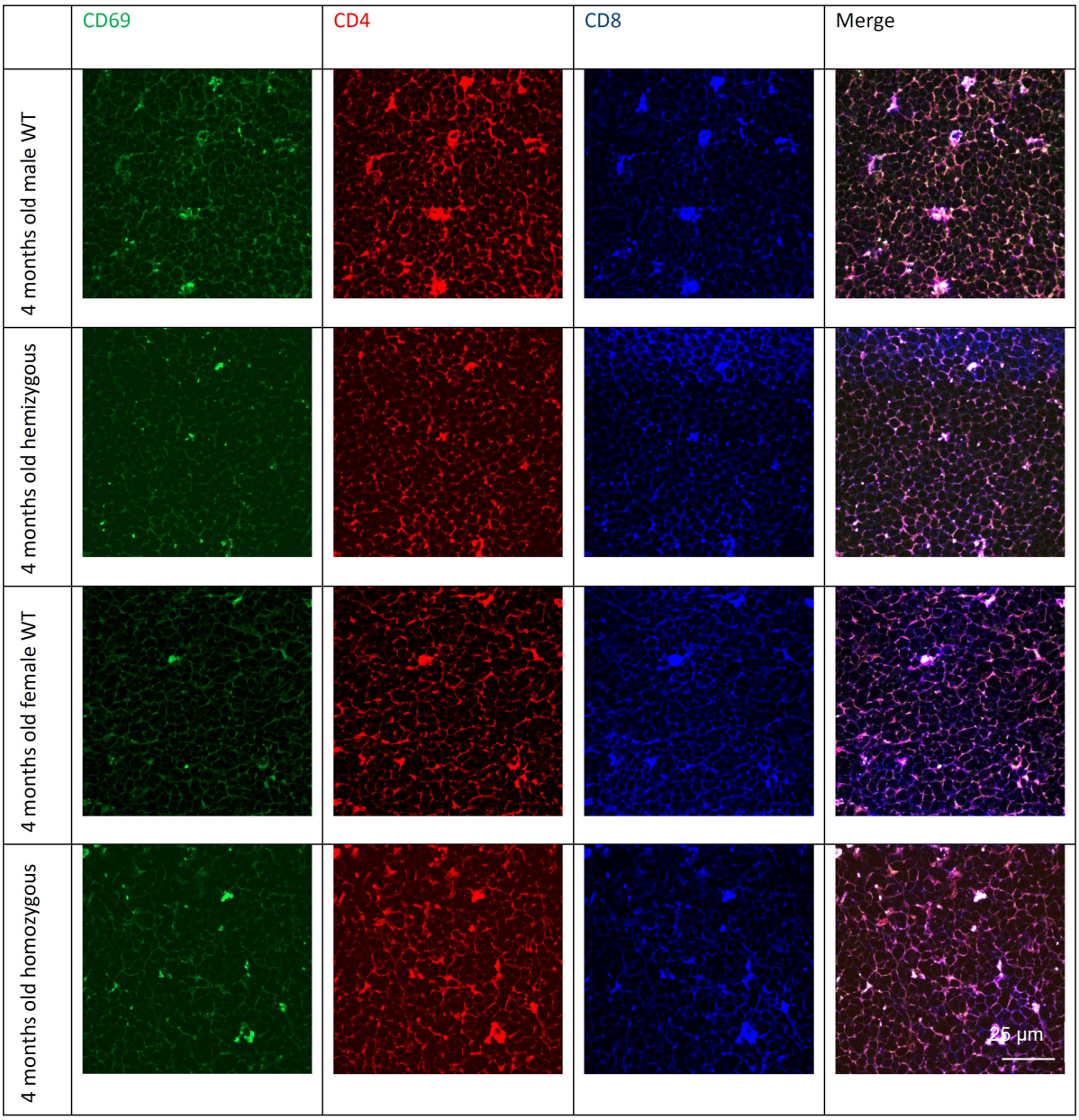

Figure 24b. Immunofluorescent staining of spleen with antibodies directed against T cell activation marker (CD69, green), CD4 (red) and CD8 (blue). n=1-3 mice. Representative images are shown. Abbreviation: WT,wildtype. Scale bar: 25 µm.

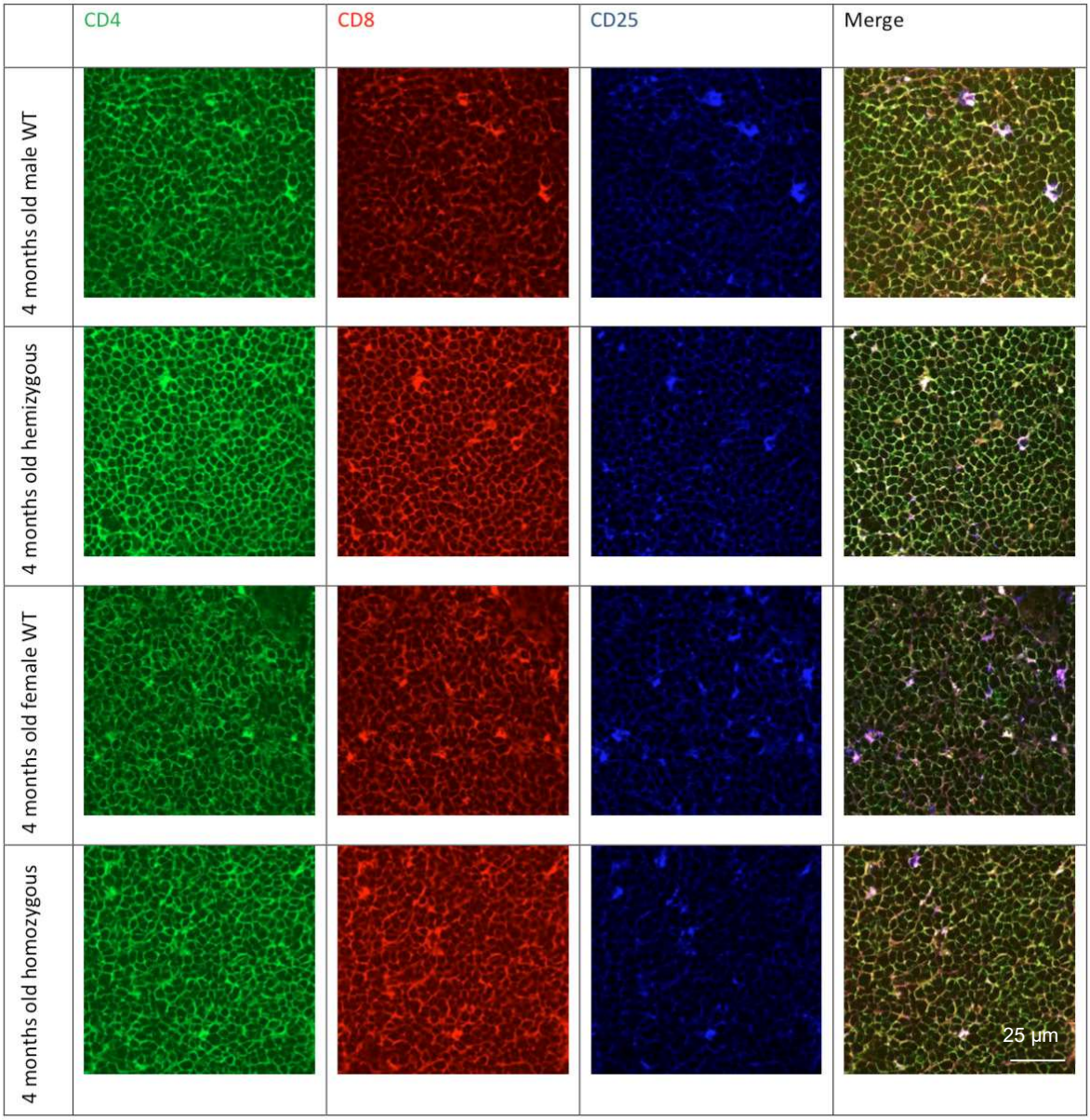

Figure 25. Immunofluorescent staining of thymus with antibodies directed against CD4 (green), CD8 (red) and T cell activation marker (CD25, blue). n=2-3 mice. Representative images are shown. Abbreviation: WT,wildtype. Scale bar: 25 µm.

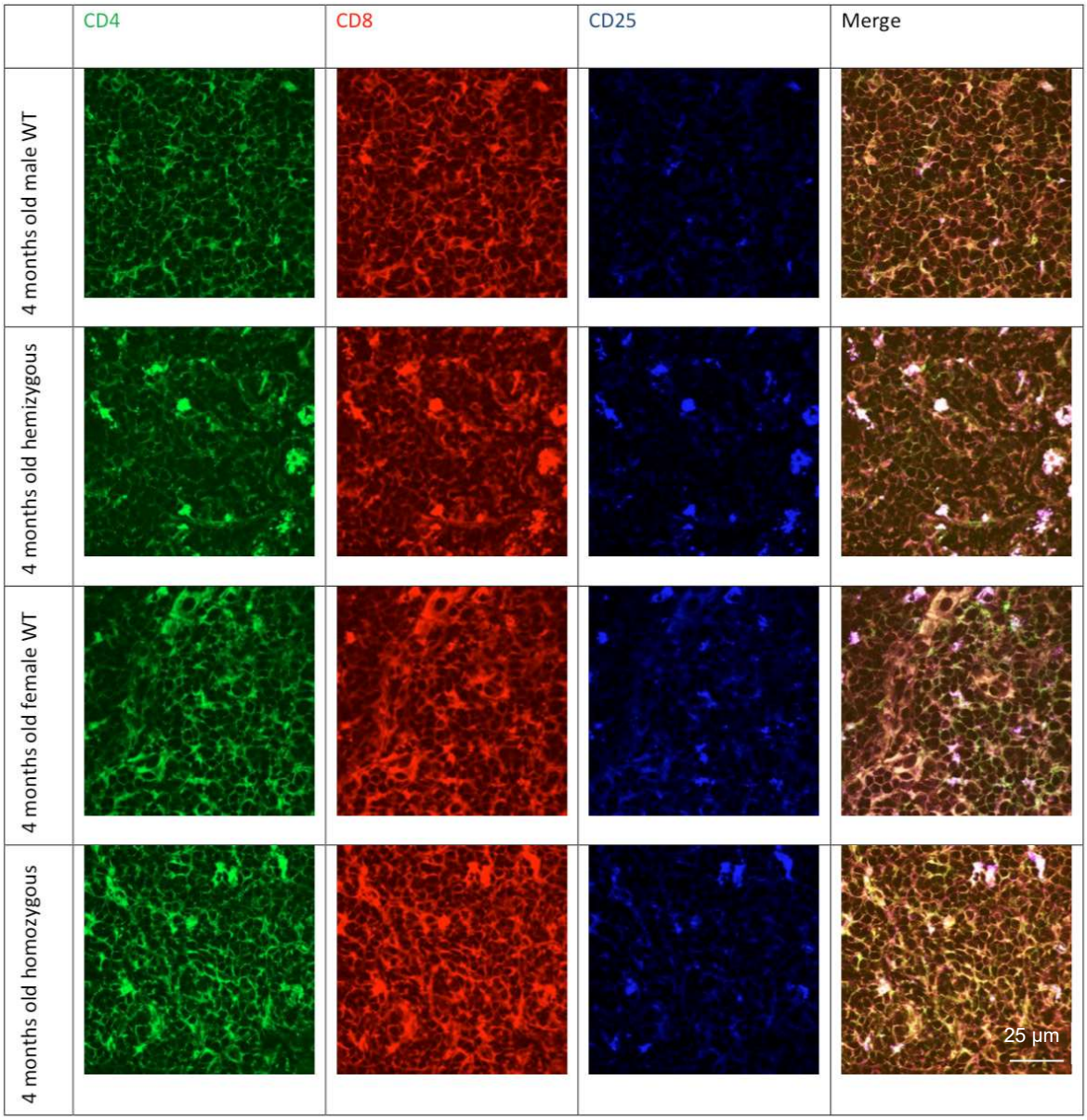

Figure 26a. Immunofluorescent staining of lymph node with antibodies directed against CD4 (green), CD8 (red) and T cell activation marker (CD25, blue). n=1-3 mice. Representative images are shown. Abbreviation: WT,wildtype. Scale bar: 25 µm.

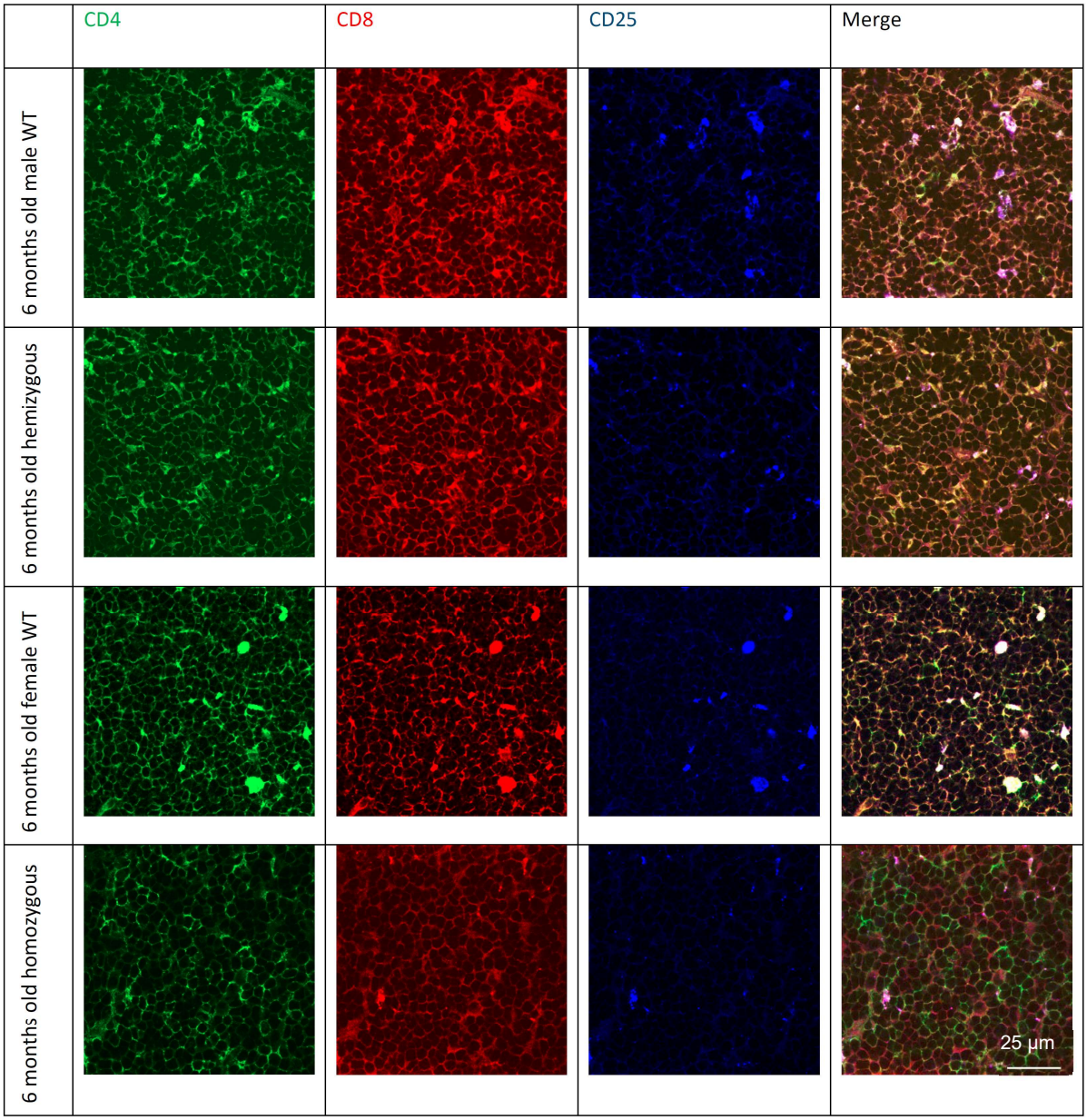

Figure 26b. Immunofluorescent staining of lymph node with antibodies directed against CD4 (green), CD8 (red) and T cell activation marker (CD25, blue). n=1-3 mice. Representative images are shown. Abbreviation: WT,wildtype. Scale bar: 25 µm.

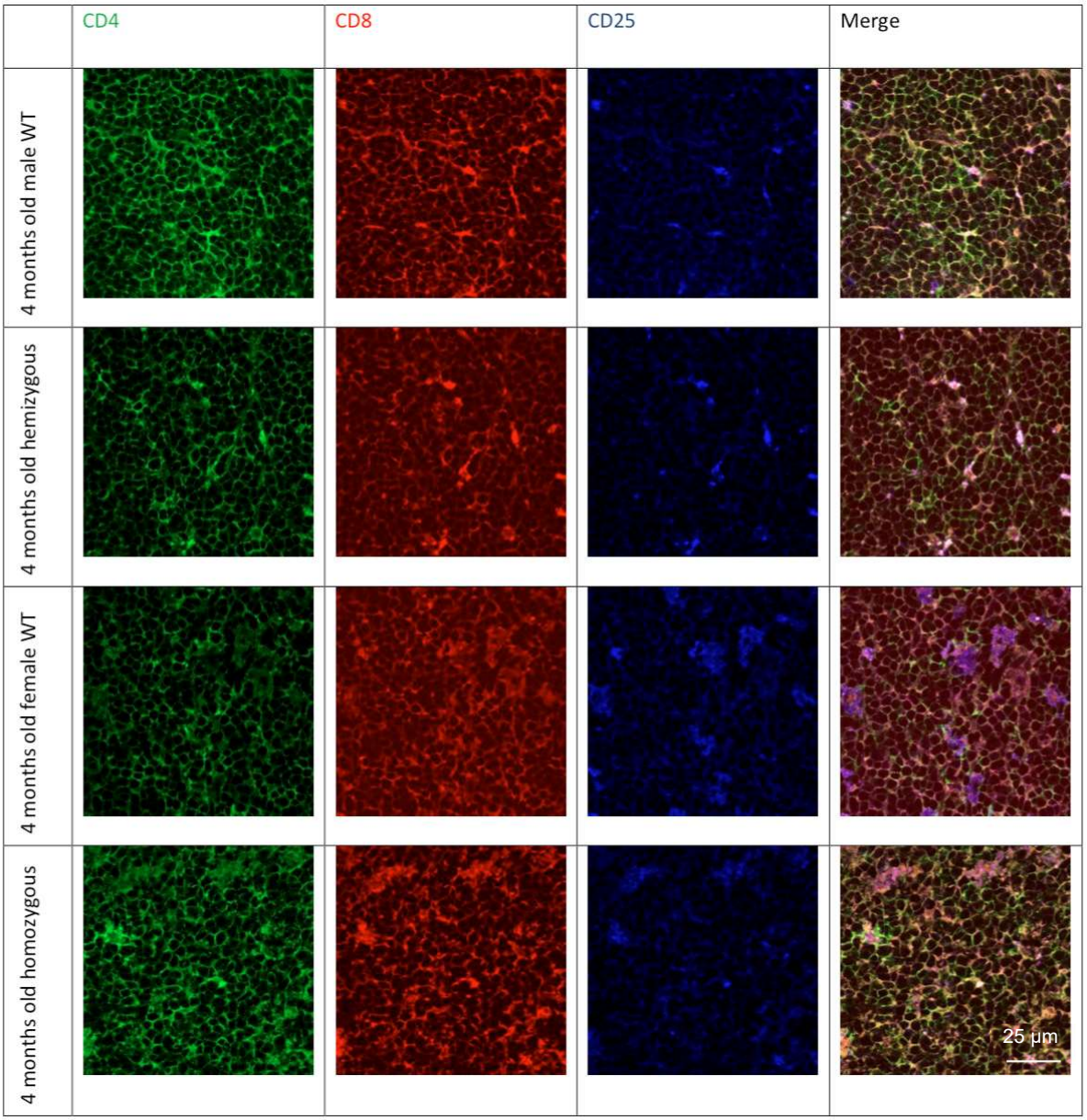

Figure 27a. Immunofluorescent staining of spleen with antibodies directed against CD4 (green), CD8 (red) and T cell activation marker (CD25, blue). n=1-3 mice. Representative images are shown. Abbreviation: WT,wildtype. Scale bar: 25 µm.

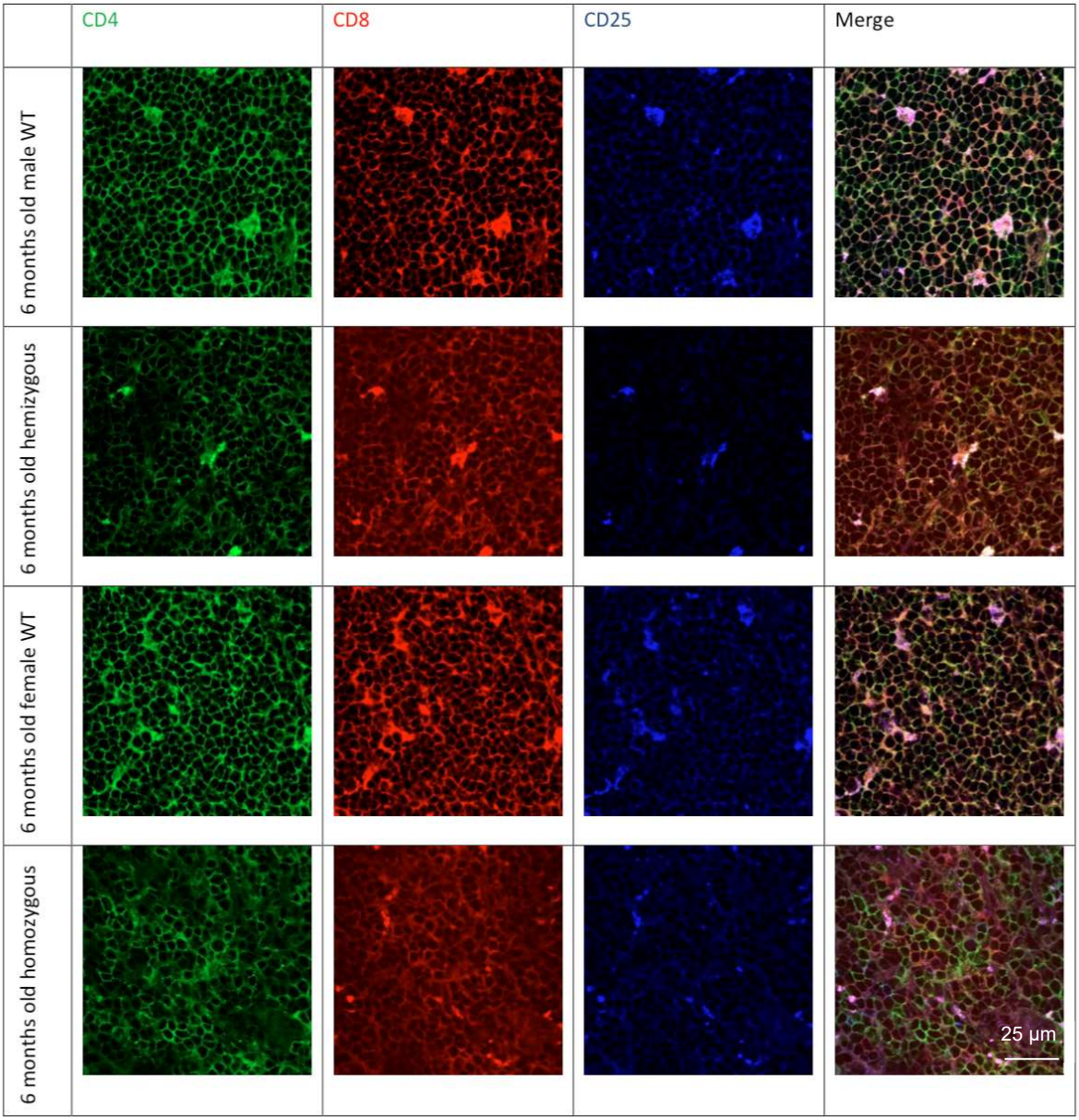

Figure 27b. Immunofluorescent staining of spleen with antibodies directed against CD4 (green), CD8 (red) and T cell activation marker (CD25, blue). n=1-3 mice. Representative images are shown. Abbreviation: WT,wildtype. Scale bar: 25 µm.

3.7 B cell population

Flow cytometry was performed to study the B cell population (Fig. 28). Anti-CD45R/B220 and anti-CD19 were used to identify B cells. CD45R/B220 is an isoform of CD45 which expresses on B cells at all stages, activated B cells, some T cell and NK cell subtypes. It is therefore used as a pan-B cell marker. CD19 is member of Ig superfamily. It is a surface marker of all pro-B cells to mature B cells. It is more specific for labeling B cells, and was used together with CD45R/B220 in this study. B cells in thymus were not identified, because the percentage of B cell population was too low.

The percentages of B cells in immune cells were unchanged in spleen and LN (Fig. 28). It was shown as well by the total cell numbers. Asm overexpression did not appear to have effect on the basal B cell population.

3.8 B and T lymphocyte localization

B and T cells are usually located at the white pulp, while in red pulp, only scattering of lymphocytes can be seen. MZB are in the pre-activated state, their cell sizes are larger than the follicular B cells and have higher expression of activation markers, such as CD69 and CD86 (Martin and Kearney 2001).

Anti-B220 antibody was for labeling B cells. The B cell follicles, marginal B cell zone, T cells zone and central arteries were identified in spleen and LN (Fig. 29-30). Since the purpose of the project was to give a general picture of the immune system, the follicular B cell or MZB were not distinguished. When comparing WT with the Tg, no difference could be seen with the B cell localization. The spleen and LN did not seem to have any depletion or increase in both follicular B cells and MZB as the sizes of the area remained similar. Anti-CD3 was used as T cell marker. In both LN and spleen there was no change of area size or CD3 expression, in between WT and Tg, regardless of age and gender.

As shown by the biochemical mass spectrometry, there was no trend in the ceramide level when comparing the genotypes. It is consistent in the IF images. No change in expression in the Tg could be observed.

Interestingly, ceramide appeared to colocalize with B cells very closely. There was a ring of high ceramide expressing cells around B cells. The ring seems to be the marginal zone.

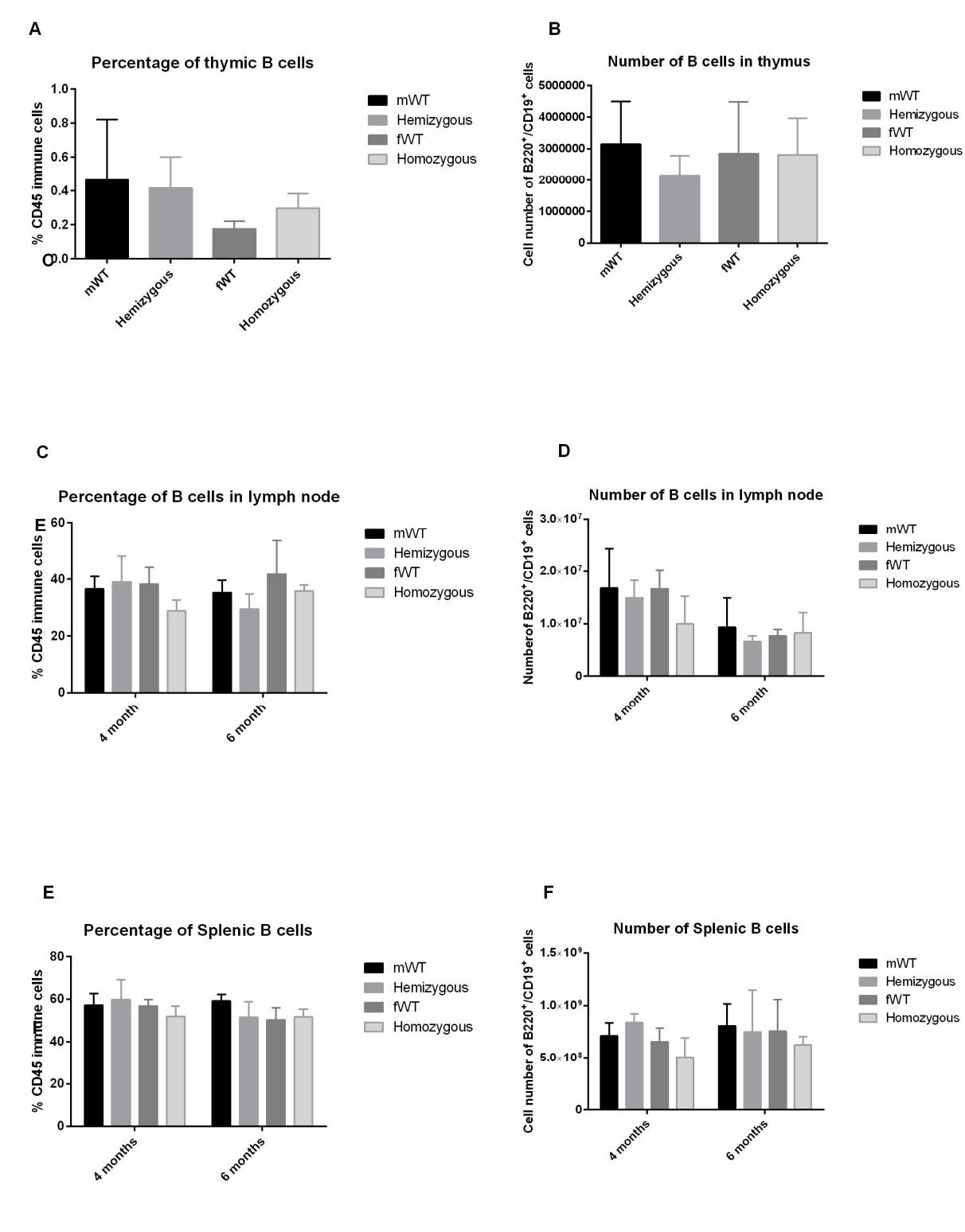

Figure 28. B cell population analysis of on (A) thymus CD19+/B220+ percentage of immune cells, (B) cell number, (C) lymph node CD19+/B220+ percentage of immune cells (D) cell number, (E) splenic CD19+/B220+ percentage of immune cells Mean ± SD. n = 3-5 mice. Significant differences were assessed by one-way ANOVA in thymus, and two-way ANOVA in lymph node and spleen. mWT,male wildtype; fWT, female wildtype.

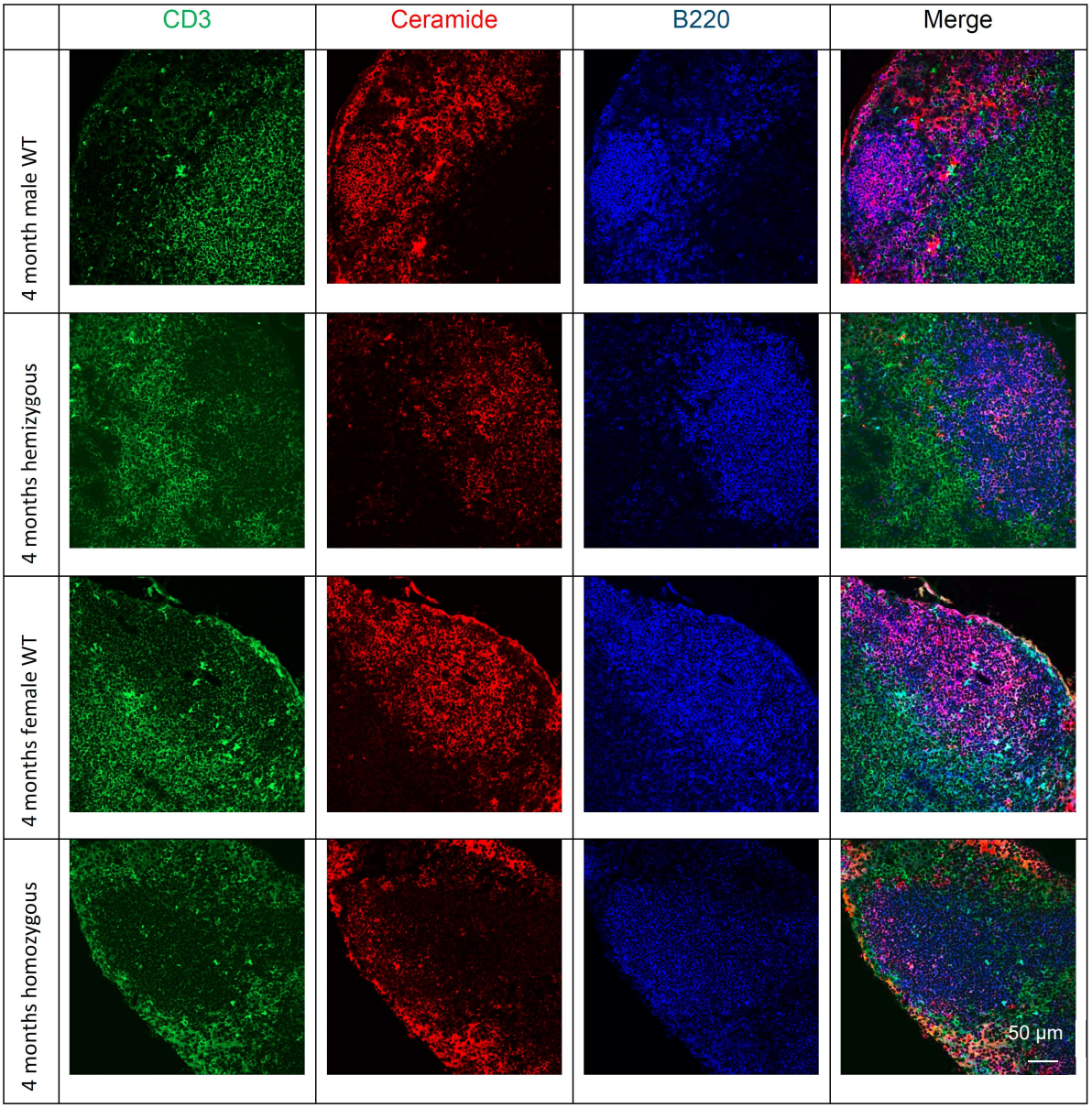

Figure 29a. Immunofluorescent staining of lymph node with antibodies directed against T cell (CD3, green), Ceramide (red) and the B cell (B220, blue). n=1-3 mice. Representative images are shown. Abbreviation: WT, wildtype. Scale bar: 50 µm.

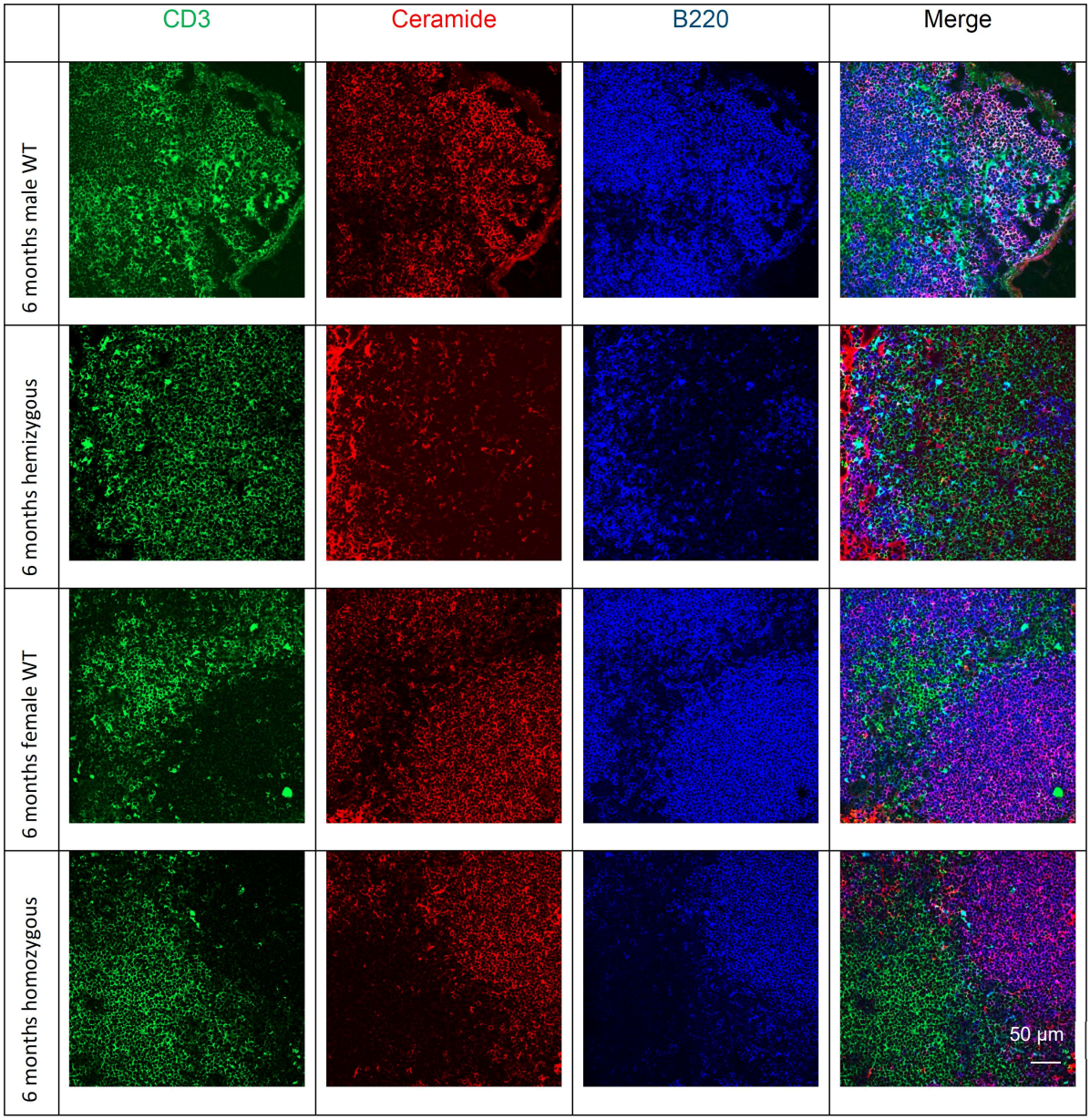

Figure 29b. Immunofluorescent staining of lymph node with antibodies directed against T cell (CD3, green), Ceramide (red) and the B cell (B220, blue). n=1-3 mice. Representative images are shown. Abbreviation: WT, wildtype. Scale bar: 50 µm.

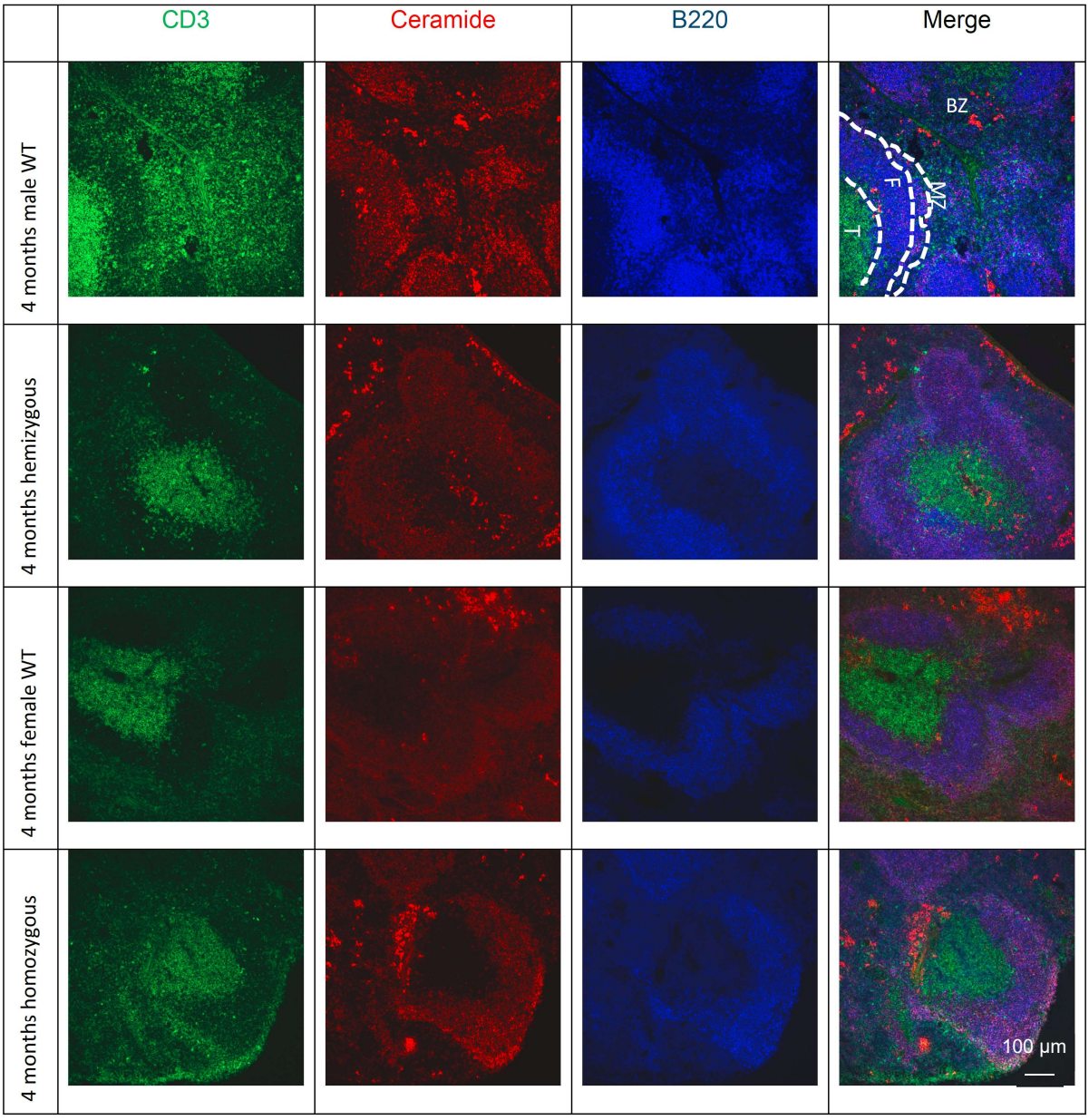

Figure 30a. Immunofluorescent staining of spleen with antibodies directed against T cell (CD3, green), Ceramide (red) and the B cell (B220, blue). n=1-3 mice. Representative images are shown. Abbreviation: WT, wildtype; MZ, marginal zone; BZ, bridging zone; T, T-cell zone, F, B cell follicle. Scale bar: 100 µm.

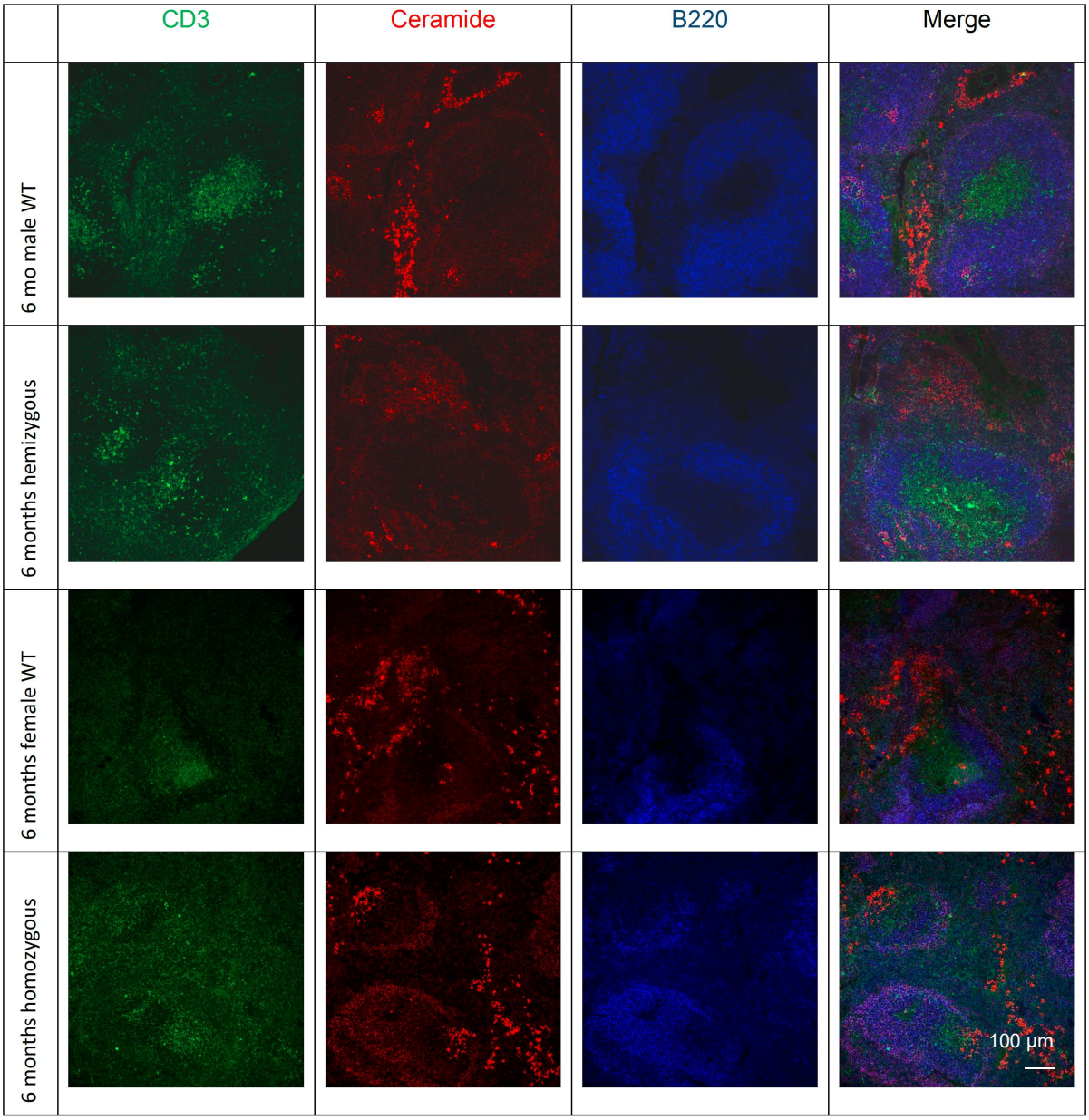

Figure 30b. Immunofluorescent staining of spleen with antibodies directed against T cell (CD3, green), Ceramide (red) and the B cell (B220, blue). n=1-3 mice. Representative images are shown. Abbreviation: WT, wildtype. Scale bar: 100 µm.

3.9 Neutrophil population

Anti-Ly6G (Clone 1A8) is widely used for the identification of neutrophils. Ly6G is expressed primarily on neutrophils, as well as some developing monocytes and subsets of eosinophils. The clone 1A8 is specific for Ly6G, unlike other clones which bind to both Ly6G and Ly6C (Rehg, 2012).

No significant differences in neutrophil numbers between the genotypes were detected in all three organs of the 4 or 6 month-old mice (Fig. 31).

3.10 Neutrophil localization

Neutrophils are migrating from blood to the lymphoid organ during inflammation. They are located at the closest to the vessels, which is the white pulp cord in spleen, the T cell zone in LN and medulla in thymus.

Images around the blood vessels in all three organs were captured (Fig. 32-34), to see the migration of neutrophils. No obvious neutrophil immigration could be found. Neutrophils were also co-stained with ceramide antibody. They did not co-localize and did not seem to have correlation. However, ceramide expressing cells were found clustering around the blood vessels. The cell type was unknown.

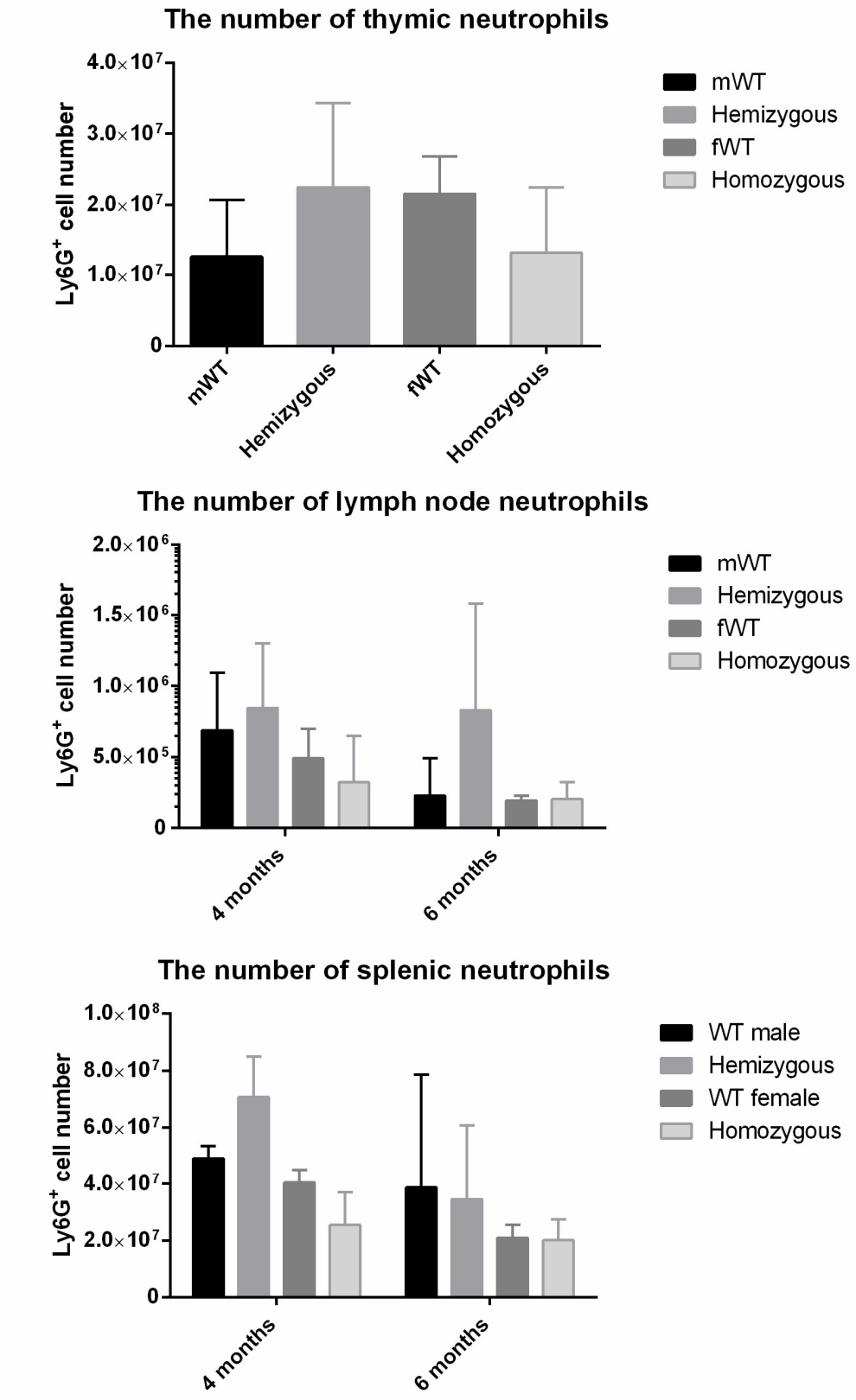

Figure 31. Neutrophil cell number of (A) thymus, (B) lymph node, (C) spleen. Mean ± SD. n = 3- 5 mice. Significant differences were assessed by one-way ANOVA in thymus, and two-way ANOVA in lymph node and spleen.

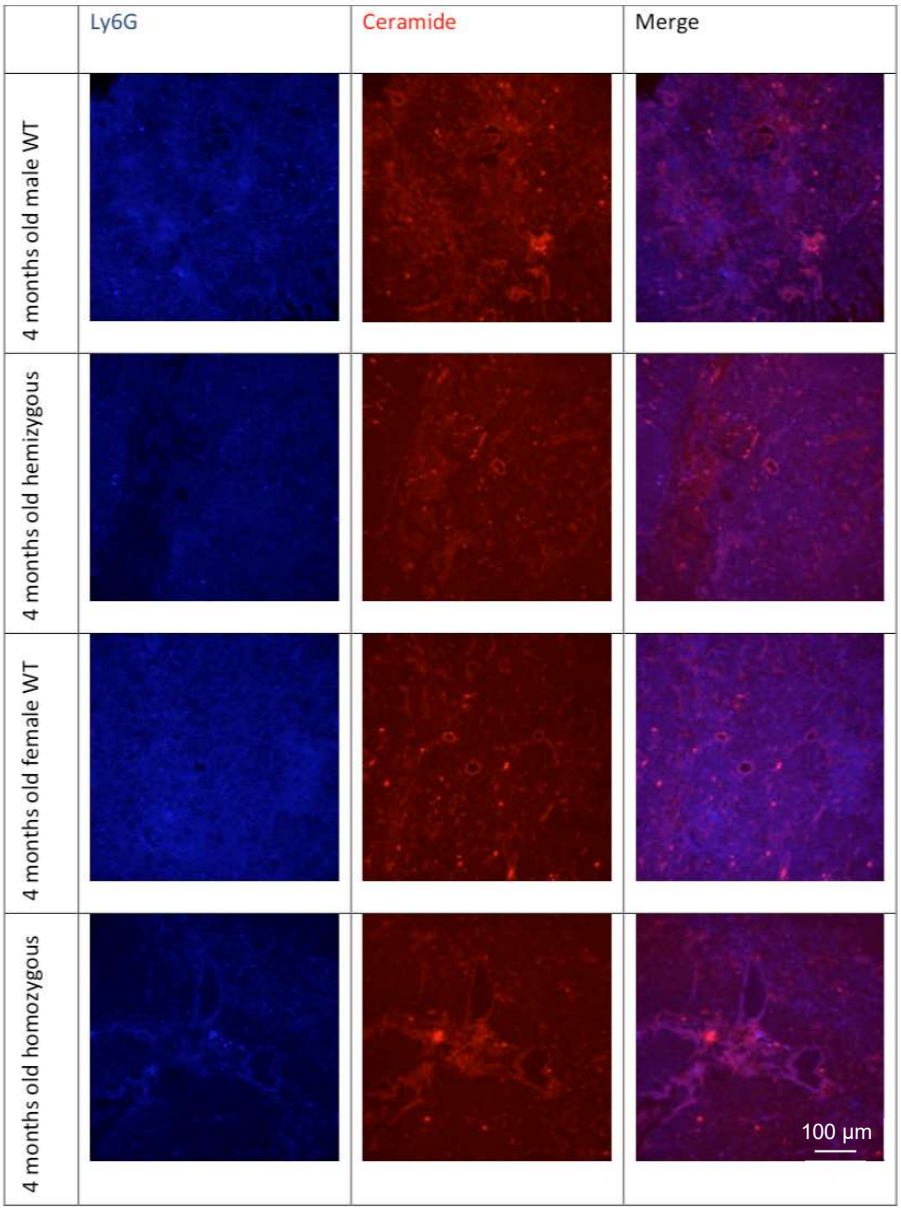

Figure 32. Immunofluorescent staining of thymus with antibodies directed against neutrophil (Ly6G, blue) and Ceramide (red). n=2-3 mice. Representative images are shown. Abbreviation: WT, wildtype. Scale bar: 100 µm.

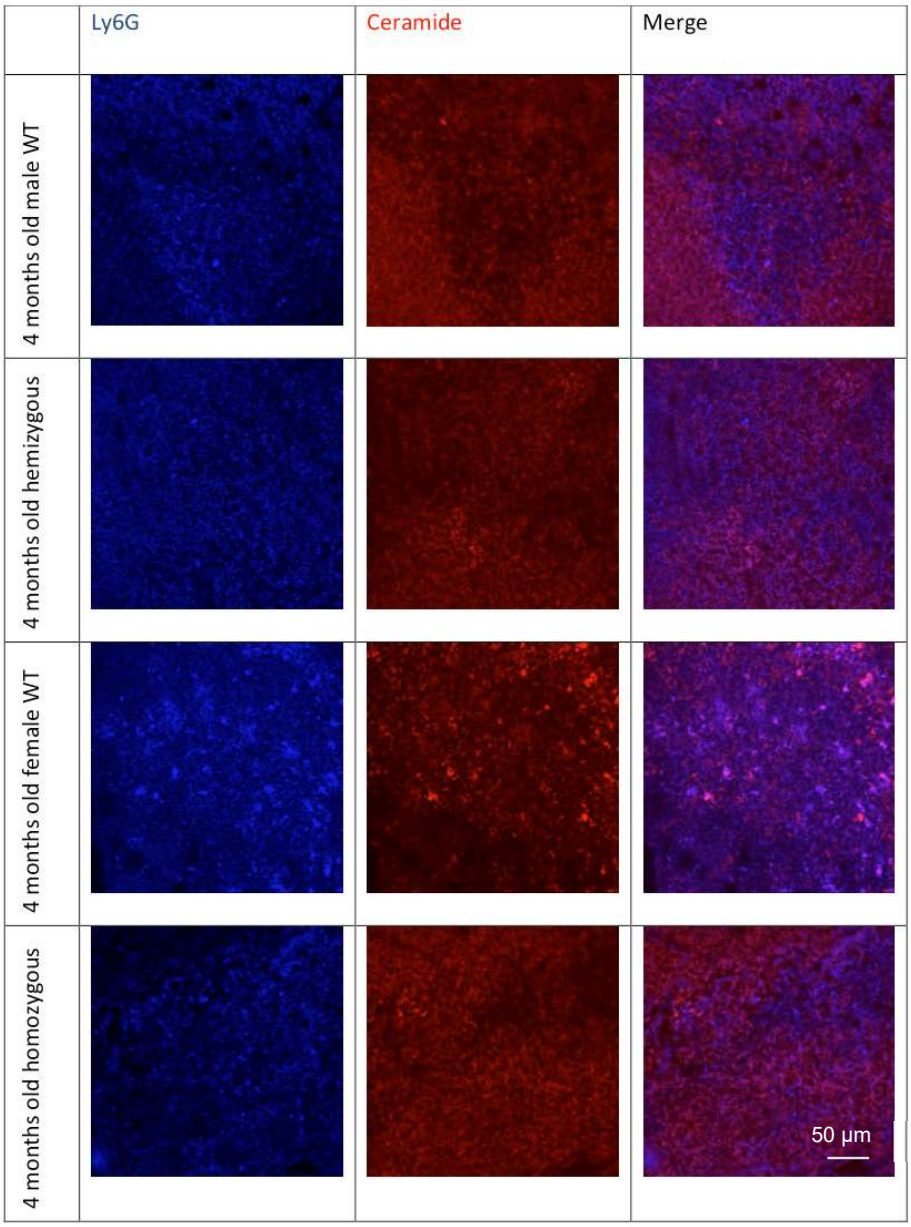

Figure 33a. Immunofluorescent staining of lymph node with antibodies directed against neutrophil (Ly6G, blue) and Ceramide (red). n=1-3 mice. Representative images are shown. Abbreviation: WT, wildtype. Scale bar: 50 µm.

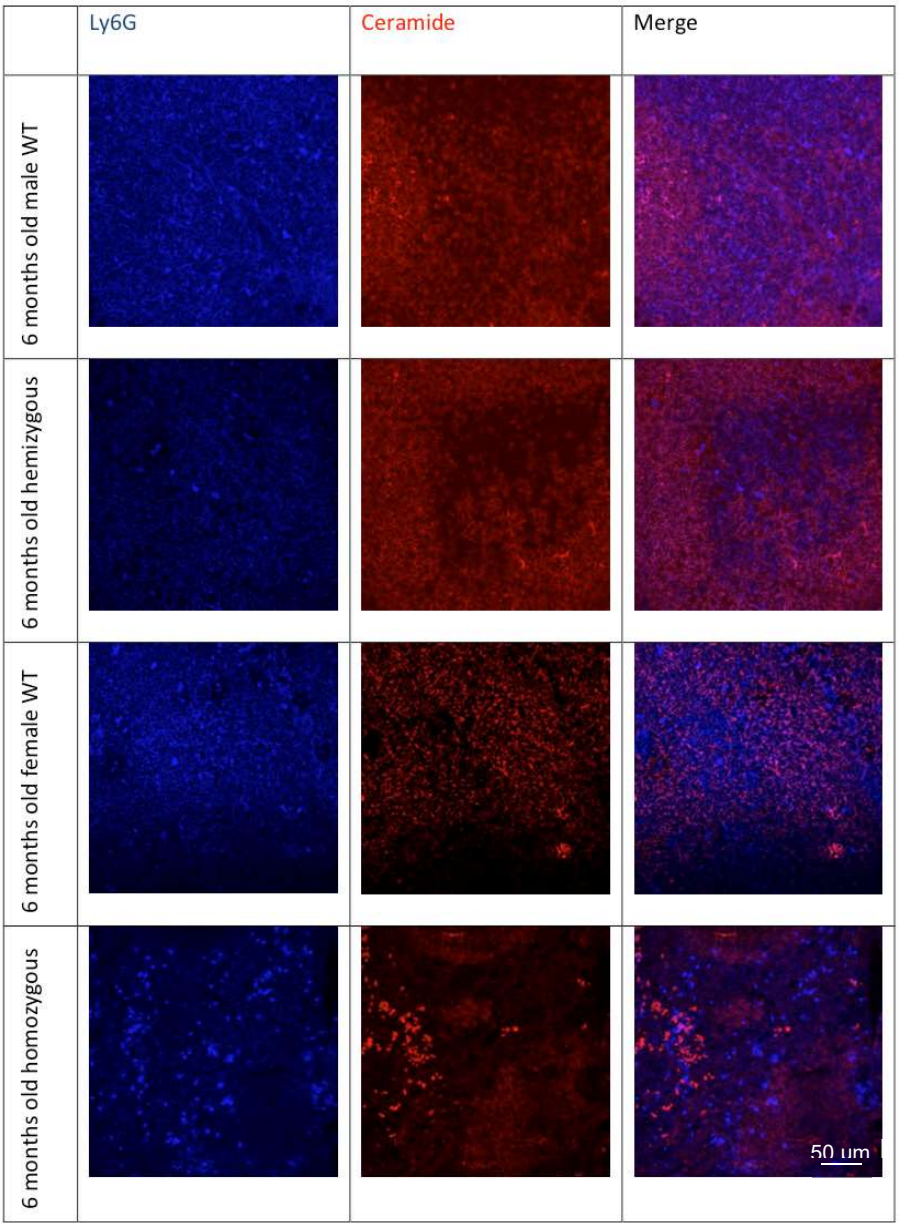

Figure 33b. Immunofluorescent staining of lymph node with antibodies directed against neutrophil (Ly6G, blue) and Ceramide (red). n=1-3 mice. Representative images are shown. Abbreviation: WT, wildtype. Scale bar: 50 µm.

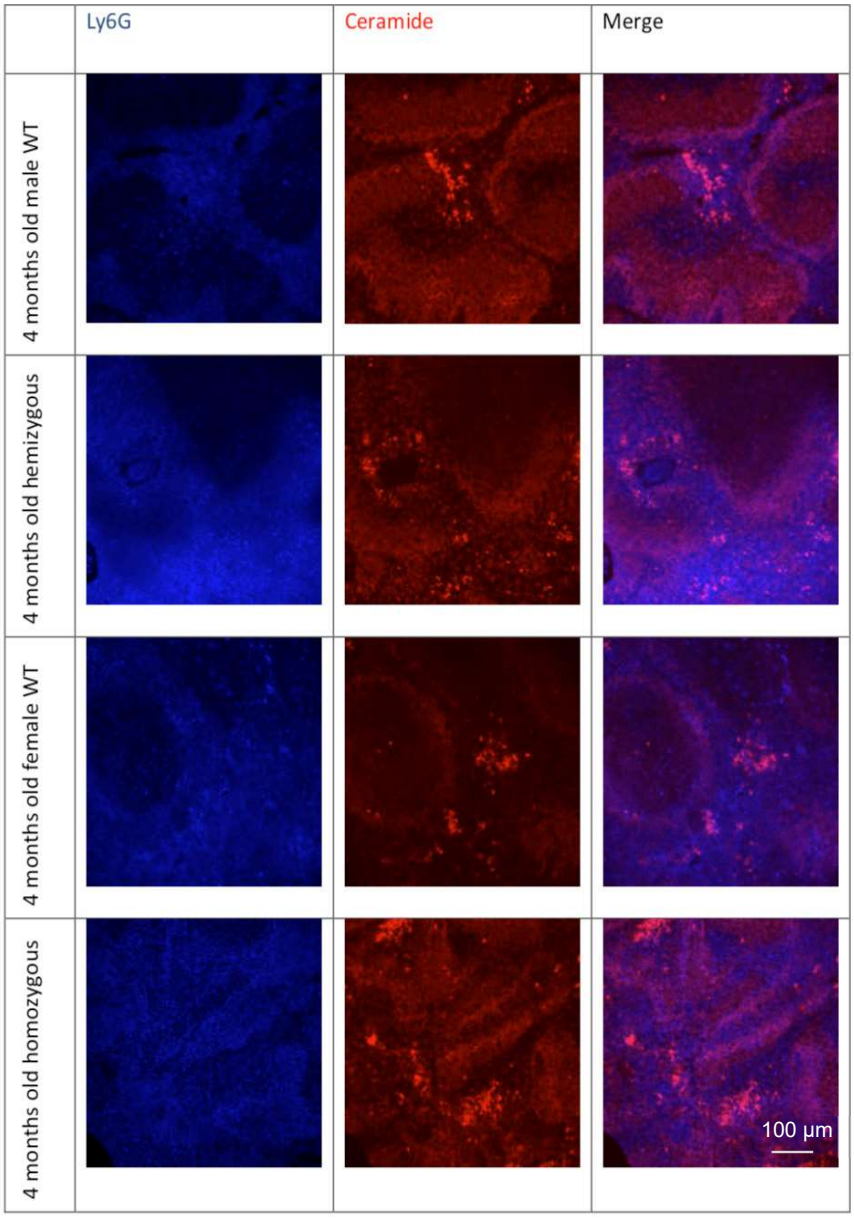

Figure 34a. Immunofluorescent staining of spleen with antibodies directed against neutrophil (Ly6G, blue) and Ceramide (red). n=1-3 mice. Representative images are shown. Abbreviation: WT, wildtype. Scale bar: 100 µm.

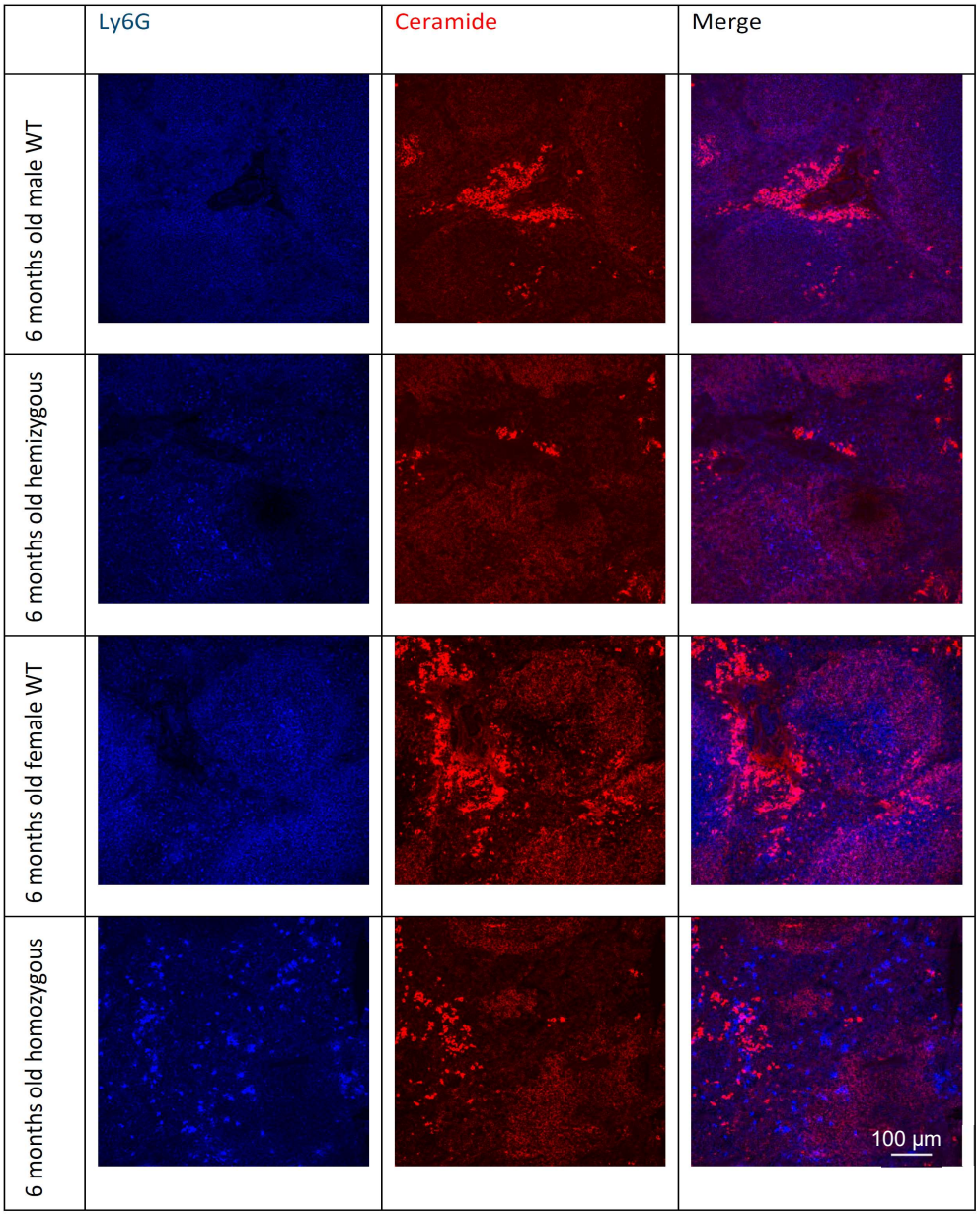

Figure 34b. Immunofluorescent staining of spleen with antibodies directed against neutrophil (Ly6G, blue) and Ceramide (red). n=1-3 mice. Representative images are shown. Abbreviation: WT, wildtype. Scale bar: 100 µm.

3.11 Macrophage population

F4/80 expresses on the membrane surface of most of the macrophages in mice. It expresses weakly in neutrophils and lymphocytes, which makes it a specific macrophage marker. It only labels the macrophage populations in splenic red pulp, lymph node medullary cords and thymic corticomedullary junction region (Rehg, 2012). Investigations on other macrophage populations are not in the scope of this project and could be studied further if necessary. The macrophages populations with flow cytometry (Fig. 35) and IF (Fig. 36-38) were inspected.

In the thymus of the 4 months old mice followed the same pattern: the male WT, hemizygous, and the homozygous mice had approximately the same macrophage numbers, but the female WT had distinctively high number of macrophages in thymus. Macrophage number in spleen showed similar trend. In LN, the numbers remained unchanged in between the WT and the Tg mice, in both genders and ages.

The trend in splenic macrophage population looked alike to that of splenic SM level, particularly SM16. In 4 months old mice, both the splenic macrophages number and the SM16 were the highest among all genotypes. And in the 6 months old mice, male WT and homozygous mice were having higher macrophage number and SM16 level than the hemizygous and female WT. Though the correlation was not statistically confirmed, it could be a preliminary idea to continue on.

3.12 Macrophages localization

Macrophages in spleen primarily localized at the red pulp for its functions. Since red pulp is made up of arteries, arterioles, sinuses and veins, macrophages can easily filter the blood. Apart from red pulp macrophages, there are two other populations of macrophages in the spleen, marginal zone and marginal metallophilic macrophages. Marginal zone macrophages form outer ring surrounding white pulp, and can be labeled with SIGNR1. The inner ring is the marginal metallophilic macrophages, expressing the cell marker CD169.

Macrophages in LN can be classified into subcapsular sinus and medullary macrophages, according to their locations. The function of medullary macrophages is similar to red pulp macrophages but instead of blood they filter lymph. Most of them are $F4/80^{+}$, $CD169^{+}$ and $Mac1^{+}$. Subcapsular sinus macrophages function to present an-

tigen to nearby follicular B cells. They express CD169 and Mac1, but not F4/80 (Gray and Cyster, 2012).

$F4/80^+$/ $Mac\text{-}2^+$ macrophages are found to distribute predominantly in the whole thymus. There are two other subtypes in the cortex and medullar: those in the cortex are positive for F4/80 antibodies, while those in medulla and corticomedullary region are positive for Mac-2 antibodies (Liu, 2013).

In the present study, anti-F4/80 (in Blue) was used to label the macrophage in cryosections (Fig. 36-38). It could only label the majority of macrophages, as the rest do not express F4/80. Monocyte marker CD11b (in green) was used in parallel.

$F4/80^+$ macrophages were very densely distributed and IF was not a good assessment to quantify the population in this case. In spleen most of the macrophages localized in red pulp, in both WT and Tg. CD11b expressions varied from mouse to mouse, and no particular trend could be observed. There were some $F4/80^-$ $CD11b^+$ cells around marginal zone. CD169 and SIGNR1 could be used for further investigation. In all genotypes of thymus, most of them were distributed throughout the sections rather than staying in the cortex.

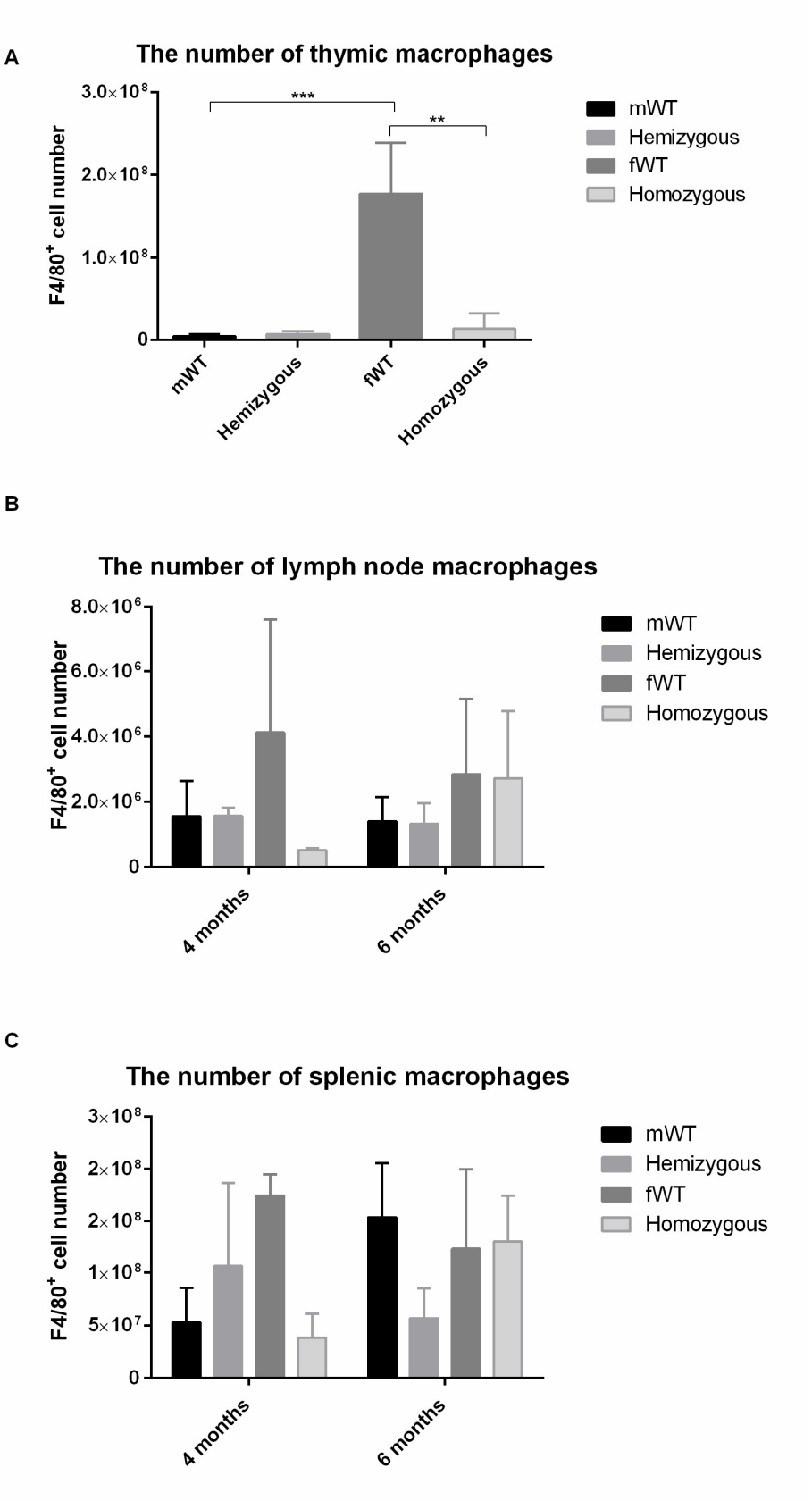

Figure 35. Macrophahge cell number of (A) thymus, (B) lymph node, (C) spleen. Mean ± SD. n = 3-5 mice. Significant differences were assessed by one-way ANOVA in thymus, and two-way ANOVA in lymph node and spleen: ** $p < 0.01$; *** $p < 0.001$. Abbreviation: mWT,male wildtype; fWT, female wildtype.

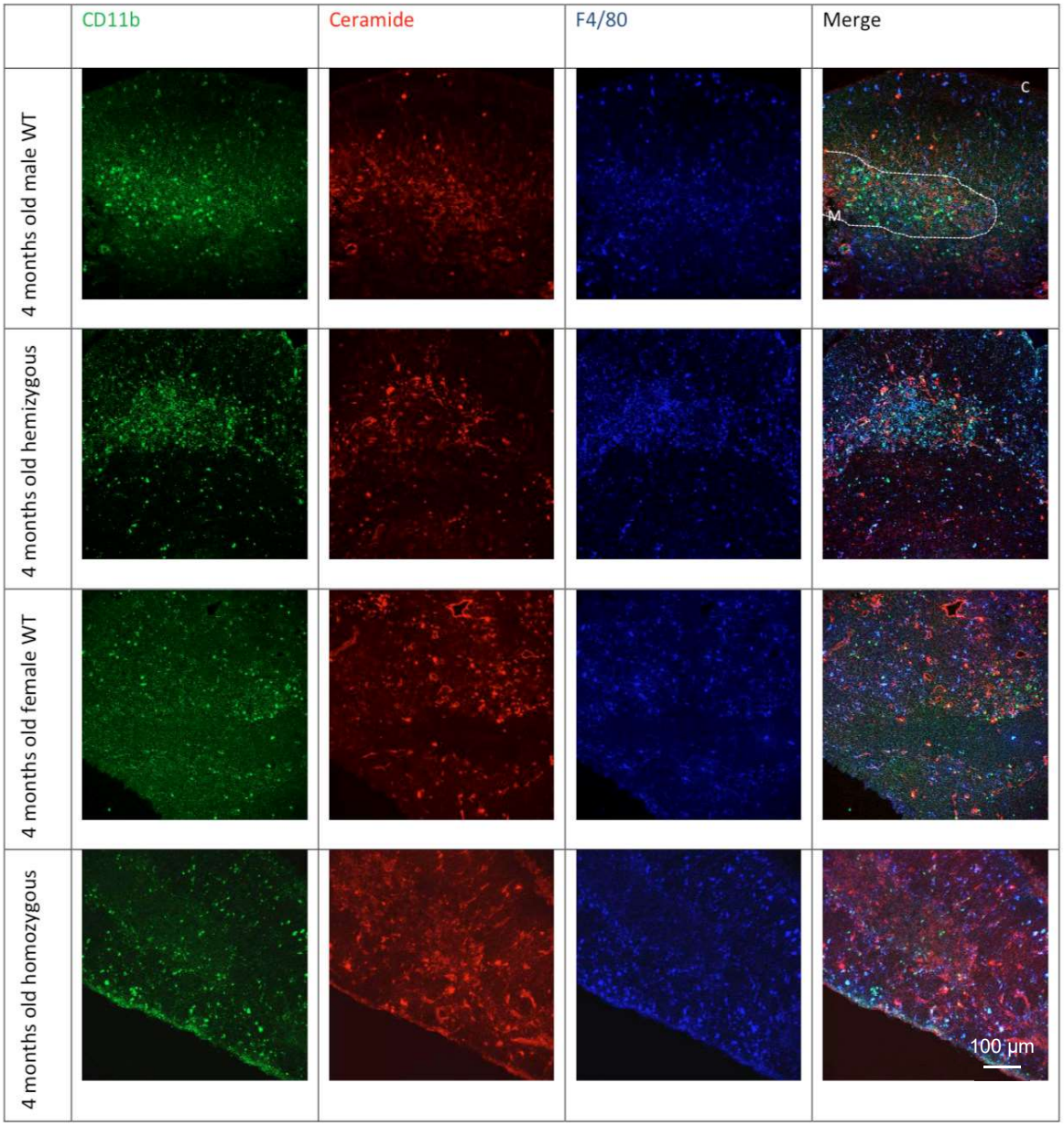

Figure 36. Immunofluorescent staining of thymus with antibodies directed against monocyte (CD11b, green), Ceramide (red) and the macrophage (F4/80, blue). n= 2-3. Representative images are shown. Abbreviation: WT, wildtype; M, medulla; C, corticomedullary region. Scale bar: 100 µm.

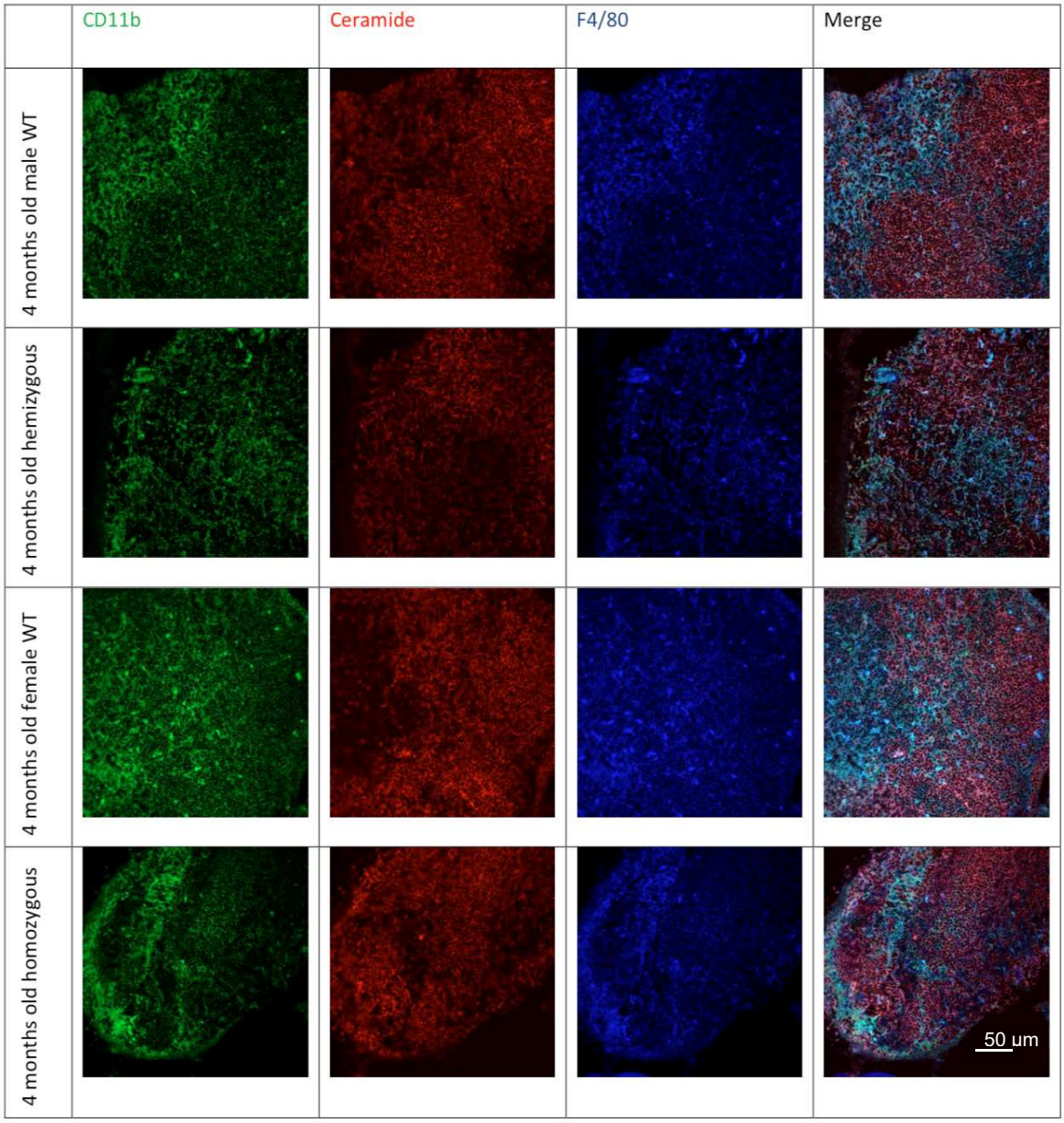

Figure 37a. Immunofluorescent staining of lymph node with antibodies directed against monocyte (CD11b, green), Ceramide (red) and the macrophage (F4/80, blue). n= 1-3. Representative images are shown. Abbreviation: WT, wildtype. Scale bar: 50 µm.

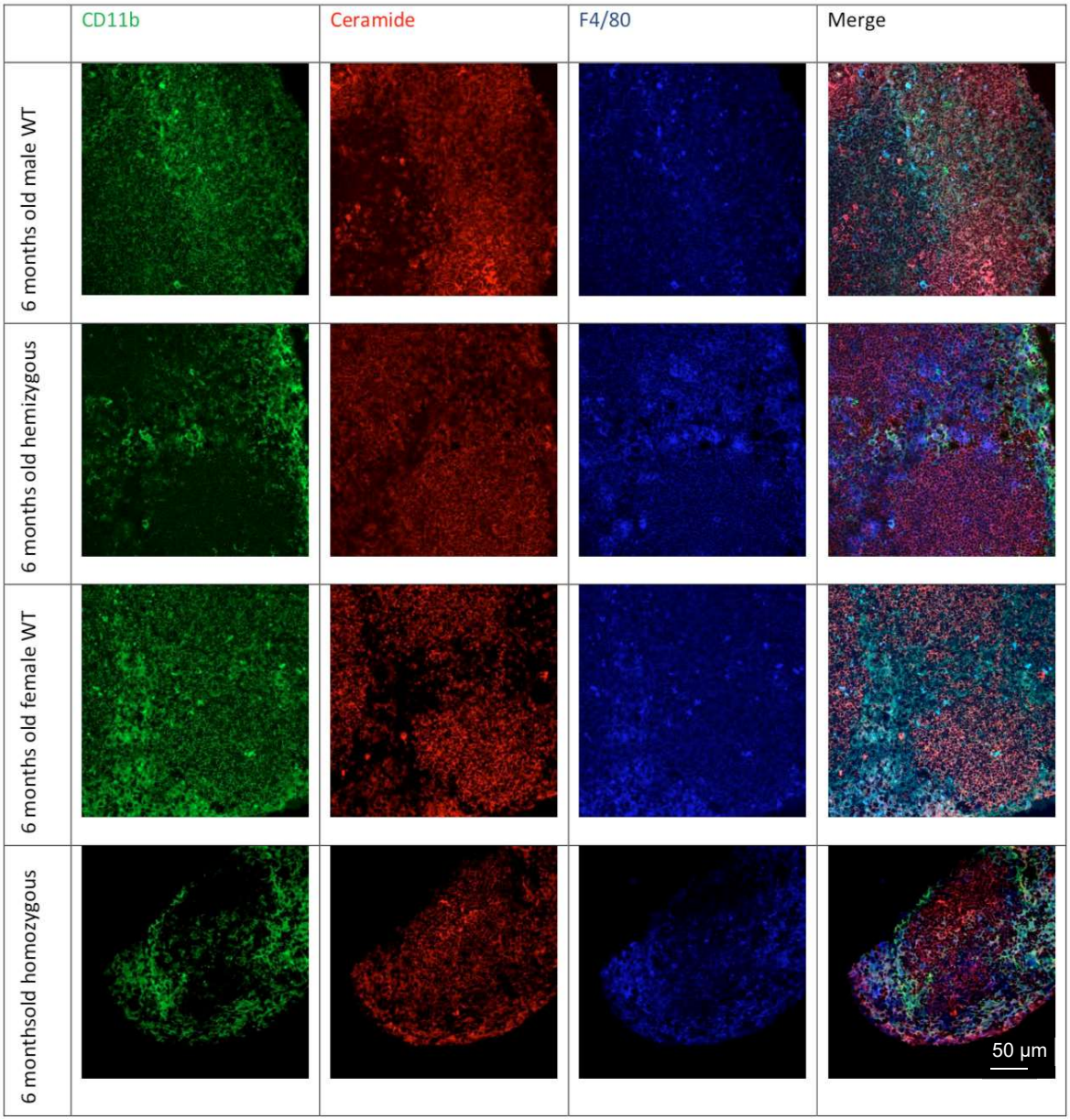

Figure 37b. Immunofluorescent staining of lymph node with antibodies directed against monocyte (CD11b, green), Ceramide (red) and the macrophage (F4/80, blue). n= 1-3. Representative images are shown. Abbreviation: WT, wildtype. Scale bar: 50 µm.

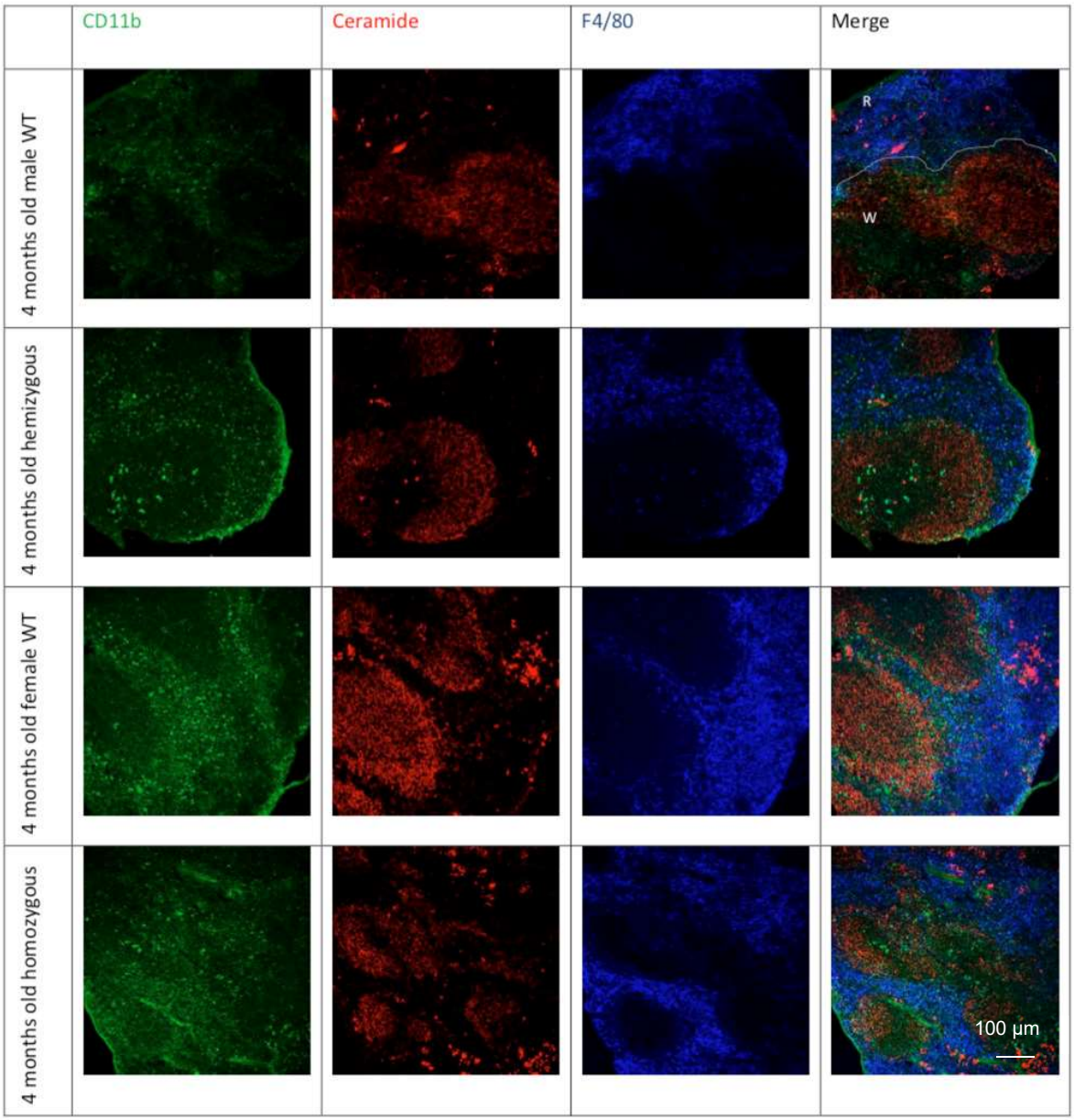

Figure 38a. Immunofluorescent staining of spleen with antibodies directed against monocyte (CD11b, green), Ceramide (red) and the macrophage (F4/80, blue). n= 1-3 mice. Representative images are shown. Abbreviation: R, red pulp; W, white pulp; WT, wildtype. Scale bar: 100 µm.

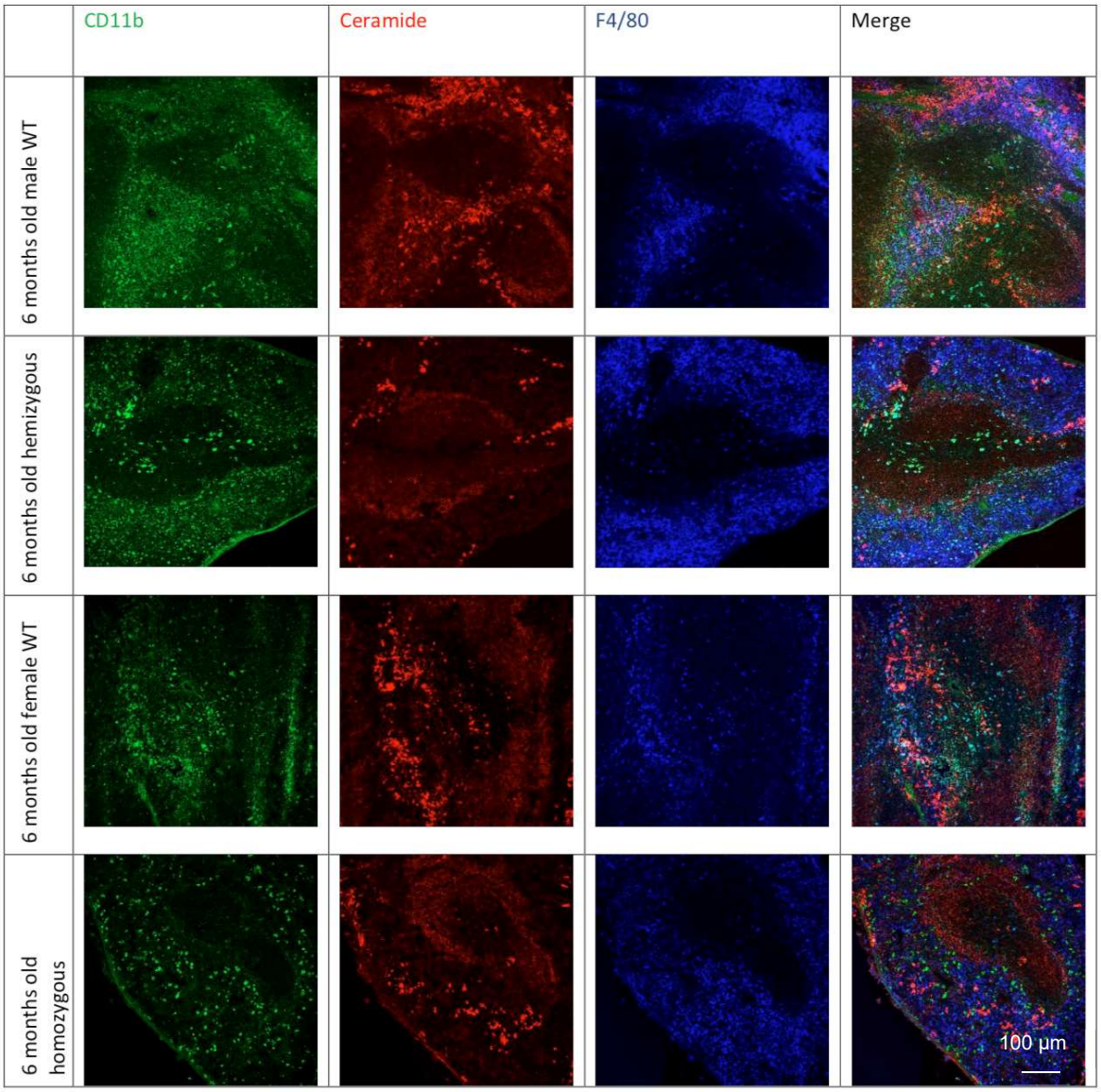

Figure 38b. Immunofluorescent staining of spleen with antibodies directed against monocyte (CD11b, green), Ceramide (red) and the macrophage (F4/80, blue). n= 1-3 mice. Representative images are shown. Abbreviation: WT, wildtype. Scale bar: 100 µm.

3.13 Dendritic cells

CD11c is a cell marker for dendritic cells and in small populations of monocytes and macrophages, as well as activated T cells and B cells. Anti-CD11c is popular to label dendritic cells in flow cytometry. It is also common to be used in frozen tissue for IF.

The trends in dendritic populations among organs were not comparable (Fig. 39). In the thymus of 4 months old mice, the female WT had the lowest number of DCs. It was significantly elevated to the highest in homozygous mice. In LN and spleen, the female mice had lower numbers of DCs. There were only slight changes between WT and Tg, and is not statistically significant.

LN had an observable reduction with age. The total numbers of DCs from both LN and spleen in 6 months old mice remain leveled among all genotypes.

3.14 Dendritic cell localization

Majority of DCs in lymphoid organs are conventional DCs. They all express high level of CD11c. Some of them express T cell marker CD4 and CD8. DCs hence are classified as $CD4^+$ $CD8^-$, $CD4^-$ $CD8^+$ and $CD4^-$ $CD8^-$ subtypes. The splenic DCs can be found in marginal zone and bridging zone (Mildner and Jung, 2014). The thymic DCs are distributed mainly in corticomedullary region and medulla (Lafontaine, 1997). Apart from residential DCs, LN also accommodates migrating DCs in the T cell zone (Turner and Mabbott 2017).

In the IF images (Fig. 40-42), $CD11c^+$ were found to be in the marginal zone in spleen and LN, and medulla in thymus. No abnormal localization was found. Ceramide was stained in parallel. Again, ceramide seemed to localize at the B cell zones in LN and spleen. Apart from these cells, there were also clusters of high ceramide-expressing cells in close proximity to the $CD11c^+$ cells. The proximity occurred in all genotypes, not only limited to Tg mice. These ceramide expressing cells were not in the B cell or T cell zones, but at the intersections instead.

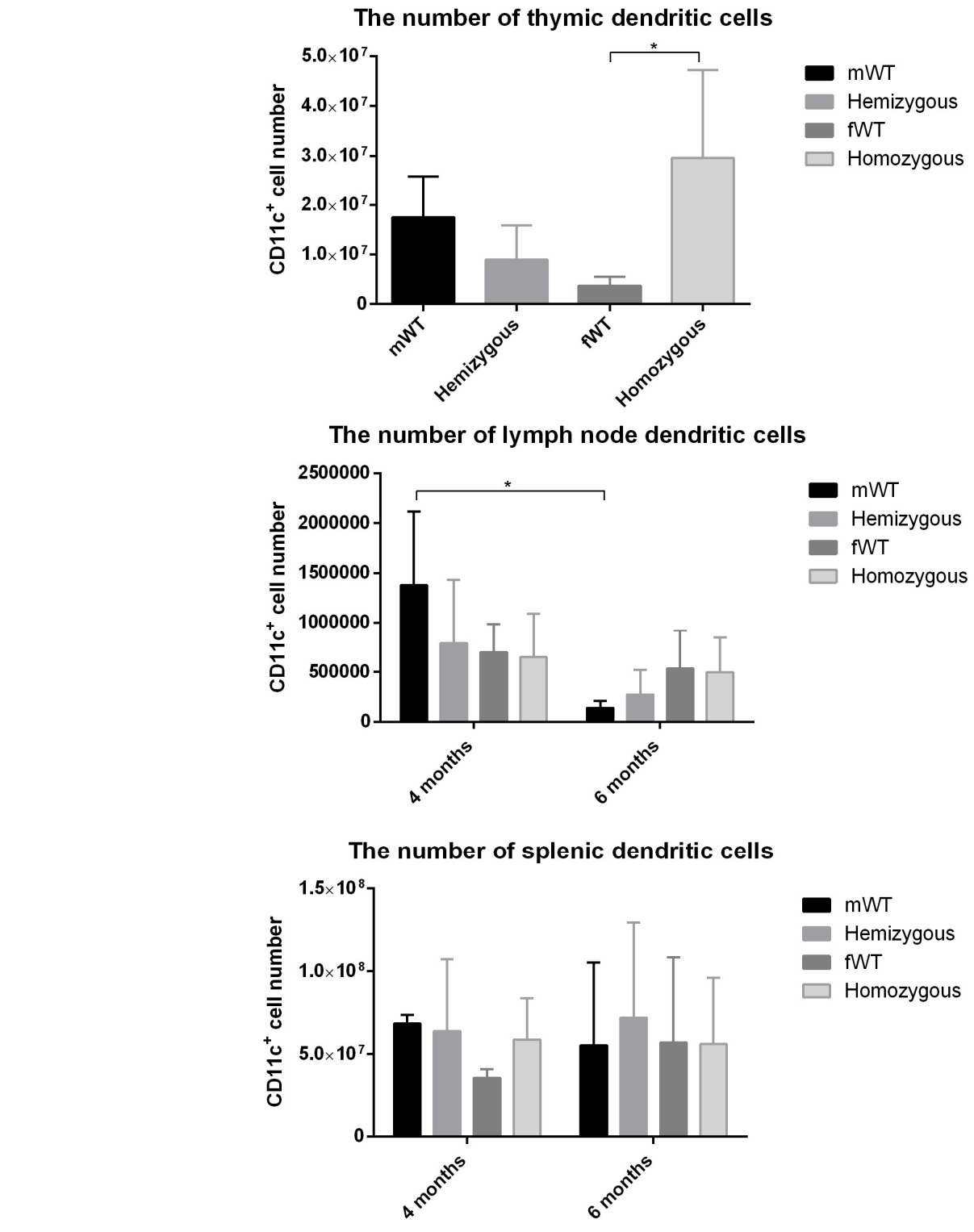

Figure 39. Dendritic cell number of (A) thymus, (B) lymph node, (C) spleen. Mean ± SD. n = 3- 5 mice. Significant differences were assessed by 1-way ANOVA in thymus, and 2-way ANOVA in lymph node and spleen: * $p < 0.05$. Abbreviation: mWT,male wildtype; fWT, female wildtype.

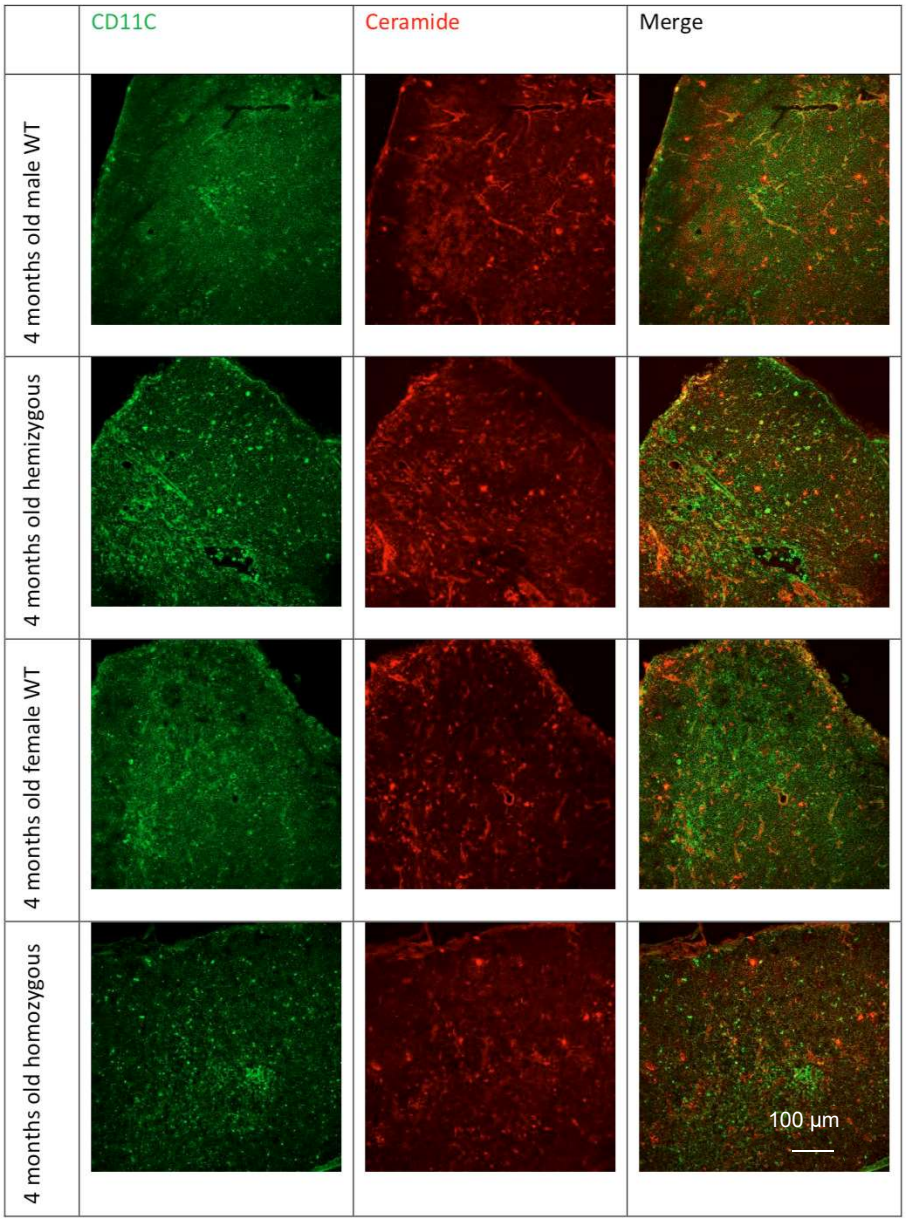

Figure 40. Immunofluorescent staining of thymus with antibodies directed against dendritic cells (CD11c, green) and Ceramide (red). n= 2- 3 mice. Representative images are shown. Abbreviation: WT, wildtype. Scale bar: 100 µm.

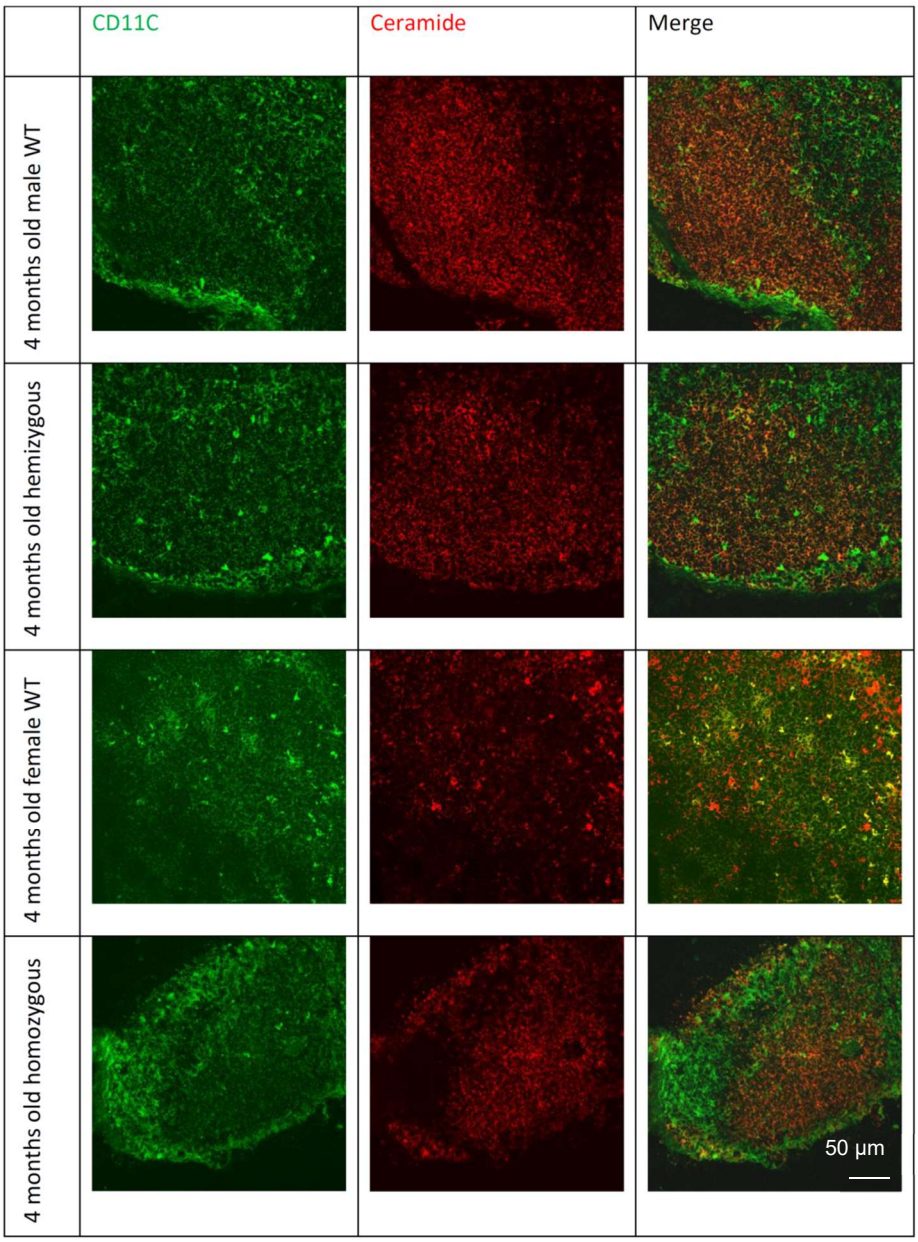

Figure 41a. Immunofluorescent staining of lymph node with antibodies directed against dendritic cells (CD11c, green) and Ceramide (red). n= 1- 3 mice. Representative images are shown. Abbreviation: WT, wildtype. Scale bar: 50 µm.

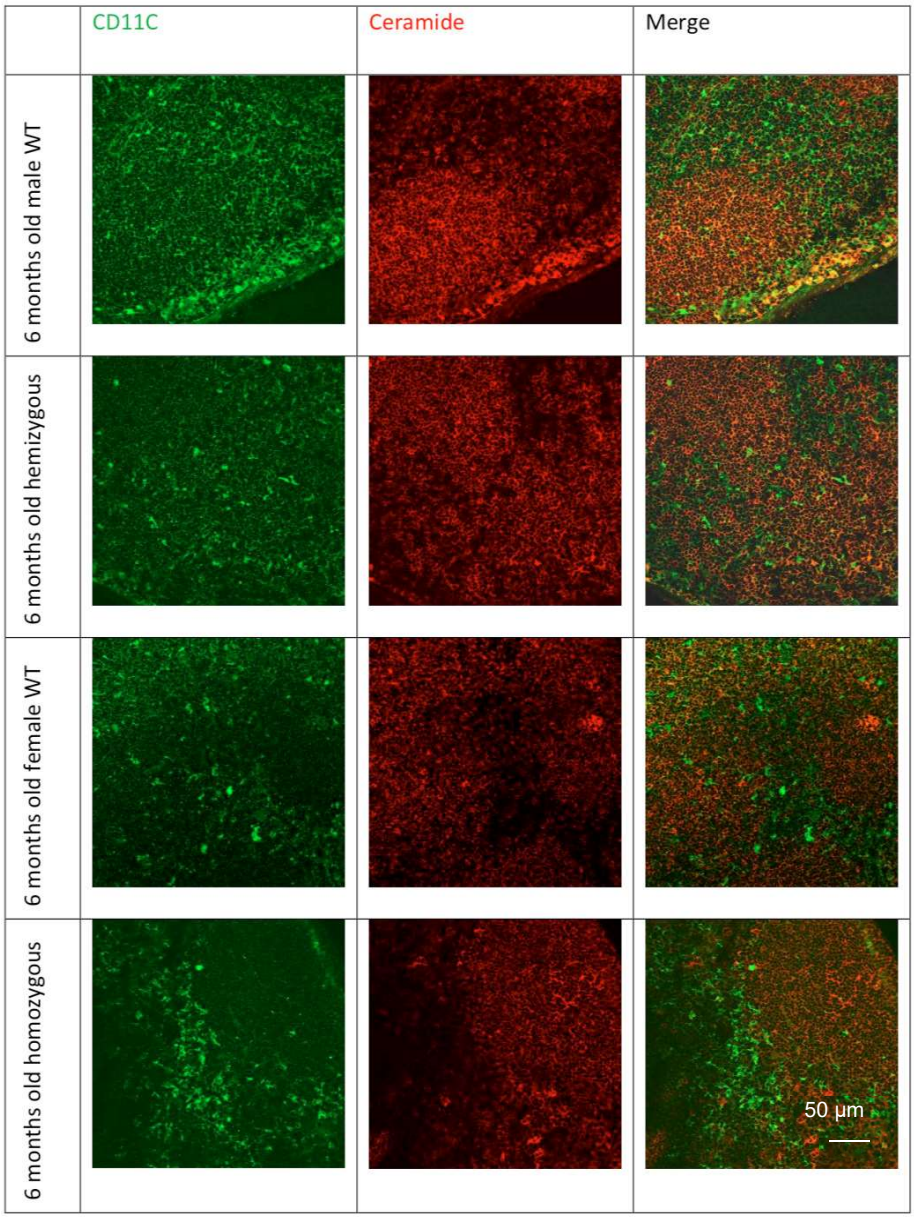

Figure 41b. Immunofluorescent staining of lymph node with antibodies directed against dendritic cells (CD11c, green) and Ceramide (red). n= 1- 3 mice. Representative images are shown. Abbreviation: WT, wildtype. Scale bar: 50 µm.

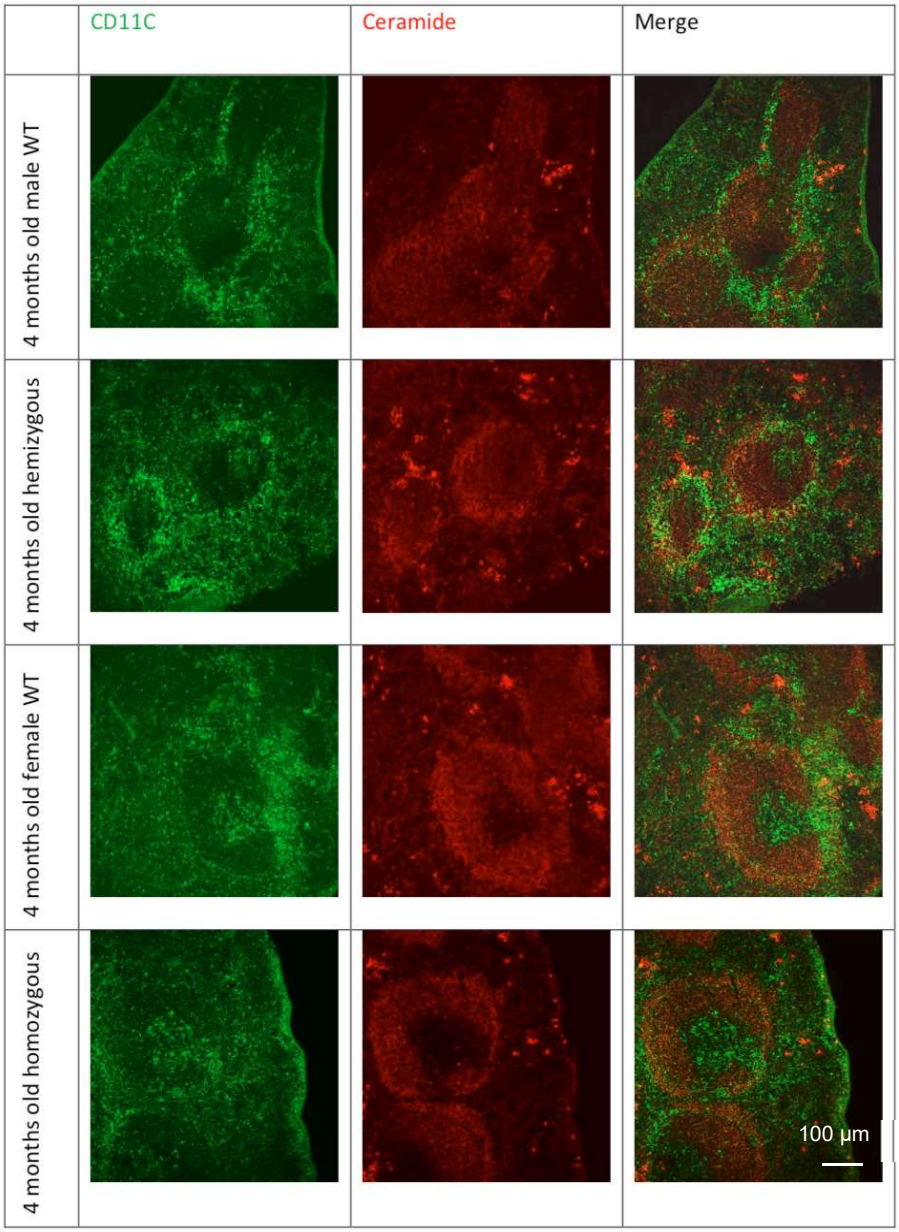

Figure 42a. Immunofluorescent staining of spleen with antibodies directed against dendritic cells (CD11c, green) and Ceramide (red). n= 1- 3 mice. Representative images are shown. Abbreviation: WT, wildtype. Scale bar: 100 µm.

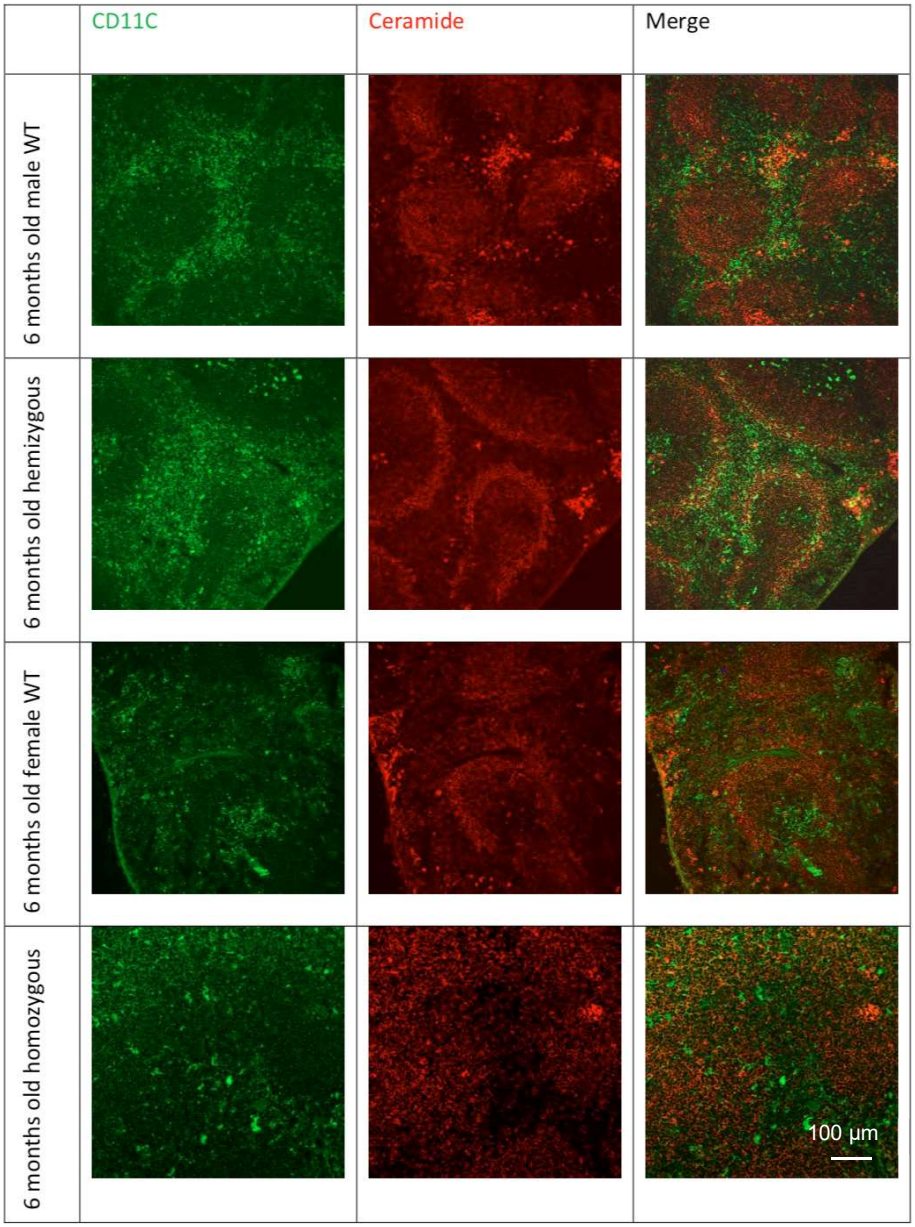

Figure 42b. Immunofluorescent staining of spleen with antibodies directed against dendritic cells (CD11c, green) and Ceramide (red). n= 1- 3 mice. Representative images are shown. Abbreviation: WT, wildtype. Scale bar: 100 µm.

Chapter 4 Discussion

The populations of T cell, B cells, macrophages, neutrophils, and dendritic cells with flow cytometry were investigated. The localization of these cells with immunofluorescence were studied. The activation markers of T cells, CD69 and CD25 were also analyzed. The experiments were carried out without immunization to study the baseline of these immune cells.

Chapter 4.1 Ceramide expressing cell

There were three populations of cells co-localizing with strong ceramide staining in the IF images.

Ceramides were found to co-localize with B cells, implying B cells express ceramide at a notable level. The ceramide expression was even higher on the marginal B cells. These cells expressed ceramide in all genotypes.

There are not a lot of published studies on association of B cells with sphingolipids. Our group has published a study on CD40 clustering in B cells. In the study, it was found that with the translocation of Asm on B cells, ceramide generated formed a lipid platform. The platform clustered CD40 and CD40 ligand for interaction of B cells and T cells. Asm deficient T cells failed to induce CD40 clustering in B cells, when WT showed normal clustering (Grassmé, 2002).

It is possible that ceramide expression in B cells is related to CD40 clustering with the lipid platform, directly or indirectly. Follicular B cells and marginal zone B cells are located next to the T cells zone for the T cell-dependent activation. However, T cell-B cell interactions in the follicle were not observed.

Ceramide expression on B cells of both WT and Tg were seen. There was no alternation in Tg mice. In the previous study, WT T cells were found forming clustering with B cells, but no clustering was found with Asm deficiency (Grassmé, 2002). No data on Asm overexpressed B cells was shown. The ceramide expression detected in the IF images could be the baseline level without stimulation.

Higher expression of ceramide was seen in MZB than in follicular B cells. MZB express higher level of immunoglobulin M (IgM), CD21 and MHC class I molecule CD1d than follicular B cells, but lower level of CD23 and immunoglobulin D (IgD). In spleen, marginal B cells are semi-activated, which means it could differentiate readily

into plasma cells once they are exposed to antigen (Kleinwort, 2018). Whether IgM, CD21 and CD1d are related to the expression of ceramide remains to be determined. It has been reported S1P is involved in follicular B cells and MZB localization. Previous studies from Cinamon and team (2004) revealed that MZB express S1P receptors, $S1P_1$ and $S1P_3$, and that $S1P_1$ prevents MZB to move to the follicle due to the chemoattraction from chemokine CXCL13. Alternation of the sphingolipid rheostat and subsequent generation of ceramide could affect these ceramide expressing cells. Asm overexpression possibly plays a role in the localization but the underlying mechanism is uncertain.

Another ceramide expressing population in the IF is localized at red pulp in spleen, subcapsular sinus and corticomedullary region in LN and thymus. They showed very robust fluorescent of ceramide. Some of them showed interactions with $CD11c^+$ cells whereas some of them co-localized with $CD11c^+$ cells. They were also in close proximity to CD11b, but rarely with F4/80, so they could be monocyte but not likely to be general population of macrophages.

One of the primary functions of DCs is to activate T cells by antigen. In LN, DCs uptake antigen entering the organs through HEV and afferent lymphatic vessels and get in contact with T cells (Cools, 2007) and arteries in spleen. In thymus, DCs helps immature T cell to undergo self-tolerance (Bouneaud, 2000. The ceramide expressing cells found in the IF could possibly be T cells executing these processes. Interestingly, ceramide fluorescence did not co-localize with CD3 staining. T cell receptors on T cell surfaces work as antigen recognition molecules, which bind to MHC with antigens on DCs. The choice of MHC molecules depends on the T cell subtype: MHC I for cytotoxic T cell, and MHC II for Th1 or Th2 $CD4^+$ cells (Soloski, 2000). To investigate more on this, both MHC I and MHC II could be looked at after immunization.

DCs are heterogeneous, but most of them express CD11c or CD11b. Resident conventional DCs are the primary DC population in spleen, but migratory cDCs enter draining LN after maturation from tissue and therefore LN has both subtypes (Merad, 2013). From the IF images the ceramide-expressing cells either interacted with $CD11b^+$ cells or co-localized with $CD11c^+$ cells. These cells were located at red pulps of spleen and paracortical and subcapsular region in LN. However the two populations could not be distinguished in the data. Migratory DCs was reported to have higher MHC II expressions, since they take up the antigen from tissue and are activated. Under the circumstances that the resident DCs are activated, MHC II is no

longer valid to distinguish the two populations (Randolph, 2005). The last ceramide expression populations were found only in spleen. They were found near the central arteriole. Since only few migratory DCs enter spleen (Randolph, 2005) under normal conditions, these cells could be of DC progenitors in bloodstream, rather than DCs. CD11c expression is the marker for cells of DC precursors. The ceramide expressing cells in red pulp, subcapsular regions and from bloodstream could also be macrophages derived from DC precursors (Merad, 2013).

Chapter 4.2 Innate immune response

Macrophages, neutrophils and dendritic cells are involved in innate immune responses. They have myeloid progenitor as precursor. They carry out innate immune responses by phagocytosis.

Neutrophils are an important cell type in innate immune responses. They were found to arrive from the inflammatory site to the draining lymph node as quickly as 15 minutes, preceded by localization of pathogens at the lymph node (Hampton, 2016). They function to phagocytose the in-coming pathogens and the foreign antigen, then destroy them with degradative enzyme. They can also secrete cytokines to regulate the adaptive immune response (Hampton, 2016, Murphy, 2011) and produce reactive oxygen species (Managó, 2015). To support the functions, the neutrophil numbers increase rapidly. In the flow cytometric data, fluctuations in number of neutrophils were observed in LN. There was no data supporting the correlation of Asm overexpression with this.

Neutrophils are recruited by residential macrophages by cytokines IL-1 or TNF-α (Kolaczkowska, 2013) into LN upon inflammation. Neutrophils usually enter the lymph node by HEV from bloodstream or afferent vessels. They localize in the subcapsular sinus where pathogens and innate immune cells are situated, with the help of subcapsular sinus macrophages (Hampton, 2016). In spleen, neutrophils are recruited through circulation by chemoattractant and inflammatory mediators (Deniset, 2017). There was no dramatic influx of neutrophils in the IF images.

Some macrophage populations in LN are exposed to lymph directly. The lymph fluid enters the LN by afferent lymphatic vessels close to subcapsular region, and leaves by efferent lymphatic vessels near medulla. Similar populations can be found in spleen red pulp. Instead of lymph, they filter blood. These macrophages have been known to filter the lymph and uptake the antigens (Gray, 2012). They are found to be

highly active phagocytes. They have enlarged lysosome and numerous vesicles (Steer, 1987). In thymus predominated macrophage population scatters throughout the cortex and medulla, and is thought to perform phagocytosis on T cells (Soga, 1997). Macrophages have been found to take in lipid (Lichtenstein, 2010), apoptotic polymorphonuclear cells and plasma cells (Koenig, 1996).

In the flow cytometry analysis, macrophage numbers in thymus decreased from 4 month-old female WT to homozygous mice significantly. Macrophage population drops in other organs were reported to be caused by apoptosis with infections when Asm was activated (Zhang, 2008; Gómez-Muñoz, 2004). Previous researches mostly involved a stimulus, such as *Pseudomonas aeruginosa* infection (Zhang, 2008) or withdrawal of growth factor macrophage colony-stimulating factor (Gómez-Muñoz A, 2004). The reason for the observed decrease in macrophage numbers in the present study is unknown.

Surprisingly, B cells in spleen can also take part in innate immune response. The phenotype of marginal zone B cells differs from the nearby follicular B cells. The MZB possess polyreactive BCR, and express high level of TLRs. When they come across antigens and microbial particles, BCR and TLR work together to produce low-affinity antibody rapidly (Cerutti, 2013). In this study, the MZB and follicular B cells were not distinguished. B220 and CD19 antibodies were used, which labeled B cells as whole. Investigation on this requires the use of CD1d or CD21 as MZB markers, as well as BCR and IgM.

Chapter 4.3 Adaptive immune responses

Follicular DCs in LN ‘free’ the foreign antigen and present it to follicular B cells. Unlike T cells, these B cells can recognize intact antigen. They then change their chemokine receptor profile, and migrate to the edge of T cell zone. B cells interact with T cells there, and receive second signal from T cells and hence induce the formation of germinal centre (GC) (Allen, 2007). In the GC they proliferate and differentiate into plasma cells and memory B cells, and undergo class-switching and antibody production (Victora, 2012). Splenic B cell activation resembles that of the LN, but it has some distinctive features. First, plasma cells can be found in red pulp for exporting antibodies into the blood stream (Allen, 2007). Second, the existence of marginal zone macrophages was reported to contribute to B cells immune responses (Koppel, 2008). GCs are transient when there are T cell-dependent activations. Dark and light

zone provide compartments for proliferation and selection (Cyster, 2000).
In T cell-independent activation, Toll-like receptors (TLR) are stimulated, or engagement of BCR. The antigens are usually presented by DCs, neutrophils or NKT cells which results in the differentiation of marginal zone B cells and B1 cells into plasma cells and production of antibodies. In this type of activation, B cells move out of follicles and proliferate, but no germinal centre is formed (Gordon, 2003).
In the IF images, only primary follicles were seen, which are the B cell follicles without germinal centre, and hence TD activation was not expected. There was no change in B cells populations, showing no proliferation of activated B cells, which suggested that B cell TI activation did not occur. Anti-B220 and anti-CD19 did not label plasma cells, so there was no data on plasma population. There was no foreign antigen in this study, which is reasonable that B cells were not activated through this pathway.
Naïve T cells enter and reside at the secondary lymphoid organs, ready for immune response. Antigen presenting cells such as dendritic cells process the antigen to form MHC-antigen complex, with either MHC I or MHC II. The complex binds to TCR on T cells as first signal. The second signal is provided by the co-stimulatory molecules on the APC, and the third signal is by the cytokines which control differentiation in effector cells. The T cells are then activated and undergo clonal expansion and differentiation into effector cells and memory cells (Pennock, 2013; Murphy, 2011). In the T cells population analysis, there was no increase in $CD4^+$, $CD8^+$, and double positive cell number, or percentage, which implied no clonal expansion.
CD69 as the early activation marker, is not expressed in resting T cells. They are expressed sharply when T cells are activated (Marzio, 1999). In the flow cytometry analysis, there was neither increase in CD69 expressing cells nor the CD69 expressions from WT to Transgenic (Tg) mice. Some fluctuations in some genotypes were seen, but they were not statistically significant. This finding was confirmed by IF. No increase in CD69 expression could be seen in correlation with Asm overexpression.
CD25 is the IL-2R α chain. IL-2 is a mitogenic cytokine, which binds to IL-2R α, β and γ chain. It has low affinity towards CD25, compare to the β and γ chain under normal condition (Kuziel, Greene, 1990). CD25 together with CD127 or Foxp3, label Tregs (Seddiki, 2006). In the current study CD25 was studied as activation marker, and there was no data regarding Tregs. In the IF and flow cytometric data, CD25 expression fluctuated insignificantly. Higher CD25 expression in response to Asm overexpression was not shown.

To carry out the functions to present antigen to T cells, immature DCs take up antigens and move to T cell zone in spleen and LN (Murphy, 2011). The localization of most DCs was found to stay near B cell follicles in spleen and LN. They did not move to T cells zone and it is suggested there was no activation of DCs judging by the localization.

Chapter 4.4 Migration

B cells from bone marrow and T cells from thymus go through a series of selections. The selected cells are naïve cells and being exported or 'home' to lymphoid organs spleen and LN. The process is under the precise control of chemokines. B cells arriving die and refill with new B cells from circulating to keep a constant number. They are controlled by CXCLl3 in chemotaxis.

The process of lymphocyte homing consists of 4 stages. Firstly, tethering and rolling, by the adhesion of addressins on HEVs to L-selectin of lymphocytes, which speeds up the lymphocyte rolling. Secondly, the activation of lymphocyte by chemokines, and the expressions of high-affinity form of integrins. Thirdly, arrest, in which the lymphocytes attach firmly to HEV luminal surface, by adhesion of intercellular cell adhesion molecules and integrins (ICAM-1). Lastly, transmigration of lymphocytes across HEV (Arbonés, 1994, Tang, 1998).

Lymphocytes enter spleen by blood. They arrive first in marginal sinus then to white pulp and leave from red pulp. In LN, they arrive through HEV to the paracortical area. The naïve T cells move to T cell zone for antigen presentation by macrophages and dendritic cells. Naive B cells move and reside at the follicle, where they are activated by specific antigen (von Andrian, 2003).

There was no data showing Asm overexpression affected the homing of T cells from the population analysis of T cells. The populations of T cells remained very stable from genotype to genotype. There was no great drop in T cell subtypes population in thymus, companied by no comparable increase in that of spleen and LN. The IF images also showed similar findings where no obvious differences in between genotype could be seen.

There was no a sudden increase in Tg in B cells population in both IF and flow cytometric data. The B cell numbers were rather equivalent among all genotypes. it is deduced that there was no homing of B cells based on data in this study. There was

no analysis on bone marrow B cell population in the present study. Nonetheless, it would not give us a different deduction.

The exit of lymphocytes from lymphoid organs is known as egress. It could either be T cells emigrating thymus or activated lymphocytes leaving the lymphoid organs to the infected site (Matloubian, 2004). The correlation of S1P and the egress has long been proven. S1P works very similarly to chemokines. Higher level of S1P is present in blood and lymph, and lower level of S1P in lymphoid organs. S1P receptors are expressed on T cell surfaces. In thymus, naïve T cells are drawn out to the circulation in response to the S1P gradient. During the period when T cells are activated in lymphoid organs, the expressions of S1P receptors are downregulated temporarily. It is caused by the expression of CD69 and internalization of S1P receptor. The temporary suspension of T cell receptor allows T cells to stay in lymphoid organs for proliferation. When the T cells are ready, CD69 expression is downregulated, and the chemoattraction is restored. The effector T cells then migrate to the infected site (Murphy, 2011).

There was no sign of egress detected in response to Asm overexpression. First of all, No change in T cell population in any genotypes in lymphoid organs was seen. Second, No $CD3^+$ cells were found gathering around vessels in spleen and LN. Thirdly, no robust fluorescence of CD69 in imaging or high level of MFI in flow cytometry could be observed. In the present study, there was no data on S1P. In case the mouse model is used for egress study in the future, it is crucial to include S1P assessment.

Summary

In the present study, I first assessed the Asm and Ac activities, and the sphingolipid levels of a transgenic Asm mouse model. I then investigated the immune cells, namely, T cells, B cells, macrophages, dendritic cell, and neutrophils in lymphoid organs, thymus, spleen, and lymph node. I employed flow cytometry to study the populations of these cells, and immunofluorescence to check their localization. While populations imply the occurrence of cellular events such as proliferation and apoptosis, the localizations indicate migrations and activations. I also looked at the activation of T cells by activation markers. I studied the innate and adaptive immune responses, as well as migration. There was no evidence that the Asm overexpressed mice encountered immune response and migration without immunization, in comparison with WT healthy mice. Interestingly, I could see in the immunofluorescent images some cells that expressed higher ceramide than other cells. The cells with high levels of ceramide are possibly B cells, as well as dendritic cells or dendritic cells-related cells. Since they expressed high ceramide levels, the Asm overexpression is likely to have effects on them. However, only populations and localization were investigated. These analyses did not seem to correlate with increased Asm activity. In the future, some other aspects such as cytokine levels and molecular interactions can be studied.

The current study showed that the untouched tAsm mice were relatively stable, showing basal levels of many immune parameters like healthy WT mice. The mouse model is a great tool to further study the immune system, in response to various challenges. The best gender and age to be used could not be defined, because their Ac activities and sphingolipid levels are not comparable.

References

Alberts, B., Johnson, A., Lewis, J., . . .Walter, P. (2002). Molecular Biology of the Cell. 4th edition. New York: Garland Science; Helper T Cells and Lymphocyte Activation.

Allen, C. D., Okada, T., & Cyster, J. G. (2007). Germinal-center organization and cellular dynamics. *Immunity, 27*(2), 190-202. doi: 10.1016/j.immuni.2007.07.009

Antonarakis, S. E., Valle, D., Moser, H. W., Moser, A., Qualman, S. J., & Zinkham, W. H. (1984). Phenotypic variability in siblings with Farber disease. *J Pediatr, 104*(3), 406-409.

Arbones, M. L., Ord, D. C., Ley, K., Ratech, H., Maynard-Curry, C., Otten, G., . . . Tedder, T. F. (1994). Lymphocyte homing and leukocyte rolling and migration are impaired in L-selectin-deficient mice. *Immunity, 1*(4), 247-260.

Artetxe, I., Sergelius, C., Kurita, M., Yamaguchi, S., Katsumura, S., Slotte, J. P., & Maula, T. (2013). Effects of sphingomyelin headgroup size on interactions with ceramide. *Biophys J, 104*(3), 604-612. doi: 10.1016/j.bpj.2012.12.026

Avota, E., Gulbins E., and Schneider-Schaulies S., *DC-SIGN mediated sphingomyelinase-activation and ceramide generation is essential for enhancement of viral uptake in dendritic cells.* PLoS Pathog, 2011. **7**(2): p. e1001290.

Bai, J., & Pagano, R. E. (1997). Measurement of spontaneous transfer and transbilayer movement of BODIPY-labeled lipids in lipid vesicles. *Biochemistry, 36*(29), 8840-8848. doi: 10.1021/bi970145r

Bajnok, A., Ivanova, M., Rigo, J., Jr., & Toldi, G. (2017). The Distribution of Activation Markers and Selectins on Peripheral T Lymphocytes in Preeclampsia. *Mediators Inflamm, 2017*, 8045161. doi: 10.1155/2017/8045161

Beckmann, N., Sharma, D., Gulbins, E., Becker, K. A., & Edelmann, B. (2014). Inhibition of acid sphingomyelinase by tricyclic antidepressants and analogons. *Front Physiol, 5*, 331. doi: 10.3389/fphys.2014.00331

Bodey, G. P. (1966). Infectious complications of acute leukemia. *Med Times, 94*(9), 1076-1085.

Bouneaud, C., Kourilsky, P., & Bousso, P. (2000). Impact of negative selection on the T cell repertoire reactive to a self-peptide: a large fraction of T cell clones escapes clonal deletion. *Immunity, 13*(6), 829-840.

Brady, R. O. (1966). The sphingolipidoses. *N Engl J Med, 275*(6), 312-318. doi: 10.1056/NEJM196608112750606

Bunting, M., Harris, E. S., McIntyre, T. M., Prescott, S. M., & Zimmerman, G. A. (2002). Leukocyte adhesion deficiency syndromes: adhesion and tethering defects involving beta 2 integrins and selectin ligands. *Curr Opin Hematol, 9*(1), 30-35.

Cambier, J. C., Gauld, S. B., Merrell, K. T., & Vilen, B. J. (2007). B-cell anergy: from transgenic models to naturally occurring anergic B cells? *Nat Rev Immunol, 7*(8), 633-643. doi: 10.1038/nri2133

Cerutti, A., Cols, M., & Puga, I. (2013). Marginal zone B cells: virtues of innate-like antibody-producing lymphocytes. *Nat Rev Immunol, 13*(2), 118-132. doi: 10.1038/nri3383

Cerutti, A., Puga, I., & Cols, M. (2012). New helping friends for B cells. *Eur J Immunol, 42*(8), 1956-1968. doi: 10.1002/eji.201242594

Cheretakis, C., Leung, R., Sun, C. X., Dror, Y., & Glogauer, M. (2006). Timing of neutrophil tissue repopulation predicts restoration of innate immune protection in a murine bone marrow transplantation model. *Blood, 108*(8), 2821-2826. doi: 10.1182/blood-2006-04-018184

Cicchetti, G., Allen, P. G., & Glogauer, M. (2002). Chemotactic signaling pathways in neutrophils: from receptor to actin assembly. *Crit Rev Oral Biol Med, 13*(3), 220-228.

Cinamon, G., Matloubian, M., Lesneski, M. J., Xu, Y., Low, C., Lu, T., . . . Cyster, J. G. (2004). Sphingosine 1-phosphate receptor 1 promotes B cell localization in the splenic marginal zone. *Nat Immunol, 5*(7), 713-720. doi: 10.1038/ni1083

Coant, N., Sakamoto, W., Mao, C., & Hannun, Y. A. (2017). Ceramidases, roles in sphingolipid metabolism and in health and disease. *Adv Biol Regul, 63*, 122-131. doi: 10.1016/j.jbior.2016.10.002

Cools, N., Ponsaerts, P., Van Tendeloo, V. F., & Berneman, Z. N. (2007). Balancing between immunity and tolerance: an interplay between dendritic cells, regulatory T cells, and effector T cells. *J Leukoc Biol, 82*(6), 1365-1374. doi: 10.1189/jlb.0307166

Cuschieri, J., & Maier, R. V. (2007). Oxidative stress, lipid rafts, and macrophage reprogramming. *Antioxid Redox Signal, 9*(9), 1485-1497. doi: 10.1089/ars.2007.1670

Cyster, J. G., Ansel, K. M., Reif, K., Ekland, E. H., Hyman, P. L., Tang, H. L., . . . Ngo, V. N. (2000). Follicular stromal cells and lymphocyte homing to follicles. *Immunol Rev, 176*, 181-193.

Dalton, D. K., Pitts-Meek, S., Keshav, S., Figari, I. S., Bradley, A., & Stewart, T. A. (1993). Multiple defects of immune cell function in mice with disrupted interferon-gamma genes. *Science, 259*(5102), 1739-1742.

Deniset, J. F., Surewaard, B. G., Lee, W. Y., & Kubes, P. (2017). Splenic Ly6G(high) mature and Ly6G(int) immature neutrophils contribute to eradication of S. pneumoniae. *J Exp Med, 214*(5), 1333-1350. doi: 10.1084/jem.20161621

Dimanche-Boitrel, M. T., Meurette, O., Rebillard, A., & Lacour, S. (2005). Role of early plasma membrane events in chemotherapy-induced cell death. *Drug Resist Updat, 8*(1-2), 5-14. doi: 10.1016/j.drup.2005.02.003

Doring, G., & Gulbins, E. (2009). Cystic fibrosis and innate immunity: how chloride channel mutations provoke lung disease. *Cell Microbiol, 11*(2), 208-216. doi: 10.1111/j.1462-5822.2008.01271.x

Dworski, S., Lu, P., Khan, A., Maranda, B., Mitchell, J. J., Parini, R., . . . Medin, J. A. (2017). Acid Ceramidase Deficiency is characterized by a unique plasma cytokine and ceramide profile that is altered by therapy. *Biochim Biophys Acta, 1863*(2), 386-394. doi: 10.1016/j.bbadis.2016.11.031

Eckhardt, M. (2010). Pathology and current treatment of neurodegenerative sphingolipidoses. *Neuromolecular Med, 12*(4), 362-382. doi: 10.1007/s12017-010-8133-7

Edelmann, B., Bertsch, U., Tchikov, V., Winoto-Morbach, S., Perrotta, C., Jakob, M., . . . Schutze, S. (2011). Caspase-8 and caspase-7 sequentially mediate proteolytic activation of acid sphingomyelinase in TNF-R1 receptosomes. *EMBO J, 30*(2), 379-394. doi: 10.1038/emboj.2010.326

Ehlert, K., Frosch, M., Fehse, N., Zander, A., Roth, J., & Vormoor, J. (2007). Farber disease: clinical presentation, pathogenesis and a new approach to treatment. *Pediatr Rheumatol Online J, 5*, 15. doi: 10.1186/1546-0096-5-15

Falcone, S., Perrotta, C., De Palma, C., Pisconti, A., Sciorati, C., Capobianco, A., . . . Clementi, E. (2004). Activation of acid sphingomyelinase and its inhibition by the nitric oxide/cyclic guanosine 3',5'-monophosphate pathway: key events in Escherichia coli-elicited apoptosis of dendritic cells. *J Immunol, 173*(7), 4452-4463.

Fenteany, G., & Glogauer, M. (2004). Cytoskeletal remodeling in leukocyte function. *Curr Opin Hematol, 11*(1), 15-24.

Ferlinz, K., Hurwitz, R., Vielhaber, G., Suzuki, K., & Sandhoff, K. (1994). Occurrence of two molecular forms of human acid sphingomyelinase. *Biochem J, 301 (Pt 3)*, 855-862.

Goggel, R., Winoto-Morbach, S., Vielhaber, G., Imai, Y., Lindner, K., Brade, L., . . . Uhlig, S. (2004). PAF-mediated pulmonary edema: a new role for acid sphingomyelinase and ceramide. *Nat Med, 10*(2), 155-160. doi: 10.1038/nm977

Gomez-Munoz, A., Kong, J. Y., Salh, B., & Steinbrecher, U. P. (2004). Ceramide-1-phosphate blocks apoptosis through inhibition of acid sphingomyelinase in macrophages. *J Lipid Res, 45*(1), 99-105. doi: 10.1194/jlr.M300158-JLR200

Gordon, S. (2003). Alternative activation of macrophages. *Nat Rev Immunol, 3*(1), 23-35. doi: 10.1038/nri978

Grassme, H., Jekle, A., Riehle, A., Schwarz, H., Berger, J., Sandhoff, K., . . . Gulbins, E. (2001). CD95 signaling via ceramide-rich membrane rafts. *J Biol Chem, 276*(23), 20589-20596. doi: 10.1074/jbc.M101207200

Grassme, H., Jendrossek, V., Bock, J., Riehle, A., & Gulbins, E. (2002). Ceramide-rich membrane rafts mediate CD40 clustering. *J Immunol, 168*(1), 298-307.

Gray, E. E., & Cyster, J. G. (2012). Lymph node macrophages. *J Innate Immun, 4*(5-6), 424-436. doi: 10.1159/000337007

Gulbins, E., & Li, P. L. (2006). Physiological and pathophysiological aspects of ceramide. *Am J Physiol Regul Integr Comp Physiol, 290*(1), R11-26. doi: 10.1152/ajpregu.00416.2005

Hampton, H. R., & Chtanova, T. (2016). The lymph node neutrophil. *Semin Immunol, 28*(2), 129-136. doi: 10.1016/j.smim.2016.03.008

Hanada, K., Kumagai, K., Yasuda, S., Miura, Y., Kawano, M., Fukasawa, M., & Nishijima, M. (2003). Molecular machinery for non-vesicular trafficking of ceramide. *Nature, 426*(6968), 803-809. doi: 10.1038/nature02188

Hannun, Y. A., & Obeid, L. M. (2011). Many ceramides. *J Biol Chem, 286*(32), 27855-27862. doi: 10.1074/jbc.R111.254359

Hannun, Y. A., & Obeid, L. M. (2018). Sphingolipids and their metabolism in physiology and disease. *Nat Rev Mol Cell Biol, 19*(3), 175-191. doi: 10.1038/nrm.2017.107

Hawthorne, J. N. (1975). A note on the life of J.L.W. Thudichum (1829-1901). *Biochem Soc Trans, 3*(5), 591.

Holopainen, J. M., Subramanian, M., & Kinnunen, P. K. (1998). Sphingomyelinase induces lipid microdomain formation in a fluid phosphatidylcholine/sphingomyelin membrane. *Biochemistry, 37*(50), 17562-17570. doi: 10.1021/bi980915e

Jakobi, V., & Petry, F. (2008). Humoral immune response in IL-12 and IFN-gamma deficient mice after infection with Cryptosporidium parvum. *Parasite Immunol, 30*(3), 151-161. doi: 10.1111/j.1365-3024.2007.01013.x

Kirschnek, S., Paris, F., Weller, M., Grassme, H., Ferlinz, K., Riehle, A., . . . Gulbins, E. (2000). CD95-mediated apoptosis in vivo involves acid sphingomyelinase. *J Biol Chem, 275*(35), 27316-27323. doi: 10.1074/jbc.M002957200

Kitatani, K., Idkowiak-Baldys, J., & Hannun, Y. A. (2008). The sphingolipid salvage pathway in ceramide metabolism and signaling. *Cell Signal, 20*(6), 1010-1018. doi: 10.1016/j.cellsig.2007.12.006

Kleinwort, A., Luhrs, F., Heidecke, C. D., Lipp, M., & Schulze, T. (2018). S1P Signalling Differentially Affects Migration of Peritoneal B Cell Populations In Vitro and Influences the Production of Intestinal IgA In Vivo. *Int J Mol Sci, 19*(2). doi: 10.3390/ijms19020391

Kobayashi, S. D., Voyich, J. M., Whitney, A. R., & DeLeo, F. R. (2005). Spontaneous neutrophil apoptosis and regulation of cell survival by granulocyte macrophage-colony stimulating factor. *J Leukoc Biol, 78*(6), 1408-1418. doi: 10.1189/jlb.0605289

Koenig, J. M., Simon, J., Anderson, D. C., Smith, E., & Smith, C. W. (1996). Diminished soluble and total cellular L-selectin in cord blood is associated with its impaired shedding from activated neutrophils. *Pediatr Res, 39*(4 Pt 1), 616-621. doi: 10.1203/00006450-199604000-00009

Kolaczkowska, E., & Kubes, P. (2013). Neutrophil recruitment and function in health and inflammation. *Nat Rev Immunol, 13*(3), 159-175. doi: 10.1038/nri3399

Koppel, E. A., Litjens, M., van den Berg, V. C., van Kooyk, Y., & Geijtenbeek, T. B. (2008). Interaction of SIGNR1 expressed by marginal zone macrophages with marginal zone B cells is essential to early IgM responses against Streptococcus pneumoniae. *Mol Immunol, 45*(10), 2881-2887. doi: 10.1016/j.molimm.2008.01.032

Kornhuber, J., Medlin, A., Bleich, S., Jendrossek, V., Henkel, A. W., Wiltfang, J., & Gulbins, E. (2005). High activity of acid sphingomyelinase in major depression. *J Neural Transm (Vienna), 112*(11), 1583-1590. doi: 10.1007/s00702-005-0374-5

Kuziel, W. A., & Greene, W. C. (1990). Interleukin-2 and the IL-2 receptor: new insights into structure and function. *J Invest Dermatol, 94*(6 Suppl), 27S-32S.

Lafontaine, M., Landry, D., & Montplaisir, S. (1997). Human thymic dendritic cells. *Microsc Res Tech, 38*(3), 267-275. doi: 10.1002/(SICI)1097-0029(19970801)38:3<267::AID-JEMT7>3.0.CO;2-J

Lang, P. A., Schenck, M., Nicolay, J. P., Becker, J. U., Kempe, D. S., Lupescu, A., . . . Lang, F. (2007). Liver cell death and anemia in Wilson disease involve acid sphingomyelinase and ceramide. *Nat Med, 13*(2), 164-170. doi: 10.1038/nm1539

Li, C., Wu, Y., Riehle, A., Orian-Rousseau, V., Zhang, Y., Gulbins, E., & Grassme, H. (2017). Regulation of Staphylococcus aureus Infection of Macrophages by CD44, Reactive Oxygen Species, and Acid Sphingomyelinase. *Antioxid Redox Signal*. doi: 10.1089/ars.2017.6994

Lichtenstein, L., Mattijssen, F., de Wit, N. J., Georgiadi, A., Hooiveld, G. J., van der Meer, R., . . . Kersten, S. (2010). Angptl4 protects against severe proinflammatory effects of saturated fat by inhibiting fatty acid uptake into mesenteric lymph node macrophages. *Cell Metab, 12*(6), 580-592. doi: 10.1016/j.cmet.2010.11.002

Liu, K., Victora, G. D., Schwickert, T. A., Guermonprez, P., Meredith, M. M., Yao, K., . . . Nussenzweig, M. (2009). In vivo analysis of dendritic cell development and homeostasis. *Science, 324*(5925), 392-397. doi: 10.1126/science.1170540

Ma, J., Gulbins, E., Edwards, M. J., Caldwell, C. C., Fraunholz, M., & Becker, K. A. (2017). Staphylococcus aureus alpha-Toxin Induces Inflammatory Cytokines via Ly-

sosomal Acid Sphingomyelinase and Ceramides. *Cell Physiol Biochem, 43*(6), 2170-2184. doi: 10.1159/000484296

Manago, A., Becker, K. A., Carpinteiro, A., Wilker, B., Soddemann, M., Seitz, A. P., . . . Gulbins, E. (2015). Pseudomonas aeruginosa pyocyanin induces neutrophil death via mitochondrial reactive oxygen species and mitochondrial acid sphingomyelinase. *Antioxid Redox Signal, 22*(13), 1097-1110. doi: 10.1089/ars.2014.5979

Mao, C., & Obeid, L. M. (2008). Ceramidases: regulators of cellular responses mediated by ceramide, sphingosine, and sphingosine-1-phosphate. *Biochim Biophys Acta, 1781*(9), 424-434. doi: 10.1016/j.bbalip.2008.06.002

Marchesini, N., & Hannun, Y. A. (2004). Acid and neutral sphingomyelinases: roles and mechanisms of regulation. *Biochem Cell Biol, 82*(1), 27-44. doi: 10.1139/o03-091

Marzio, R., Mauel, J., & Betz-Corradin, S. (1999). CD69 and regulation of the immune function. *Immunopharmacol Immunotoxicol, 21*(3), 565-582. doi: 10.3109/08923979909007126

Matloubian, M., Lo, C. G., Cinamon, G., Lesneski, M. J., Xu, Y., Brinkmann, V., . . . Cyster, J. G. (2004). Lymphocyte egress from thymus and peripheral lymphoid organs is dependent on S1P receptor 1. *Nature, 427*(6972), 355-360. doi: 10.1038/nature02284

Merad, M., Sathe, P., Helft, J., Miller, J., & Mortha, A. (2013). The dendritic cell lineage: ontogeny and function of dendritic cells and their subsets in the steady state and the inflamed setting. *Annu Rev Immunol, 31*, 563-604. doi: 10.1146/annurev-immunol-020711-074950

Merrill, A. H., Jr., Stokes, T. H., Momin, A., Park, H., Portz, B. J., Kelly, S., . . . Wang, M. D. (2009). Sphingolipidomics: a valuable tool for understanding the roles of sphingolipids in biology and disease. *J Lipid Res, 50 Suppl*, S97-102. doi: 10.1194/jlr.R800073-JLR200

Merrill, A. H., Jr., Wang, M. D., Park, M., & Sullards, M. C. (2007). (Glyco)sphingolipidology: an amazing challenge and opportunity for systems biology. *Trends Biochem Sci, 32*(10), 457-468. doi: 10.1016/j.tibs.2007.09.004

Michel, C., van Echten-Deckert, G., Rother, J., Sandhoff, K., Wang, E., & Merrill, A. H., Jr. (1997). Characterization of ceramide synthesis. A dihydroceramide desaturase introduces the 4,5-trans-double bond of sphingosine at the level of dihydroceramide. *J Biol Chem, 272*(36), 22432-22437.

Mikati, M. A., Zeinieh, M., Habib, R. A., El Hokayem, J., Rahmeh, A., El Sabban, M., . . . Dbaibo, G. (2008). Changes in sphingomyelinases, ceramide, Bax, Bcl(2), and caspase-3 during and after experimental status epilepticus. *Epilepsy Res, 81*(2-3), 161-166. doi: 10.1016/j.eplepsyres.2008.05.009

Mildner, A., & Jung, S. (2014). Development and function of dendritic cell subsets. *Immunity, 40*(5), 642-656. doi: 10.1016/j.immuni.2014.04.016

Monick, M. M., Carter, A. B., Robeff, P. K., Flaherty, D. M., Peterson, M. W., & Hunninghake, G. W. (2001). Lipopolysaccharide activates Akt in human alveolar macrophages resulting in nuclear accumulation and transcriptional activity of beta-catenin. *J Immunol, 166*(7), 4713-4720.

Murphy K. Janeway's Immunobiology. 8th ed. Garland Science; 2011.

Niedergang, F., & Chavrier, P. (2004). Signaling and membrane dynamics during phagocytosis: many roads lead to the phagos(R)ome. *Curr Opin Cell Biol, 16*(4), 422-428. doi: 10.1016/j.ceb.2004.06.006

O'Riordain, M. G., Falconer, J. S., Maingay, J., Fearon, K. C., & Ross, J. A. (1999). Peripheral blood cells from weight-losing cancer patients control the hepatic acute phase response by a primarily interleukin-6 dependent mechanism. *Int J Oncol, 15*(4), 823-827.

Okino, N., He, X., Gatt, S., Sandhoff, K., Ito, M., & Schuchman, E. H. (2003). The reverse activity of human acid ceramidase. *J Biol Chem, 278*(32), 29948-29953. doi: 10.1074/jbc.M303310200

Paris, F., Fuks, Z., Kang, A., Capodieci, P., Juan, G., Ehleiter, D., . . . Kolesnick, R. (2001). Endothelial apoptosis as the primary lesion initiating intestinal radiation damage in mice. *Science, 293*(5528), 293-297. doi: 10.1126/science.1060191

Pearse, G. (2006). Histopathology of the thymus. *Toxicol Pathol, 34*(5), 515-547. doi: 10.1080/01926230600978458

Pennock, N. D., White, J. T., Cross, E. W., Cheney, E. E., Tamburini, B. A., & Kedl, R. M. (2013). T cell responses: naive to memory and everything in between. *Adv Physiol Educ, 37*(4), 273-283. doi: 10.1152/advan.00066.2013

Plate, J. M., Lukaszewska, T. L., Bustamante, G., & Hayes, R. L. (1988). Cytokines involved in the generation of cytolytic effector T lymphocytes. *Ann N Y Acad Sci, 532*, 149-157.

Qiu, H., Edmunds, T., Baker-Malcolm, J., Karey, K. P., Estes, S., Schwarz, C., . . . Van Patten, S. M. (2003). Activation of human acid sphingomyelinase through modification or deletion of C-terminal cysteine. *J Biol Chem, 278*(35), 32744-32752. doi: 10.1074/jbc.M303022200

Raas-Rothschild, A., Pankova-Kholmyansky, I., Kacher, Y., & Futerman, A. H. (2004). Glycosphingolipidoses: beyond the enzymatic defect. *Glycoconj J, 21*(6), 295-304. doi: 10.1023/B:GLYC.0000046272.38480.ef

Randolph, G. J., Angeli, V., & Swartz, M. A. (2005). Dendritic-cell trafficking to lymph nodes through lymphatic vessels. *Nat Rev Immunol, 5*(8), 617-628. doi: 10.1038/nri1670

Reddy, M., Eirikis, E., Davis, C., Davis, H. M., & Prabhakar, U. (2004). Comparative analysis of lymphocyte activation marker expression and cytokine secretion profile in stimulated human peripheral blood mononuclear cell cultures: an in vitro model to monitor cellular immune function. *J Immunol Methods, 293*(1-2), 127-142. doi: 10.1016/j.jim.2004.07.006

Rehg, J. E., Bush, D., & Ward, J. M. (2012). The utility of immunohistochemistry for the identification of hematopoietic and lymphoid cells in normal tissues and interpretation of proliferative and inflammatory lesions of mice and rats. *Toxicol Pathol, 40*(2), 345-374. doi: 10.1177/0192623311430695

Reis e Sousa, C. (2006). Dendritic cells in a mature age. *Nat Rev Immunol, 6*(6), 476-483. doi: 10.1038/nri1845

Richard, A., Bourgoin, S., Naccache, P. H., L'Heureux, G. P., Krump, E., McColl, S. R., & Pelletier, G. (1996). C2-ceramide primes specifically for the superoxide anion production induced by N-formylmethionylleucyl phenylalanine (fMLP) in human neutrophils. *Biochim Biophys Acta, 1299*(2), 259-266.

Scheel-Toellner, D., Wang, K., Craddock, R., Webb, P. R., McGettrick, H. M., Assi, L. K., . . . Lord, J. M. (2004). Reactive oxygen species limit neutrophil life span by activating death receptor signaling. *Blood, 104*(8), 2557-2564. doi: 10.1182/blood-2004-01-0191

Schuchman, E. H. (2010). Acid sphingomyelinase, cell membranes and human disease: lessons from Niemann-Pick disease. *FEBS Lett, 584*(9), 1895-1900. doi: 10.1016/j.febslet.2009.11.083

Schuchman, E. H., Levran, O., Pereira, L. V., & Desnick, R. J. (1992). Structural organization and complete nucleotide sequence of the gene encoding human acid sphingomyelinase (SMPD1). *Genomics, 12*(2), 197-205.

Seddiki, N., Santner-Nanan, B., Martinson, J., Zaunders, J., Sasson, S., Landay, A., . . . Fazekas de St Groth, B. (2006). Expression of interleukin (IL)-2 and IL-7 receptors discriminates between human regulatory and activated T cells. *J Exp Med, 203*(7), 1693-1700. doi: 10.1084/jem.20060468

Shah, D. K., & Zuniga-Pflucker, J. C. (2014). An overview of the intrathymic intricacies of T cell development. *J Immunol, 192*(9), 4017-4023. doi: 10.4049/jimmunol.1302259

Shumilina, E., Xuan, N. T., Schmid, E., Bhavsar, S. K., Szteyn, K., Gu, S., . . . Lang, F. (2010). Zinc induced apoptotic death of mouse dendritic cells. *Apoptosis, 15*(10), 1177-1186. doi: 10.1007/s10495-010-0520-x

Soga, H., Nakamura, M., Yagi, H., Kayaba, S., Ishii, T., Gotoh, T., & Itoh, T. (1997). Heterogeneity of mouse thymic macrophages: I. Immunohistochemical analysis. *Arch Histol Cytol, 60*(1), 53-63.

Soloski, M. J., Szperka, M. E., Davies, A., & Wooden, S. L. (2000). Host immune response to intracellular bacteria: A role for MHC-linked class-Ib antigen-presenting molecules. *Proc Soc Exp Biol Med, 224*(4), 231-239.

Steer, H. W., & Foot, R. A. (1987). Changes in the medulla of the parathymic lymph nodes of the rat during acute gastro-intestinal inflammation. *J Anat, 152*, 23-36.

Steiniger, B. S. (2015). Human spleen microanatomy: why mice do not suffice. *Immunology, 145*(3), 334-346. doi: 10.1111/imm.12469

Takahashi, K. (1994). [Development and differentiation of macrophages and their related cells]. *Hum Cell, 7*(3), 109-115.

Tang, M. L., Steeber, D. A., Zhang, X. Q., & Tedder, T. F. (1998). Intrinsic differences in L-selectin expression levels affect T and B lymphocyte subset-specific recirculation pathways. *J Immunol, 160*(10), 5113-5121.

Teichgraber, V., Ulrich, M., Endlich, N., Riethmuller, J., Wilker, B., De Oliveira-Munding, C. C., . . . Gulbins, E. (2008). Ceramide accumulation mediates inflammation, cell death and infection susceptibility in cystic fibrosis. *Nat Med, 14*(4), 382-391. doi: 10.1038/nm1748

Turner, V. M., & Mabbott, N. A. (2017). Structural and functional changes to lymph nodes in ageing mice. *Immunology, 151*(2), 239-247. doi: 10.1111/imm.12727

van Kooyk, Y., & Geijtenbeek, T. B. (2003). DC-SIGN: escape mechanism for pathogens. *Nat Rev Immunol, 3*(9), 697-709. doi: 10.1038/nri1182

van Meer, G., & Hoetzl, S. (2010). Sphingolipid topology and the dynamic organization and function of membrane proteins. *FEBS Lett, 584*(9), 1800-1805. doi: 10.1016/j.febslet.2009.10.020

Victora, G. D., & Nussenzweig, M. C. (2012). Germinal centers. *Annu Rev Immunol, 30*, 429-457. doi: 10.1146/annurev-immunol-020711-075032

Vieira, O. V., Botelho, R. J., & Grinstein, S. (2002). Phagosome maturation: aging gracefully. *Biochem J, 366*(Pt 3), 689-704. doi: 10.1042/BJ20020691

von Andrian, U. H., & Mempel, T. R. (2003). Homing and cellular traffic in lymph nodes. *Nat Rev Immunol, 3*(11), 867-878. doi: 10.1038/nri1222

Wang, J. P., Bowen, G. N., Padden, C., Cerny, A., Finberg, R. W., Newburger, P. E., & Kurt-Jones, E. A. (2008). Toll-like receptor-mediated activation of neutrophils by influenza A virus. *Blood, 112*(5), 2028-2034. doi: 10.1182/blood-2008-01-132860

Wang, S. W., Parhar, K., Chiu, K. J., Tran, A., Gangoiti, P., Kong, J., . . . Gomez-Munoz, A. (2007). Pertussis toxin promotes macrophage survival through inhibition of acid sphingomyelinase and activation of the phosphoinositide 3-kinase/protein kinase B pathway. *Cell Signal, 19*(8), 1772-1783. doi: 10.1016/j.cellsig.2007.04.001

Wardemann, H., Yurasov, S., Schaefer, A., Young, J. W., Meffre, E., & Nussenzweig, M. C. (2003). Predominant autoantibody production by early human B cell precursors. *Science, 301*(5638), 1374-1377. doi: 10.1126/science.1086907

Wu, W., Mosteller, R. D., & Broek, D. (2004). Sphingosine kinase protects lipopolysaccharide-activated macrophages from apoptosis. *Mol Cell Biol, 24*(17), 7359-7369. doi: 10.1128/MCB.24.17.7359-7369.2004

Xuan, N. T., Shumilina, E., Schmid, E., Bhavsar, S. K., Rexhepaj, R., Gotz, F., . . . Lang, F. (2010). Role of acidic sphingomyelinase in thymol-mediated dendritic cell death. *Mol Nutr Food Res, 54*(12), 1833-1841. doi: 10.1002/mnfr.200900577

Yu, Z. F., Nikolova-Karakashian, M., Zhou, D., Cheng, G., Schuchman, E. H., & Mattson, M. P. (2000). Pivotal role for acidic sphingomyelinase in cerebral ischemia-induced ceramide and cytokine production, and neuronal apoptosis. *J Mol Neurosci, 15*(2), 85-97. doi: 10.1385/JMN:15:2:85

Zeidan, Y. H., & Hannun, Y. A. (2007). Translational aspects of sphingolipid metabolism. *Trends Mol Med, 13*(8), 327-336. doi: 10.1016/j.molmed.2007.06.002

Zhang, Y., Li, X., Carpinteiro, A., & Gulbins, E. (2008). Acid sphingomyelinase amplifies redox signaling in Pseudomonas aeruginosa-induced macrophage apoptosis. *J Immunol, 181*(6), 4247-4254.

Appendix

Conferences and presentations

Hung WY, Gulbins E. The characterization of the immune cells in Asm-overexpressed mice. Poster, International Workshop ,Sphingolipids - from basic science to novel therapeutic concepts, Würzburg, Germany. 28-30 June 2018

Hung WY, Gulbins E. The characterization of the immune cells in Asm-overexpressed mice. Presentation, Meeting of SFB 1039 and GRK 2098, Frankfurt, Germany. 26-27 June 2018

Acknowledgement

First of all, I would like to thank my supervisor Prof. Erich Gulbins, for taking me as his PhD student. Thank you for giving me the opportunity to work in Germany and in New York.

I would also like to thank my supervisor in New York, Prof. Edward Schuchman. You are a truly inspiring mentor. Working with you, Lila and your team was definitely a very pleasant experience.

And I would like to thank the thesis committee for your time and attention.

My collaboration partner Dr. Fabian Schumacher from University of Potsdam helped me with the mass spectrometry. I am very grateful for that.

Another person I want to thank is Dr. Xingxuan He from Mount Sinai Hospital. You guided me with a very logical and scientific mentality. I learnt a lot from you. I will remember your wise words, and good sense of humour.

I also want to say thank you to Ms Maggie from Mount Sinai Hospital. You helped me a lot with the mouse work in New York. Apart from that, we had really fun times eating out in New York. I have been away from home for a long time. You took care of me like my mom and gave me the feeling of home. I am really thankful for that.

I am so happy to have met my best friends, Anne Koch, Salina Begum and Yuqing Wu. Anne you helped me a lot with the difficult works. You helped me with my personal life. You helped me to an extent I am more than grateful. Seriously I owe you so much. Salina you are always the careful one and I always just run to you for all the details. Thank you for being patient with me. Yuqing we share the same culture and we always have good laughs. Thank you for supporting me all the time, laughing with me and crying for me. And your daughter is the cutest little girl I know.

Simone Keitsch, you are the friendliest person I have met. You have helped me a lot, with work and with my life in Germany. I will never forget you were the first person who asked me out for dinner when I was new to this place.

Thank you Dr. Stephanie Kadow, you taught me a lot about immunology. You were always patient and gave me good advice. I am impressed how well-organised you are and have learnt a lot from you.

Ms Helga Pätsch and Ms Bettina Peter helped me a lot with the administrative work. Particularly Helga, you take care of my visa issue, our graduate school and organise everything very well. Without your efforts, our graduate school would not have run so efficiently.

Svenja Plöhn you are my best company. We have had great time in New York, and I learnt most of my German (and the German drinking culture) from you. Thank you for being a good German teacher.
Thank you for my lab in Germany, Hannelore Disselhoff, Dr. Heike Grassmé, Dr. Katrin Becker-Flegler, Claudine Kühn, Jie Ma, Segfried Moyrer, Eyad Naser, Gabriele Hessler and Melanie Kramer, Dr. Alexander Carpinteiro, Bärbel Pollmeier, Andrea Riehle, Carolin Sehl, Matthias Soddeman and Barbara Wilker for being very great colleagues. Katrin I am very grateful for your help with my project, especially with the mice and all the good advice. Matthias thank you for teaching me how to do sectioning. Your cheerful greeting in the morning always warms my heart.
I want to thank everyone in the GRK 2098, for the sensible discussions during our literature seminars and progress presentations. Kristina, Klaus, Julian, Matthias and Jana you all are great mates. Thank you for the great experience together.
I want to show my gratitude to Ms Phyllis Cheung. It is very lovely to know you and your family. We stay close when we are homesick and that gives me power. Thank you also for the technical advices.
Ms Xiaoming Fang, my best friend and a brilliant scientist, has given me lots of supports technically and emotionally throughout these three years. Thank you for encouraging me and being always by my side.
Finally, I would like to say thank you to my family and my boyfriend Matthew, for being so supportive. You bore with me when I was busy and moody, and are so proud of me. I want to thank Matthew especially for taking care of me during my highs and lows. I would not have made it without you all.

Declarations

Erklärung:

Hiermit erkl**ä**re ich, gem. § 7 Abs. (2) d) + f) der Promotionsordnung der Fakultät für Biologie zur Erlangung des Dr. rer. nat., dass ich die vorliegende Dissertation selbständig verfasst und mich keiner anderen als der angegebenen Hilfsmittel bedient, bei der Abfassung der Dissertation nur die angegeben Hilfsmittel benutzt und alle wörtlich oder inhaltlich übernommenen Stellen als solche gekennzeichnet habe.

Essen, den _____ _____

Unterschrift der Doktorandin

Erklärung:

Hiermit erkl**ä**re ich, gem. § 7 Abs. (2) e) + g) der Promotionsordnung der Fakultät für Biologie zur Erlangung des Dr. rer. nat., dass ich keine anderen Promotionen bzw. Promotionsversuche in der Vergangenheit durchgeführt habe und dass diese Arbeit von keiner anderen Fakultät/Fachbereich abgelehnt worden ist.

Essen, den _____ _____

Unterschrift der Doktorandin

Erklärung:

Hiermit erkl**ä**re ich, gem. § 6 Abs. (2) g) der Promotionsordnung der Fakultät für Biologie zur Erlangung der Dr. rer. nat., dass ich das Arbeitsgebiet, dem das Thema *The characterization of immune cells in Asm-overexpressed mice* zuzuordnen ist, in Forschung und Lehre vertrete und den Antrag Wing Yee Hung befürworte und die Betreuung auch im Falle eines Weggangs, wenn nicht wichtige Gründe dem entgegenstehen, weiterführen werde.

_____

Name des Mitglieds der Universität Duisburg-Essen in Druckbuchstaben

Essen, den _____ _____

Unterschrift eines Mitglieds der Universität Duisburg-Essen